The Role of Protein Tyrosine Kinase 6 in UVB-Induced Signaling and Skin Carcinogenesis

BY

Michael Chastkofsky
B.S., University of Georgia, 2003
M.S., University of Wisconsin – Madison, 2006

THESIS

Defense Committee:

Angela Tyner, PhD Chair and Advisor
Luisa DiPietro PhD, DDS
David Crowe PhD, DDS
Xiaofeng Zhou PhD
Pradip Raychaudhuri PhD, Biochemistry and Molecular Genetics

This thesis is dedicated to my wonderful wife, Rivka, whose immeasurable support and

encouragement has helped me during these years.

Acknowledgements

I would like to express my deepest thanks and appreciation to my thesis advisor Dr. Angela L. Tyner for her guidance and support. She has been a wonderful role model as a scientist and as a mentor. I could not have accomplished this thesis and my doctorate without her direction and advice.

I would also like to thank my thesis committee Dr. Luisa DiPietro, Dr. David Crowe, Dr. Charles Zhou, and Dr. Pradip Raychaudhuri for their helpful suggestions and their support. I would like to thank my collaborators Dr. Susan Ball-Kell, for contribution to my research and for explicating the pathology reports, and Dr. Yu-Ying He, for providing me with human biopsy samples to corroborate the mouse data. I would also like to thank our lab manager June Bie for all her help in managing the mouse colony, her aid in mouse surgeries, and for her help in UVB irradiating the mice.

I would like to thank my family for the help and support they have given me, especially my wife, Rivka. I would also like to thank my parents, Dr. Leonard Chastkofsky and Dr. Barbara Redman, for motivating me and supporting me.

TABLE OF CONTENTS

TABLE OF CONTENTS
(continued)

LIST OF FIGURES

LIST OF ABBREVIATIONS

AKT	Ak mouse strain, transforming
ALT-PTK6	Alternatively spliced protein tyrosine kinase
AOM	Azoxymethane
ATCC	American type culture collection
ATP	Adenosine triphosphate
BCAR1	Breast cancer anti-estrogen resistance protein 1
BKS	BRK kinase substrate
BPH	Benign prostatic hyperplasia
BrdU	5-Bromo-2-deoxyuridine
BRK	Breast tumor kinase
BSA	Bovine Serum Albumin
BSK	β-cell Src-homology tyrosine kinase
cDNA	complementary DNA
CSK	C-Src tyrosine kinase
DAB	3, 3'-Diaminobenzidine tetrahydrochloride
DAPI	4, 6'-diamidino-2-phenylindole
DBS	Double stranded break
DMEM	Dulbecco's modified eagle medium
DNA	Deoxyribonucleic acid
Dok1	Docking protein 1
EDTA	Ethylenediaminetetraacetic acid
EGF	Epidermal growth factor
EGFR	Epidermal growth factor receptor
EGTA	Ethylene glycol tetraacetic acid
EMK	Embryonic mouse keratinocyte
EMT	Epithelial to mesenchymal transition
ER	Estrogen receptor
ERK	Extracellular signal-regulated kinase
FAK	Focal adhesion kinase
FBS	Fetal bovine serum
FITC	Fluorescein isothiocyanate
FRK	Fyn-related kinase
GAP	GTPase activating protein
HaCaT	Human adult-calcium-temperature
HEK	Human embryonic kidney
HEPES	4-(2-hydroxyethyl)-1-piperazineethanesulfonic acid
HIF	Hypoxia induced factor
HER2	Human epidermal growth factor receptor 2
HGF	Hepatocyte growth factor
HNSCC	Head and neck squamous cell carcinoma
IF	Immunofluorescence
IGF	Insulin-like growth factor
IgG	Immunoglobin G
IHC	Immunohistochemistry

LIST OF ABBREVIATIONS
(continued)

IRS	Insulin receptor substrate
Jak	Janus kinase
KAP3A	Kinesin-associated protein 3A
KGFR	Keratinocyte growth factor receptor
MAPK	Mitogen-activated protein kinase
MCF	Michigan Cancer Foundation
MDM2	Mouse double minute 2 homolog
MEF	Mouse embryonic fibroblast
MMR	Mismatch repair
MOI	Multiplicity of infection
NER	Nucleotide excision repair
OSCC	Oral squamous cell carcinoma
p130Cas	p130 Crk-associated substrate
PBS	Phosphate buffered saline
PC	Prostate cancer
PCR	Polymerase chain reaction
PI3K	Phosphoinositide-3 kinase
PIN	Prostatic intraepithelial neoplasia
PMSF	Phenylmethylsulfonyl fluoride
PR	Progesterone receptor
PSF	Polypyrimidine tract-binding protein-associated splicing factor
PTEN	Phosphatase and tension homolog
PTK6	Protein tyrosine kinase 6
PY	Phosphotyrosine
RACK1	Receptor of activated C kinase
RNA	Ribonucleic acid
ROS	Radical oxygen species
Sam68	Src-associated in mitosis, 68 kDa
SCC	Squamous cell carcinoma
SCT	Spindle cell tumor
SDS-PAGE	Sodium dodecyl sulfate-polyacrylamide gel electrophoresis
SENCAR	Sensitive to carcinogenesis
SH	SRC-homology domain
shRNA	small hairpin RNA
Sik	Src-related intestinal kinase
siRNA	small interfering RNA
SLM	Sam68-like mammalian protein
SRC	Sarcoma
SRMS	SRC-related kinase lacking C-terminal regulatory tyrosine and N-terminal myristoylation sites
STAP	Signal transducer and activator protein
STS	Skin tumor sensitive
STAT	Signal transducer and activator of transcription

LIST OF ABBREVIATIONS
(continued)

SV	Simian vacuolating virus
TCR	T cell factor
TBST	Tris-buffered saline with Tween 20
TNT	Tris-NaCl-Tween buffer
UVB	Ultraviolet B
VSVG	Vesicular stomatitis virus glycoprotein
WT	Wild type
YAMC	Young adult mouse colonic cells

SUMMARY

Protein tyrosine kinase 6 (PTK6; also called BRK for Breast tumor Kinase or Sik for Src-related Intestinal Kinase) is an intracellular tyrosine kinase. PTK6 shares structural similarity with the Src family of tyrosine kinases, but it lacks an N-terminal myristoylation consensus sequence for localization to the membrane. As a result, PTK6 localizes to different parts of the cells, such as the cytoplasm and the nucleus. PTK6 is most strongly expressed in non-dividing, differentiating epithelial cells, particularly in the skin, gastrointestinal tract, and oral epithelia. Characterization of the Ptk6-/- mouse showed increased intestinal epithelial cell turnover and impaired enterocyte differentiation. PTK6 is traditionally thought to promote terminal differentiation and inhibit proliferation in those tissues. However, PTK6 can also play an oncogenic role in certain tissues and conditions. PTK6 is over-expressed in 80% of breast cancers, despite low expression in normal breast tissue. In the gastrointestinal tract, gamma-irradiation and induce PTK6 expression in the proliferating crypt cells, where it promotes DNA-damage induced apoptosis. PTK6 targets several oncogenic signaling pathways that promote cancer cell proliferation, survival, and migration, such as STAT3, AKT, FAK, and BCAR1. Additionally, localization of PTK6 has been shown to affect oncogenesis in the prostate, suggesting that localization may play a role in how PTK6 functions.

PTK6 localizes to the suprabasal layer of skin epithelium. We determined that PTK6 localization is disrupted in SENCAR (SENsitive to CARcinogenesis) mice, such that PTK6 is present in all layers of the epithelium. PTK6 is also less phosphorylated in SENCAR mice, as compared with C57BL/6 mice, in which total PTK6 is expressed primarily in the suprabasal layers, but there is a small pool of phosphorylated PTK6 in

the basal layer. Knocking out PTK6 results in increased proliferation in neonatal mouse skin, but has no significant effect on adult mouse skin, suggesting PTK6 has a different effect on developing skin than on mature skin. Keratinocyte differentiation does not seem to be affected in either adult or neonatal mice, as keratin-14, a marker for undifferentiated basal cells, remains confined to the basal layer.

UVB irradiation induces proliferation in the skin, causing the skin to become thicker to protect against the damaging effects of UV. After regularly treating mouse skin with UVB, PTK6 expression increases significantly within 10 days, and becomes activated at the basal layer. PTK6 still does not seem to have a significant impact on proliferation or epithelial architecture. PTK6 promotes STAT3 Y705 phosphorylation and localization to the nucleus in the UVB-treated skin. PTK6 also promotes phosphorylation of FAK and BCAR, suggesting that PTK6 may play a role in increased keratinocyte motility after UVB irradiation.

Ptk6-/- mice are more resistant to UVB-induced inflammation than *Ptk6*+/+ mice. *Ptk6*+/+ mice developed inflammatory lesions on the lower dorsal skin, while *Ptk6*-/- mice experience only a slight erythema. PTK6 promotes tumor formation of UVB-induced skin tumors, as *Ptk6*+/+ mouse developed more tumors than did *Ptk6*-/- mice. *Ptk6*+/+ mice also exhibited a higher mortality rate than *Ptk6*-/- mice. In *Ptk6*+/+ mouse skin tumors, PTK6 was Y342 phosphorylated and localized to the membrane in hyperplastic skin to the cytoplasm in invading non-adhering epithelial cells. In the invading non-adhering epithelial cells, Y342 phosphorylated PTK6 co-localized with keratin-14, indicating that these cells are of epithelial origin. PTK6 did not co-localize with keratin-10, and is present primarily in poorly differentiated carcinomas.

PTK6 also promotes Y705 phosphorylation of STAT3, which enables STAT3 to dimerize and translocate to the nucleus to transcribe target genes. FAK and BCAR1 are also phosphorylated by PTK6. *Ptk6-/-* mouse skin contained noticeably less phosphorylated STAT3, FAK, and BCAR1 than *Ptk6+/+* mouse skin, suggesting that these pathways are the primary methods for PTK6 to promote carcinogenesis in UVB-damaged skin.

We then studied expression and phosphorylation of PTK6 in human skin to corroborate our finding in mouse skin. We determined that PTK6 becomes Y342 phosphorylated and localizes to the membrane in squamous cell carcinomas tissue. We also found that PTK6 transcription decreases in the early stages of tumorigenesis in head and neck squamous cell carcinoma. We have performed some additional experiments in HaCaT cells in which we successfully knocked down PTK6 using shRNA, although further studies need to be done in that area.

Our findings suggest that PTK6 plays an important role in promoting UVB-induced carcinogenesis. UVB irradiation causes an increase in PTK6 expression and Y342 phosphorylation. Disrupting *Ptk6* increases resistance to UVB-induced injury to skin, and inhibits phosphorylation of STAT3, FAK, and BCAR1. Targeting PTK6 may improve patient outcomes in treating squamous cell carcinomas.

I. INTRODUCTION

1. **PTK6 family**

Protein Tyrosine Kinase 6 (PTK6) is an intracellular tyrosine kinase that regulates growth and differentiation in epithelial tissues, as well as the response to DNA damage (Brauer et al. 2010). PTK6 is related to Src, but is non-myristoylated and is involved in normal epithelial homeostasis and cancer. PTK6 was originally cloned from human melanocytes (Lee et al. 1993) and soon discovered to play a role in breast cancer, receiving the name BReast tumor Kinase (BRK) (Mitchell et al. 1994). The mouse orthologue was subsequently cloned from small intestinal epithelial cell RNA, identified as a regulator of epithelial cell differentiation, and was named Src-related Intestinal Kinase (SIK) (Siyanova et al. 1994).

PTK6 belongs to a larger family of tyrosine kinases, which includes Fyn-Related Kinase (FRK) and Src-Related kinase lacking C-terminal regulatory tyrosine and N-terminal Myristylation Sites (SRMS) (Brauer et al. 2009). This family of tyrosine kinases is highly conserved and is distinct from other tyrosine kinase families, particularly the Src family (Serfas et al. 2003).

FRK (also called RAK, BSK, Iyk, and Gtk) was identified in human breast cancer, normal intestinal epithelium, kidney, liver, lung, and mammer gland (Brauer et al. 2009). FRK acts as a tumor suppressor by inhibiting cell proliferation and invasion (Yim et al. 2009). FRK phosphorylates PTEN on Tyr336, preventing PTEN degradation (Yim et al. 2009).

SRMS was identified as part of a screen for non-receptor protein tyrosine kinases in mouse embryonic neuroepithelial cells (Kohmura et al. 1994) and mouse skin

(Kawachi et al. 1994). SRMS expression is ubiquitous, but is particularly abundant in liver, lung, spleen, kidney, and testes (Kohmura et al. 1994). SRMS is known to target Dok1, a scaffolding protein which is a target of Src and may act as a tumor suppressor (Goel et al. 2013).

2.   PTK6 structure

The human PTK6 gene is found on human chromosome 20q13.3 and contains 8 exons which extend across 10 kilobases (Park et al. 1997). While PTK6 shares 44% amino acid similarity with the SRC family of protein tyrosine kinases, the *PTK6* gene only shares 2 exon boundaries (Serfas et al. 2003) with *Src*. There is at least one alternative splice transcript of PTK6, lacking exon 2. As a result, the reading frame is shifted and the final protein is truncated, containing only the amino terminus and SH3 domain of full length PTK6, in which the catalytic domain is inactive and there is a novel C-terminus. This *PTK6* transcript, known as ALT-PTK6, is expressed in human breast carcinoma cell lines (Easty et al. 1997) and in normal prostate cell lines, where it negatively regulates growth and can modulate PTK6 activity (Brauer et al. 2011).

PTK6 structurally resembles Src kinase, but lacks the N-terminal myristoylation consensus sequence, which targets Srk to the membrane. Like Src, PTK6 contains SH2 and SH3 Src Homology domains, a catalytic tyrosine kinase domain, and a C-terminal regulatory domain (Fig. 1). The SH2 and SH3 domains are involved in protein-protein interactions and substrate recognition. SH2 domain recognizes phosphorylated tyrosine residues and regulates catalytic activity (Mitchell et al. 2000, Born et al. 2005). The SH3 domain interacts with proline rich regions and is involved in

Figure 1. Structure of Src and PTK6 Tyrosine Kinases

Src is a 60-kDa protein that contains 536 amino acids. It contains Src homology domains SH2 and SH3, as well as a tyrosine kinase domain and an N-terminal SH4 domain, which contains a consensus sequence for myristoylation and palmitoylation in Src family members. Tyrosine 527 in Src regulates kinase activity. Tyrosine 416 in Src is autophosphorylated, resulting in full kinase activity. Lysine 295 in Src is in the ATP binding site and is required for catalytic activity.

PTK6 is a 48-kDa protein that contains 451 amino acids. PTK6 proteins contain Src homology domains SH2 and SH3, as well as a tyrosine kinase domain. Tyrosine 447 in PTK6 regulates kinase activity. Tyrosine 342 in PTK6 is autophosphorylated, resulting in full kinase activity. Lysine 219 in PTK6 is in the ATP binding site and is required for catalytic activity. PTK6 does not contain an N-terminal SH4 domain, and can localize to different places in the cell.

ALT-PTK6 is an alternatively spliced isoform of PTK6 that is only 15-kDa in size, has 134 amino acids, and contains an SH3 domain and a novel proline rich carboxy-terminal sequence.

Src — SH4, SH3, SH2, Catalytic (K295, Y416, Y527)

PTK6 — SH3, SH2, Catalytic (K219, Y342, Y447)

ALT-PTK6 — SH3, PR
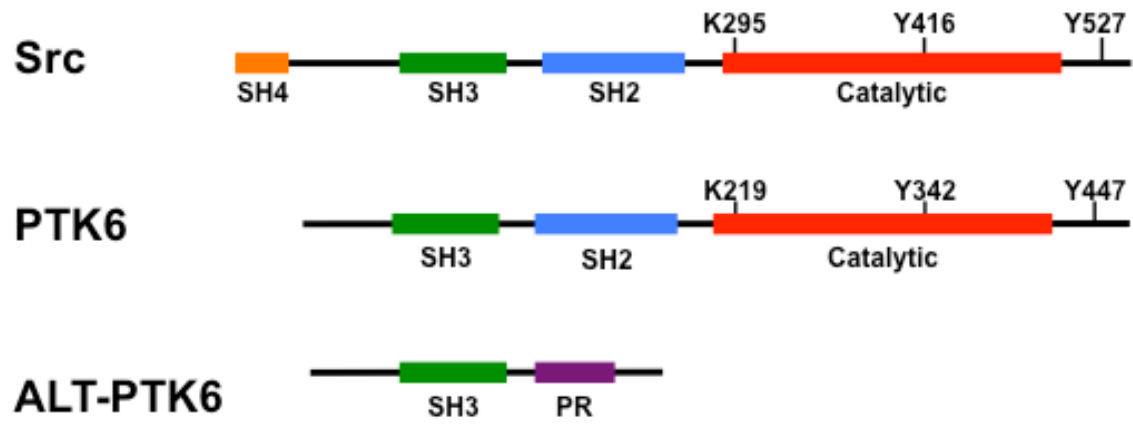
regulation of kinase activity and cellular localization, as well as playing a role in substrate interactions (Derry et al. 2000, Qiu et al. 2004, Born et al. 2005).

PTK6 is autophosphorylated at tyrosine residue 342, which causes the activation loop to disassociate from the substrate-binding site, enabling access to substrates (Qiu et al. 2002). Additionally, tyrosine residue 447 is a negative regulatory site. Phosphorylation of Y447 causes it to bind to the SH2 domain of PTK6, resulting in catalytic inactivation. The SH3 domain further stabilizes the inactive conformation by preventing ATP binding. Mutating Y447 to phenylalanine prevents this inactivation and constitutively activates PTK6 (Derry et al. 2000, Qiu et al. 2002). While CSK (C-Src tyrosine kinase) is known to phosphorylate the comparable site on Src, it is unknown which kinase performs this function for PTK6. PTK6 can be inhibited by SOCS3 (Suppressor of Cytokine Signaling 3), which interacts with the SH2 domain of PTK6, binds to the kinase domain, and inhibits catalytic activity (Gao et al. 2012). PTK6 can also be regulated by hypoxia through HIF-1α/2α (Hypoxia Induced Factors) (Regan Anderson et al. 2013).

3. PTK6 expression in skin

PTK6 is developmentally regulated and in mice it is first detected late in gestation, at embryonic day 15.5, when the skin becomes stratified into the basal proliferating cells and granular layers (Vasioukhin et al. 1995). It is later expressed in the differentiating intestine at embryonic day 18.5 (Siyanova et al. 1994, Vasioukhin et al. 1995). In adult mice, PTK6 is most highly expressed in the differentiated layers of skin, oral epithelium, and the gastrointestinal tract (Vasioukhin et al. 1995). It is also found in the nucleus of epithelial cells in the prostate (Derry et al. 2003). There is low expression

of PTK6 in normal human breast tissue (Peng et al. 2014) but it is not detected in any stage of mouse mammary gland differentiation (Llor et al. 1999, Peng et al. 2013).

PTK6 is believed to play a role in differentiation by negatively regulating proliferation and promoting epithelial cell differentiation. PTK6 is induced in embryonic mouse keratinocyte (EMK) cells following differentiation (V. Vasioukhin 1997) and is localized to differentiating cells in the suprabasal layers of the skin (Wang et al. 2005). Calcium induced differentiation of embryonic mouse keratinocytes also results in increased PTK6 activity, and overexpression of PTK6 promotes expression of the skin differentiation marker filaggrin (V. Vasioukhin 1997). In HaCaT cells, confluence induces PTK6 expression, as well as the skin differentiation marker keratin-10 (Wang et al. 2005). In squamous cell carcinomas, PTK6 expression is reduced and Y342 phosphorylated PTK6 is excluded from the nucleus (Petro et al. 2004). PTK6 expression also increases during differentiation in Caco-2 cells, a colon adenocarcinoma cell line which spontaneously polarizes in culture, suggesting that PTK6 is involved in signaling pathways which promote differentiation (Llor et al. 1999). There is also a study suggesting that in primary human keratinocytes, reduction in PTK6 expression results in a decrease in epidermal growth factor receptor (EGFR) along with an increase in keratin-10 (Tupper et al. 2011), suggesting that under certain conditions, PTK6 may depart from its typical role in differentiation and act as an oncogene.

4.   PTK6 function in normal epithelium

A *Ptk6*-null mouse model has been established in the C57BL/6 genetic background in order to study the role of PTK6 *in vivo*. Cells in the gastrointestinal tract divide in the crypt compartment and migrate into the villi, where they undergo terminal

differentiation. *Ptk6*-null mice exhibit reduced differentiation of intestinal epithelial linings (Haegebarth et al. 2006), and villus length is significantly longer than in the wild type intestine, along with an expanded proliferation zone and delayed enterocyte differentiation. There is also increased proliferation in intestinal crypt cells in *Ptk6 -/-* mice than in the wild type mice, along with greater cell turnover, proliferation, and activation of AKT throughout the intestinal epithelia (Haegebarth et al. 2006). These mice also exhibit increased levels of nuclear β-catenin, suggesting that PTK6 may also potentially play a role in regulating the Wnt pathway, which plays an important role in regulation of epithelial turnover in the skin and gastrointestinal tract. PTK6 inhibits β-catenin by directly phosphorylating it and targeting it for degradation (Palka-Hamblin et al. 2010).

PTK6 also has an impact on cell survival. In an immortalized nontransformed Rat1A cell line, expression of PTK6 sensitizes the cell to apoptotic stimuli, such as serum deprivation and UV irradiation (Haegebarth et al. 2005). Additional studies show that after gamma irradiation, PTK6 is induced in the intestinal crypt cells, promoting DNA-damaged induced apoptosis. Eliminating *Ptk6* results in an increase in the MAPK pro-survival signaling pathway and impedes apoptosis in irradiated mice (Haegebarth et al. 2009). These data suggest that PTK6 plays a role in limiting cell growth in connection with differentiation of skin and intestinal epithelia.

5.   PTK6 substrates

A.   RNA binding proteins

Many different proteins have been identified as substrates for PTK6. Among this list of substrates are RNA-binding proteins Sam68, SLM-1, SLM-2 (Sam68-like

mammalian proteins), and PSF (Polypyrimidine tract-binding protein-associated splicing factor) (Derry et al. 2000, Haegebarth et al. 2004, Lukong et al. 2005, Lukong et al. 2009). PTK6 co-localizes with Sam68 in the nucleus, where it directly phosphorylates Sam68, inhibiting its RNA-binding function. This phosphorylation results in disruption in Sam68 localization and interactions (Sellier et al. 2010). HaCaT human keratinocytes and MDA-MB-231 breast cancer cells need Sam68 expression for hepatocyte growth factor (HGF) induced migration, and in both cell lines, a phospho-mutant of Sam68 lacking ERK kinase consensus sequences inhibits HGF-induced migration (Locatelli et al. 2012). PTK6 phosphorylates SLM-1 and SLM-2 in a similar manner, negatively regulating RNA-binding activity (Haegebarth et al. 2004). PTK6 phosphorylates PSF in BT20 cells after EGF stimulation and causes PSF to relocalize from the nucleus to the cytoplasm, resulting in cell cycle arrest (Lukong et al. 2009).

B.   Transcription factors

Signal transducers and activators of transcription (STATs) are an important class of transcription factors that regulate proliferation, cell survival, angiogenesis, and the immune response (Balsas et al. 2009). There are seven members of the STAT family (STAT1, STAT2, STAT3, STAT4, STAT5a, STAT5b, and STAT6), which contain six conserved domains and are activated through phosphorylation on C-terminal tyrosine residues, which causes STAT proteins to dimerize (Turkson 2004). STATS localize to the cytoplasm when inactive, and translocate to the nucleus when activated by Janus kinases (Jaks) (Yu et al. 2004), where they promote transcription of downstream target genes (Schaefer et al. 2001).

STAT3 plays an important role in skin (Sano et al. 2008), and disrupting the *Stat3* gene impairs hair cycle progression and wound healing (Sano et al. 1999, Sano et al. 2000, Sano et al. 2005), as well as reduces tumorigenesis (Chan et al. 2004, Kim et al. 2007, Kim et al. 2009). STAT3 is phosphorylated on tyrosine residue 705, and activates numerous downstream targets that regulate proliferation, survival, angiogenesis, and the immune response (Grivennikov et al. 2010). STAT3 is activated in skin after exposure to ultraviolet B radiation (Kim et al. 2007), potential providing a mechanism for PTK6 function in skin following DNA damage. STAT3 initiates proliferation after injury and may promote replacement of damaged tissues.

There are a number of transcription factors which are substrates of PTK6, most notably STAT3 (Liu et al. 2006) and STAT5b (Weaver et al. 2007). The STAT family of transcription factors has been identified as mediators of cytokine signaling, and can be activated by growth factors like EGF and PDGF. PTK6 directly phosphorylates and activates STAT3 and STAT5b, which promotes breast cancer cell proliferation, but does not target other members of the STAT family (Liu et al. 2006). PTK6 catalytic activity is needed for STAT3 Y705 phosphorylation, and cell lacking PTK6 exhibit decreased STAT3 activation. SOCS3 inhibition of PTK6 results in impaired STAT3 signaling and inhibits breast cancer cell proliferation (Gao et al. 2012). Co-expression of PTK6 and STAT3 promote cellular proliferation. Disruption of the *Ptk6* gene in mice impairs STAT3 activation after AOM injection, and a stable knockdown of PTK6 results in reduced basal levels of phosphorylated STAT3 and impairs EGF-induced STAT3 activation in HCT116 cells (Gierut et al. 2011).

PTK6 phosphorylates STAT5b at Tyr699 *in vitro* and in breast cancer cells, resulting in increased STAT5b activity and increased cellular proliferation (Weaver et al. 2007). Additionally, PTK6 substrate signal transducing adapter protein 2 (STAP-2, also referred to as BKS) modulates STAT3 activity (Mitchell et al. 2000). STAP-2 is an adaptor protein containing pleckstrin homology (PH) and SH2 domains, in addition to a STAT3 binding domain. Knocking down STAP-2 in T47D cells causes impaired PTK6-induced activation of STAT3 and inhibits cell proliferation (Ikeda et al. 2010).

Another direct substrate of PTK6 is β-catenin, which plays an essential role in the Wnt signaling pathway. Activation of the Wnt pathway results in stabilization of β-catenin, which then accumulates in the nucleus to promote transcription (Liu et al. 2010). PTK6 phosphorylates β-catenin at multiple tyrosine residues, including Tyr64 (the primary target), Tyr142, Tyr331, and/or Tyr333 (Palka-Hamblin et al. 2010). PTK6 regulation of β-catenin transcriptional activity is dependent on PTK6 localization. Nuclear-targeted PTK6 negatively regulates endogenous β-catenin/TCF transcriptional activity, while membrane-targeted PTK6 promotes it (Palka-Hamblin et al. 2010). β-catenin is phosphorylated and degraded by PTK6, which results in inhibited cell growth.

C.   EGFR/ERB2 family

Epidermal Growth Factor Receptor (EGFR) is frequently associated with breast cancer and is part of the ERB2 family of receptor tyrosine kinases. This family includes EGFR, ErbB2 (HER2/Neu), ErbB3, and ErbB4. PTK6 interacts with ErbB1 (EGFR) and promotes EGF-induced cellular proliferation in normal mammary epithelial cells (Kamalati et al. 1996). EGFR is a substrate of PTK6, which promotes EGFR signaling by phosphorylating it on Tyr845, preventing its downregulation (Li et al. 2012). PTK6

enhances ERK1/2 activation in MCF10A cells, which overexpress ErbB2, which results in increased cellular proliferation (Xiang et al. 2008). In normal mammary epithelial cells overexpressing PTK6, EGF stimulation results in increased interation between ErbB3 and PI3K, resulting in increased ErbB3 tyrosine phosphorylation and AKT signaling (Kamalati et al. 2000). Heregulin, a ligand for ErbB3 and ErbB4, activates PTK6 and promotes activation of Erk5 and p38 MAPK in breast cancer cells (Ostrander et al. 2007). PTK6 co-precipitates with ErbB2, ErbB3, and ErbB4 in T47D human breast cancer cells (Aubele et al. 2008). PTK6 interacts with the ErbB family in order to promote survival and proliferation.

EGFR is expressed in keratinocytes in the basal layer of the skin (Gaffney et al. 2014). Keratinocytes express decreasing levels of EGFR as they progress into the suprabasal layers of the epidermis. Additionally, EGFR localizes to both the membrane and the cytoplasm in the basal layer, but only in the membrane in the spinous layer (Gaffney et al. 2014). ErbB2 can be induced by exposure to UVA, which can promote ROS formation, in both hairless mice and in HaCaT cells (Han et al. 2008). Inhibition of ErbB family receptors protects keratinocytes from UVB-induced apoptosis (Lewis et al. 2003). It is possible that lower levels of EGFR in the post-mitotic cells of the suprabasal layer reduce UVB-induced apoptosis in those cells, and that promotion of proliferation in these cells will result in apoptosis instead.

Malignant cells express 50-100 times more EGFR than normal keratinocytes (Cowley et al. 1986). Nearly all Head and Neck Squamous Cell Carcinomas overexpress EGFR, and cetuximab, an antibody which targets EGFR, is a drug which has been used to treat HNSCC in patients (Cohen 2014). Both mutations in EGFR and amplification of

EGFR have been reported in HNSCCs, which may result in constitutive signaling through spontaneous EFGR dimerization (Bose et al. 2013). However, due to the heterogeneity of HNSCCs, it is difficult to identify a consistent mechanism for EGFR-induced carcinogenesis. Further data suggests the existence of an active autocrine loop, and there are multiple phosphorylation sites in EGFR that interact with a variety of protein partners to initiate different downstream effects (Leemans et al. 2011).

D. Integrin signaling

Focal adhesion kinase (FAK) is a tyrosine kinase that associates with proteins localized within the focal adhesion contacts of normal cells (Parsons 2003). It is regulated by integrin mediated cell adhesion by activation of growth factor receptor and G-protein linked receptor signaling (Schaller 2001). FAK plays a role in multiple cellular functions, such as proliferation, survival, motility, and invasion (Schaller 2001, Schlaepfer et al. 2004). FAK can activate PI3K/AKT signaling to promote fibroblast survival (Xia et al. 2004). FAK can also form signaling complexes with Paxillin or BCAR1 and transmit survival signals to fibroblast and epithelial cells (Zouq et al. 2009). Nuclear FAK promotes cell survival by enhancing Mdm2-dependent p53 ubiquitination to promote p53 turnover (Lim et al. 2008). Overexpression of FAK positively correlates with histological grade and proliferation (Theocharis et al. 2009), and inhibition of FAK expression in mammary glands inhibits tumor formation and metastasis in mice (Provenzano et al. 2008).

PTK6 directly phosphorylates FAK, which then activates AKT (Zheng et al. 2012). Co-expression of FAK and membrane-targeted Y342 phosphorylated PTK6 enhances FAK and AKT activation and promotes cell survival in mouse embryonic

fibroblasts (MEFs). In the PC3 human prostate cell line, knocking down PTK6 inhibits FAK and AKT activation and promotes anoikis, and exogenous expression of FAK can reverse this effect (Zheng et al. 2012).

BCAR1 (Breast Cancer Anti-estrogen Resistance 1), also known as p130CAS (P130 Crk-associated substrate), is a hyperphosphorylated protein first identified in v-Crk and v-Src transformed cells (Reynolds et al. 1989, Kanner et al. 1991), and localizes to focal adhesions (Petch et al. 1995). The gene *BCAR1* was identified in a screen for genes promoting resistance to antiestrogen tamoxifen (Brinkman et al. 2000). In the course of the integrin signaling cascade, FAK and Src phosphorylate BCAR1 at multiple tyrosine residues, forming binding sites for adaptor protein Crk, promoting membrane ruffling, cytoskeletal remodeling, and cell migration (Sakai et al. 1994, Tachibana et al. 1997, Smith et al. 2008). BCAR1 is also needed for Src-induced transformation of primary fibroblasts (Honda et al. 1998), and elevated BCAR1 expression has been found to correlate with EGFR expression in metastatic prostate cancer (Fromont et al. 2007). Overexpression of BCAR1 resulted in extensive mammary epithelial hyperplasia and delayed involution (Cabodi et al. 2006). Overexpression of BCAR1 and ErbB2 in MMTV-Her2/Neu mice causes multifocal mammary tumors that exhibit significantly reduced latency (Cabodi et al. 2006), and BCAR1 expression is inversely correlated with survival in human breast cancer (Dorssers et al. 2004). BCAR1 is necessary for ErbB2-dependent foci formation and anchorage-independent growth, and inhibiting BCAR1 expression in mammary glands reduces the growth of ErbB2-induced breast tumors (Cabodi et al. 2010).

PTK6 phosphorylates BCAR1 and promotes the formation of peripheral adhesion complexes as well as cell migration (Zheng et al. 2012). Integrin signaling appears to be upstream of PTK6 activation, and the formation of peripheral adhesion complexes is dependent on PTK6 localization and kinase activity. Expression of membrane-targeted PTK6 leads to increased cell migration, which can be reversed by knocking down BCAR1 or ERK5 (Zheng et al. 2012). PTK6 can phosphorylate BCAR1 in a FAK-independent manner, and seems to interact with BCAR1 in a different manner than Src, using its SH2 domain instead of the SH3 domain.

Another factor in integrin signaling is paxillin, a signal transduction adaptor protein that localizes to the leading edges of cells after initiation of migration. Paxillin is a multidomain protein that acts as a molecular scaffold at the plasma membrane and interacts with tyrosine kinases such as Src and FAK, as well as structural proteins such as vinculin. Many of the proteins that paxillin interacts with are involved in regulating the actin cytoskeleton organization, and so phosphorylation of paxillin has important implications for cell motility and migration. PTK6 phosphorylates paxillin at Tyr31 and Tyr118 after EGF stimulation, resulting in activation of small GTPase Rac1 to promote cell migration and invasion (Chen et al. 2004).

E. Signaling factors

There are a wide variety of additional signaling molecules phosphorylated by PTK6. PTK6 phosphorylates p190RhoGAP-A to stimulate activity, resulting in RhoA inactivation and the activation of Ras, which affects PTK6-mediated migration and proliferation in breast cancer cells (Shen et al. 2008). PTK6 also phosphorylates ARAP1

on Y231, which inhibits EGFR downregulation, promoting EGF/EGFR signaling in breast cancer cells (Kang et al. 2010).

IRS-4 (Insulin receptor substrate) interacts with PTK6 in A431 human epidermoid carcinoma cells (Qiu et al. 2005). IRS-4 enhanced PTK6 tyrosine phosphorylation after IGF-1 stimulation in MCF-1 breast cancer cells, and PTK6 forms a complex with the IGF-1 receptor. IGF-1R is a substrate of PTK6 (Fan et al. 2013) and overexpressed PTK6 regulates IGF-1R in MCF-10A mammary epithelial cells to promote anchorage-independent survival (Irie et al. 2010). PTK6 phosphorylates KAP3A (Kinesin-associated protein 3A), resulting in KAP3A relocalization from the nucleus to the cytoplasm to promote migration (Lukong et al. 2008). Knocking down KAP3A in breast cancer cells impairs PTK6-induced migration (Lukong et al. 2008).

PTK6 also directly phosphorylates AKT, inhibiting AKT kinase activity and downstream signaling. EGF-stimulation causes this complex to disassociate, enabling the resumption of AKT singaling (Zhang et al. 2005). Additional data suggest that PTK6 can actually activate AKT and promote oncogenic signaling (Zheng et al. 2010), and that knocking down PTK6 in BPH-1 human prostate cells results in decreased EGF-induced AKT activation. Finally, there is evidence that PTK6 forms complexes with both MAPK and PTEN (Aubele et al. 2008). PTK6 clearly has a wide variety of interaction with many different signaling molecules in the cell.

6.   PTK6 in cancer

A considerable amount of research into the contribution of PTK6 to cancer has been done in breast tissue. PTK6 is expressed in up to 86% of human breast tumors, and is most strongly expressed in advanced tumors (Mitchell et al. 1994, Barker et al. 1997,

Lofgren et al. 2011). Recently, it has been determined that PTK6 is phosphorylated on Y342 at the membrane in in breast cancer (Peng et al. 2014). PTK6 can promote breast cancer cell proliferation and migration through a variety of mchanisms, including activation of STAT transcription factors, EGFR/ErbB receptors, and p190rhogAP-A. PTK6 regulates IGF-1-mediated anchorage-independent breast tumor cell survival (Irie et al. 2010). Using a PTK6 transgenic mouse, mammary glands that express PTK6 exhibit delayed involution, most likely due to activation of p38 MAPK pro-survival pathway (Lofgren et al. 2011). PTK6 has further been shown to promote breast cancer through Y705 phosphorylation of STAT3 (Peng et al. 2013). Overexpressing PTK6 in immortalized human breast cell line HB4a caused increased cellular proliferation and anchorage-independent growth, and this increase required PTK6 kinase activity (Kamalati et al. 1996). It also sensitizes human mammary epithelial cells to the mitogenic effects of EGF. Similarly, overexpression of PTK6 in human T47D breast tumor cells resulted in induced EGF-stimulated or serum-stimulated proliferation (Harvey et al. 2003, Ostrander et al. 2007). Knocking down PTK6 in chemo-resistant breast cancer cells sensitizes them to the EGFR-blocking antibody cetuximab (Li et al. 2012). PTK6 expression is also needed for heregulin-induced activation of p38 MAPK and ERK5 in T47D cells, which promotes cell migration (Ostrander et al. 2007). Hypoxic conditions in solid breast tumors regulate PTK6 via HIF1α/2α (Regan Anderson et al. 2013).

PTK6 is co-amplified with ErbB2 in breast cancers, and the co-expression of PTK6 with ErbB2 in non-tumorigenic MCF-10A cells caused an increase in MEK 1/2 and ERK 1/2 activity (Xiang et al. 2008). Knocking down both PTK6 and ErbB2 decreases phosphorylation of pro-survival pathways such as MAPK 1/3, ERK1/2, and

p38MAPK (Ludyga et al. 2013). ErbB2 regulates PTK6 stability by upregulating calpastatin, which inhibits calpain and calpain-1-mediated proteolysis of PTK6 (Ai et al. 2013). Overexpression of ErbB2 in MCF-7 cells results in elevated levels of PTK6 and reduced phosphorylation of Src at Y416 (Ai et al. 2013). PTK6 is activated to promote VEGF expression, tumor progression, and angiogenesis in human MDA-MB-231 cells when stimulated by osteopontin in a xenograft model (Chakraborty et al. 2008). PTK6 further promotes survival in breast cancer cells under anchorage-independent conditions by downregulating autophagy protein Beclin (Harvey et al. 2009). Knocking down PTK6 in breast cancer cell lines T47D, BT474, and JIMT-1 result in decreased phosphorylation of HER-2 and PTEN, resulting in reduced cell migration (Ludyga et al. 2011).

As in normal breast tissue, PTK6 is not expressed in normal ovarian epithelia. However, PTK6 is expressed in 70% of high grade serous ovarian carcinomas (Schmandt et al. 2006). PTK6 is expressed in nine human ovarian cancer cell lines (OVCAR5, OVCAR8, TOV21G, DOV13, 2774, OVCA420, OVCA433, HEY, and HEYC2), but is not found in immortalized ovarian epithelium. PTK6 was amplified in six primary ovarian carcinomas using fluorescence *in situ* hybridization (FISH) (Schmandt et al. 2006). Downregulation of PTK6 in ovarian cancer cells corresponds to increased sensitivity to anoikis and inhibition of IFG-1 induced anchorage independent growth, as well as an enhanced basal level of cell death (Irie et al. 2010). Furthermore, knocking down PTK6 reduced prosphorylation of IGF-1 receptor after IGF-1 stimulation, resulting in decreased downstream signaling, such as the AKT and ERK pathways.

Similarly, PTK6 expression has been found in human cutaneous T-cell lymphomas and transformed T- and B- cell populations, even though they are not

epithelial specific. PTK6 expression has been detected in normal and malignant T-cells, although not in normal human peripheral blood mononuclear cells (Kasprzycka et al. 2006). Overexpression of PTK6 in immature mouse B-cell line BaF3 results in inhibition of apoptosis and increased proliferation in the absence of serum and cytokines, and this reaction was found to be dependent on PTK6 kinase activity. Knocking down PTK6 inhibited proliferation and increased apoptosis in human malignant T-cell lines (Kasprzycka et al. 2006). These results further suggest that PTK6 may promote malignant cell transformation and promote carcinogenesis.

In normal prostate epithelial cells, PTK6 localizes to the nucleus. When prostate cancer progresses from benign hyperplasia to prostatic intraepithelial neoplasia (PIN) and becomes a high grade prostate tumor, nuclear localization is lost (Derry et al. 2003). PC3 cells are a highly aggressive and metastatic human prostate cell line in which PTK6 localizes to the cytoplasm. Knocking down endogenous cytoplasmic PTK6 results in reduced cellular proliferation and colony formation (Brauer et al. 2010). Re-expressing nuclear-targeted PTK6 results in decreased PC3 cell growth. Additionally, prostate tumors cells contain a greater full-length PTK6 to ALT-PTK6 ratio than normal prostate cells (Brauer et al. 2011). Overexpressing ALT-PTK6 in PC3 cells inhibits β-catenin target genes c-Myc and Cyclin D1, resulting in decreased proliferation and colony formation, suggesting a potential role for ALT-PTK6 (Brauer et al. 2011). These data suggest that PTK6 localization may play an important role for its function in the cell.

PTK6 plays an important role in cellular response to DNA-damage in the gastrointestinal tract. In the intestine, PTK6 is expressed in the differentiated villus cells, but not in the proliferating crypt cells (Haegebarth et al. 2006), similar to PTK6

expression in differentiated keratinocytes. PTK6 is induced in the intestinal crypt cell 6 hours after gamma-irradiation (Haegebarth et al. 2009). The intestinal epithelial linings in PTK6-null mice have an increased resistance to apoptosis (Haegebarth et al. 2009). Additionally, the MAPK pathway is more strongly activated after gamma-irradiation in *Ptk6*-null mice. Intestinal crypt cells in wild-type mice became more proliferative in response to DNA-damage than crypt cells in *Ptk6*-null mice (Haegebarth et al. 2009).

While PTK6 is normally expressed in differentiated colon epithelial cells, PTK6 is upregulated in colon cancer (Llor et al. 1999). When treated with azoxymethane (AOM), *Ptk6*-null mice exhibit increased resistance to colonic tumor formation compared with wild type mice (Gierut et al. 2011). PTK6 expression is induced in the colonic crypt cells after AOM treatment, and there is more apoptosis in *Ptk6 +/+* crypts than in *Ptk6 -/-* crypts. These mice exhibited a compensatory proliferation and STAT3 activation, and knocking out PTK6 reduced STAT3 activation after AOM treatment (Gierut et al. 2011). Stable shRNA knockdown of PTK6 impaired basal STAT3 activation in HCT116 human colon cancer cells (Gierut et al. 2012). PTK6 was further found to promote STAT3 activation in YAMC cells.

While PTK6 is found exclusively in the suprabasal layer of skin epithelial cells, primarily in the cytoplasm (Vasioukhin et al. 1995), PTK6 expression is reduced in many human skin tumors, including squamous cell carcinomas, basal cell carcinomas, and melanomas (Wang et al. 2005). This reduction in PTK6 expression is mirrored in human oral squamous cell carcinoma cell lines as well as in oral squamous cell carcinoma tissue samples (Petro et al. 2004). PTK6 was also downregulated in esophageal squamous cell carcinoma (Ma et al. 2012). PTK6 localization is also affected, where PTK6 is localized

to both nuclear and cytoplasmic fractions in normal oral epithelial cells, while PTK6 was perinuclear in oral carcinoma cell lines. This re-localization was confirmed using subcellular fractionation, immunoblot analysis, and immunofluorescence (Petro et al. 2004).

7.   Skin development

The skin is largest organ in the human body and plays an important protective role by providing a renewable barrier against disease and injury. One of the most common forms of injury is ultraviolet radiation found in natural sunlight, which causes DNA damage and can initiate carcinogenesis. The epidermal skin layer consists of proliferative basal cell layer at the bottom, resting on the basement membrane above the dermis (Figure 3). Basal cells are set in an infrastructure of intermediate filaments called keratins, specifically keratin-5 and keratin-14 (Fuchs et al. 2008). This cellular infrastructure maintains cell anchorage and cell polarity. As keratinocytes exit the cell cycle, they migrate towards the surface of the skin, entering the spinous and granular layers where they differentiate into mature keratinocytes. As they differentiate and move into the suprabasal layer, they cease production of keratin-5 and keratin-14 and produce keratin-1 and keratin-10. This "keratin switch" is transcriptionally controlled and is an indicator of cell which have exited the cell cycle (Fuchs et al. 2008). During this transition from the granular layer to the corneal layer, an increase in intracellular calcium activates transglutaminases, which promote crosslinking of different structural proteins to form the cornified envelope (Lippens et al. 2009).

Figure 2: Architecture of the skin

Human epidermal skin consists of multiple stratified layers of keratinocytes. Above the dermis is the basement membrane consisting of structural laminins and proteoglycans. The basal cell layer sits on the basement layer. Cells migrate into the spinous layer and differentiate. The cells then undergo programmed cell death and expel their cellular contents in the granular layer. The corneal layer consists of the remaining keratin filaments and cellular structure as a barrier to the outside environment.

Ca²⁺

Corneal layer

Granular layer

Spinous layer

Basal layer
Basement membrane
Dermis
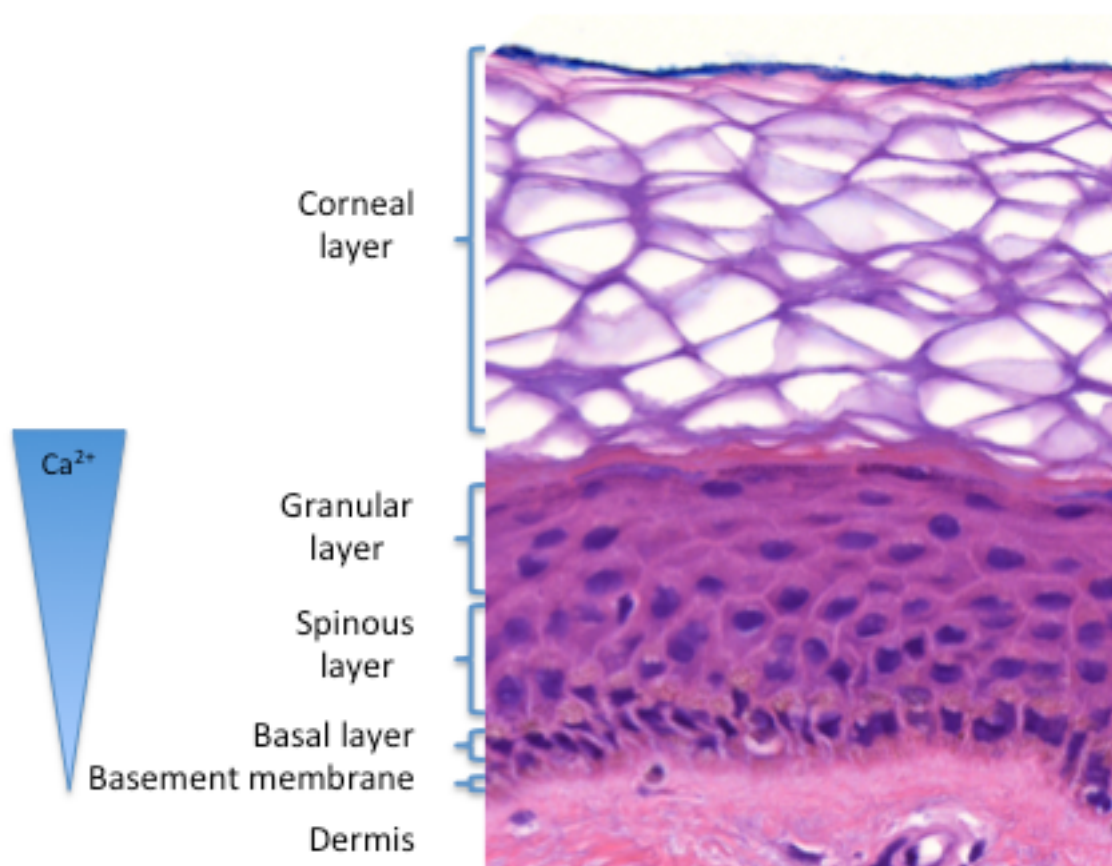
As keratinocytes reach the upper layers of the suprabasal layer, they undergo a process of organized cell death that is similar to apoptosis, and they eventually eject their cellular contents and enter the corneal layer, leaving a mass of keratinous filaments at the surface of the skin. There are several skin-specific proteases involved in programmed cell death, and the proteases responsible for apoptosis are not typically involved in this process of cell death (Lippens et al. 2009). The dead cells act as a barrier to protect the basal epidermis from environmental injury. While this barrier prevents UVB from penetrating the body, the skin itself is still exposed to DNA damage, which can lead to squamous cell carcinomas and even malignant melanoma.

8. UVB-induced DNA damage

Skin cancer is the most common form of cancer in the United States, as it is difficult to limit exposure to ultraviolet radiation. Control over proliferation and differentiation of keratinocytes is essential for proper maintenance of skin and prevention of cancer. There are three main types of skin cancer: basal cell carcinoma, squamous cell carcinoma, and melanoma. While basal and squamous cell carcinomas are not generally fatal, they can still damage the skin and result in scarring. Melanomas are often malignant and can be dangerous, even resulting in death. Most skin cancers are caused by UV radiation, usually from natural sunlight, but also through tanning beds and sunlamps. Our goal is to better understand the role of PTK6 in UVB-induced skin cancer.

UVB promotes carcinogenesis though DNA damage. High-energy UVB rays interfere with genomic integrity by causing misincorporation of bases in DNA replication, deamination of bases, oxidative damage, and alkylating agents which then modify bases of DNA (Rastogi et al. 2010). While this can result in a wide variety of

DNA injury, such as double stranded breaks (DSB) and generation of reactive oxygen species (ROS), the most common form of injury is generation of DNA lesions such as pyrimidine dimers. These injuries promote DNA damage response pathways, such as nucleotide excision repair (NER) and mismatch repair (MMR) (Rastogi et al. 2010). If these injuries to DNA structure become too severe, cells can induce apoptosis to prevent becoming cancerous. Mutations that negatively affect pro-apoptotic pathways or promote pro-survival pathways can result in cancer.

In addition to DNA damage pathways, there are other intracellular signaling pathways that are responsive to UVB, including growth factor receptors belonging to receptor tyrosine kinase families. These families include Epidermal Growth Factor Receptor (EGFR), Keratinocyte Growth Factor Receptor (KGFR), and Insulin-like Growth Factor Receptor-1 (IGF-1R) (Van Laethem et al. 2009). EGFR is one of the more significant of the receptor tyrosine kinases, although downstream signaling pathways are still being investigated (Rho et al. 2011). UVB and also act through ROS to promote activation of the MAPK pathway (Van Laethem et al. 2009). These pathways can interact with IGF-1R, and p38 MAPK may be important for these interactions (Lippens et al. 2009, Van Laethem et al. 2009, Rho et al. 2011). The PI3K-AKT pathway has been found to be deregulated in skin lesions, and keratinocytes that overexpress AKT show increased proliferation and decreased apoptosis (Rho et al. 2011). Additionally, the ERK1/2 pathway, which controls cell growth and proliferation, has also been implicated in skin tumorigenesis (Lippens et al. 2009).

STAT3 is an important downstream signaling molecule for skin carcinogenesis. Phosphorylated STAT3 dimerizes and translocates to the nucleus to regulate

proliferation, survival, angiogenesis, invasion, and metastasis. STAT3 promotes transcription of anti-apoptotic genes and pro-proliferation genes. Deletion of *Stat3* results in impaired wound healing and *Stat3*-deficient mice are resistant to both two-stage carcinogenesis and UVB-induced carcinogenesis (Rho et al. 2011). STAT3 promotion of proliferation as part of wound healing and increasing the skin barrier to UVB may play an important role in skin oncogenesis.

9.   Hypothesis

Previous data suggest that PTK6 can perform two different roles under different circumstances. In normal epithelial cells, PTK6 promotes differentiation and inhibits proliferation. Under conditions of DNA damage, PTK6 can promote apoptosis (Haegebarth et al. 2009, Gierut et al. 2011) but also functions as an oncogene and can promote carcinogenesis and tumor formation (Gierut et al. 2011). The goal of this thesis work is to better understand the role of PTK6 in both normal skin homeostasis and in skin cancer. My hypothesis is that PTK6 will maintain both a role in skin epithelium, promoting differentiation in normal skin and carcinogenesis/tumor formation in mouse skin after UVB treatment.

II. MATERIALS AND METHODS

1.   Experimental Mice

SENCAR (SENsitive to CARcinogenesis) mice are particularly sensitive to skin tumor formation. SENCAR mice were not genetically engineered, but were generated by crossing Charles River CD1 mice with skin tumor-sensitive mice (STS). These mice were then selected for over 8 generations for increased skin tumor multiplicity as well as decreased tumor latency. These mice have been tested for sensitivity for DMBA/TPA-induced carcinogenesis as well as UVB-induced carcinogenesis. SENCAR mice are less resistant to forming tumors than C57BL/6 mice and are commonly used in cancer research (Strickland 1982, Nesnow et al. 1986, Slaga 1986, Slaga et al. 1986, Strickland 1986, Strickland 1986, Strickland 1986, Imamoto et al. 1993, Lynch et al. 2007). Our lab has previously characterized a *Ptk6*-null mouse model (B6.129SV-*Ptk6*^{tm1Aty}) in C57BL/6 mice (Haegebarth 2006). These mice were crossed with SENCAR mice and backcrossed for 10 generations to generate a SENCAR *Ptk6-/-* mouse model.

2.   UVB Treatment

The backs 8 week-old male adult mice were shaved 24 hours prior to each UVB treatment. SENCAR mice were irradiated using an FB-UVXL-1000 UV crosslinker (Spectroline) fitted with 5 UVB bulbs at the top of the crosslinker for dorsal exposure only. The UVB bulbs were positioned 8 inches above animals allowing for dorsal exposure only. The mice were not restrained during UVB treatment in order to reduce physical and psychological stress, and moved freely around in the crosslinker. Mice were shaved the day prior to UVB treatment. The mice were then exposed to the appropriate dosage of UVB, which consisted of turning on the UVB lamps for a set period of time.

Short-term UVB treatments consisted of five doses of 220 mJ/cm^2 UVB five times over the course of 10 days. Neonatal mice were irradiated with a single dose of 220 mJ/cm^2 UVB. The mice were injected intraperitoneally with BrdU (100 μg/g body weight) in PBS 2 hours before sacrifice to measure proliferation. Mice were sacrificed by CO_2 anesthesia followed by cervical dislocation.

3.   Incrementally graded UVB

For the incrementally graded UVB treatments, the dorsal epidermis was exposed to 220 mJ/cm^2 UVB irradiation three times per week for weeks 1-6, 260 mJ/cm^2 UVB for weeks 7-8, 300 mJ/cm^2 UVB for weeks 9-10, 360 mJ/cm^2 UVB for weeks 11-12, 405 mJ/cm^2 UVB for weeks 13-14 and 450 mJ/cm^2 UVB for weeks 15-30. To achieve 220-450 mJ/cm^2 UVB irradiation mice were irradiated for 3-6.5 minutes. UVB irradiation was stopped at 31 weeks and mice were kept without further treatment for 43 weeks. The mice were sacrificed after 43 weeks and their skin harvested. Control animals were not exposed to UVB.

Mice were photographed and weighed prior to each UVR treatment. During the course of the incrementally graded UVB protocol mice were visually monitored for changes in skin condition after UVB exposure so that any effects of irradiation that might interfere with an animal's ability to ambulate, eat, drink, urinate and defecate would be detected and those animals would be euthanized. Mice were also euthanized if the combined tumor load exceeded 2 cm in diameter. Mice were also monitored for tumor ulceration, lethargy and discomfort in conformation with animal welfare protocols. The mice were weighed every week to observe changes in weight over time. Mice were also

sacrificed if they experience a 15% weight gain or 20% weight loss compared to their baseline weight or compared to age animals.

4.   Cell Culture

The human HaCaT cell culture line was cultured in Dulbecco's modified Eagle medium (DMEM) containing 10% fetal bovine serum. The HaCaT cells were provided by Dr. Luisa DiPietro (University of Illinois at Chicago, Chicago, IL). HaCaT cells were maintained at subconfluent levels to prevent differentiation and maintain a basal phenotype. The cells were grown to 80% of confluence, washed in PBS, trypsinized, and then passaged at a ratio of 1:10. Cells were typically passaged twice a week. The human embryonic kidney cell line 293 (HEK-293) (ATCC CRL-1573) was used to generate lentivirus for transfection of HaCaT cells. HEK-293 cells were grown and passaged under similar conditions as HaCaT cells.

5.   PTK6 knockdown and UVB treatment

We used lentivirus expressing TCRN0000021549 (shRNA 49), TCRN0000021552 (shRNA 49), and a scramble control vector to knock down PTK6 expression in HaCaT cells. Pre-designed Mission TCR shRNA in the PLKO-1 lentiviral expression vectors were purchased from Sigma Aldrich. For lentivirus production, PLKO-1 vector was cotransfected with compatible packaging plasmids HIV-trans and VSVG in HEK-293FT packaging cell line. Fresh DMEM was changed 24 hours after transfection, and lentivirus was collected 48 hours and 72 hours after transfection.

HaCaT cells were infected by lentivirus in growth media containing 5ug/ml polybrene at a multiplicity of infection (MOI) of 500 for 24 hours. Stable cell lines were selected in complete growth media containing 1μg/ml puromycin for a week.

HaCaT cells were plated at 1×10^6 cells/plate on a 10 cm dish the day before treatment. Cells were serum starved for 48 hours and then treated with 25 mJ/cm^2 of UVB and harvested 10 minutes, 30 minutes, and 60 minutes after UVB treatment.

6.   Antibodies

Anti-human PTK6 (G6), anti-mouse PTK6 (C17), FAK (C20), and Cytokeratin-14 were purchased from Santa Cruz Biotechnology (Santa Cruz, CA). Antibodies against STAT3, P-STAT3 (Tyr705), P-FAK (Tyr576/Tyr577), P-FAK (Tyr925), P-BCAR1 (Tyr165), ERK5, P-ERK5 (Thr218/Tyr220), ERK1/2, P-ERK1/2 (Thr202/Tyr204), AKT, P-AKT (Thr308), P-AKT (Ser473), cleaved caspase-3 (Asp175) and GAPDH (14C10) were purchased from Cell Signaling Technology (Danvers, MA). The anti-BCAR1 and anti-β-catenin antibodies came from BD Pharmingen. The anti-P-PTK6 (Tyr342) antibody came from Millipore. Anti-cytokeratin-10 and anti-ki67 antibodies were purchased from Abcam (Cambridge, MA). For secondary antibodies, Donkey anti-rabbit and sheep anti-mouse antibodies conjugated to horseradish peroxidase were used as secondary antibodies in Western blots (Amersham Biosciences) and were detected by chemiluminescence using SuperSignal West Dura extended duration substrate from Pierce (Rockford, IL).

7.   Immunoblot analysis

Skin tissue was harvested and homogenized using a plolydron dispersing and mixing device in 1% Triton X-100 lysis buffer (1% Triton X-100, 20 mM HEPES, pH 7.4, 150 mM NaCl, 1 mM EDTA, 1 mM EGTA, 10 mM sodium pyrophosphate, 100 mM NaF, 5 mM iodoacetic acid, 0.2 mM phenylmethylsulfonyl fluoride (PMSF), protease inhibitor mixture (Roche Applied Science). The samples were incubated in this

lysis buffer for 30 minutes at 4°C, after which the samples were pelleted at maximum speed for 30 minutes and the supernatants removed to a new Eppendorf tube. Protein concentration was determined using Bradford reagent (Bio-Rad) and the Bio Mate 3 spectrophotometer (Thermo Spectronic) and stored at -80°C.

Fresh growth medium was added to cells 24 hours before harvesting. Cells are placed on ice, the medium is aspirated, and the cells are washed in PBS and then lysed in lysis buffer. Cell lysates are collected in a 1.5 mL Eppendorf tube, incubated in an end-over-end rotor at 4°C for 30 minutes, pelleted at maximum speed for 10 minutes at 4°C, and then the supernatant is transferred to a new Eppendorf tube. The protein lysates are then quantified and stored at -80°C.

For protein analysis, equivalent lysate concentrations were placed in 5X Laemmli buffer (200mM Tris-Hcl pH 6.8, 10% Sodium dodecyl sulfate, 20% Glycerol, 0.05% Bromophenol blue, 10% β-mercaptoethanol in water). Protein samples were then separated by SDS-PAGE and transferred onto Immobilon-P PVDF (Millipore) membranes in cold transfer buffer (3 g/L Tris, 14.4 g/L Glycine, 20% Methanol) for 90 minutes at 4°C. Membranes are stained in Ponceau reagent (0.5% Ponceau S, 1% Glacial acetic acid) to visualize total protein, and then destained in 1% Glacial acetic acid and washed in TBST (150mM NaCl, 10mM Tris pH 7.5, 0.1% Tween20).

The membranes were blocked in 5% milk/TBST for 1 hour at room temperature or overnight at 4°C. Primary antibodies were diluted in 5% milk/TBST and incubated for 1 hour at room temperature. Cell Signaling antibodies were incubated overnight at 4°C. Secondary horseradish peroxidase–conjugated antibodies were diluted 1:5,000 in milk

and were added to blots for one hour at room temperature. Protein bands were visualized using SuperSignal West Dura chemiluminescence and exposed to X-ray film.

8.   Immunohistochemistry and immunofluorescence

Skin tissue was harvested and fixed in 10% neutral-buffered formalin, embedded in paraffin blocks, and cut into 5 mm sections. The slides were deparaffinized in xylene and rehydrated by sequential passage through decreasing ethanol solutions. These slides were stained with hematoxylin and eosin to analyze the histology.

For immunofluorescence microscopy, the slides were deparaffinized by xylenes, dehydrated with ethanol, and rehydrated in PBS. Antigen retrieval was performed by incubation in 0.01 M citrate buffer (pH 6.0) at 75°C for 20 minutes. To quench endogenous peroxidase activity, the slides were incubated with 3% H_2O_2 in methanol for 10 minutes. Samples were then blocked in goat and horse serum in TNT (0.1M Tris-Hcl pH 7.5, 0.15M NaCl, 0.05% Tween20) for 1 hour at room temperature. The primary antibody was diluted 1:100 in blocking buffer and incubated overnight at 4°C. The slides were then washed in TNT, followed by the secondary incubation with biotinylated anti-rabbit or anti-mouse secondary antibodies at room temperature for 30 minutes. Immunohistochemistry was performed using the Vectastain ABC Kit (Vector Laboratories) according to the manufacturer's protocols. Reactions were visualized with 3,3'-diaminobenzidine (DAB) and counterstained with hematoxylin. For immunofluorescence, sections were stained with fluorescein isothiocyanate (FITC)-conjugated avidin (Vector Laboratories, Burlingame, CA). For double staining, FITC-conjugated anti-mouse secondary antibodies (Sigma-Aldrich) were used to detect primary antibodies made in mouse (green), and biotinylated anti-rabbit secondary antibodies

(Vector Laboratories) were used and then incubated with AlexaFluor594-conjugated avidin (Life Technologies) to detect primary antibodies made in rabbit (red). Slides were mounted in Vectashield fluorescent mounting medium containing 4',6-diamidino-2-phenylindole (DAPI) (Vector Laboratories). The skin was then viewed using standard UV, rhodamine, or FITC filters under 20x and 40x differential interference contrast objectives using a Zeiss LSM 5 PASCAL confocal microscope. Images were taken using an Axiocam HRc color digital camera and LSM 5 PASCAL software (Zeiss, Jena, Germany).

9. Statistics

A dataset containing 41 head an neck squamous cell carcinoma samples were extracted from the Oncomine database (Ginos Head-Neck Dataset (Ginos et al. 2004)) The sample data included information on type, differentiation, lymph node status, stage, N stage, T stage, perineural invasion, and primary/recurrent. Patients were classified according to their N stage status (0-3), which describes whether the cancer has been found in the lymph nodes. A low N stage value indicates few tumors present in the lymph nodes, while a high N stage value indicates many tumors found in the lymph nodes. For all statistical studies studies, p-values were determined using a two-tailed Student's t-test (Microsoft Excel 2011).

<center>**III. RESULTS**</center>

1.   PTK6 expression is upregulated following UVB irradiation

A.   PTK6 expression in SENCAR mice

PTK6 localizes to the suprabasal layers of the skin (Vasioukhin et al. 1995).

However, since adult mouse skin is very thin, only a single cell layer thick, PTK6

localization is not clearly apparent. Neonatal mice were used to study PTK6 localization

in skin because neonatal skin is much thicker than adult skin and the differentiated layer

is easily distinguishable from the basal layer. We decided to use SENCAR (SENsitive to

CARcinogenesis) mice because they are prone to forming skin tumors when exposed to

DNA damage. However early immunohistochemical stains for PTK6 did not reveal a

clear suprabasal PTK6 localization pattern in SENCAR skin. Using immunoblotting to

compare PTK6 expression in SENCAR and C57BL/6 mouse skin, I found that PTK6 is

much more strongly expressed in the tumor sensitive SENCAR mice than in the tumor

resistant C57BL/6 mice (Figure 3A), and quantification revealed this difference to be

significant (p-value = 0.005) (Figure 3B). A comparison of PTK6 localization in the

different mouse backgrounds revealed that while PTK6 is largely confined to the

differentiated squamous layer of the skin in C57BL/6 mice, there is a more diffuse

localization in SENCAR mice, although PTK6 is less concentrated in the basal layer

(Figure 3C). C57BL/6 skin contained more Y342 phosphorylated PTK6 than SENCAR

skin (Figure 3D). It is striking that Y342 phosphorylated PTK6 is primarily present in the

basal layer of C57BL/6 skin, where there is minimal expression of PTK6 protein. It is

also possible that the elevated expression of PTK6 in SENCAR mice corresponds with

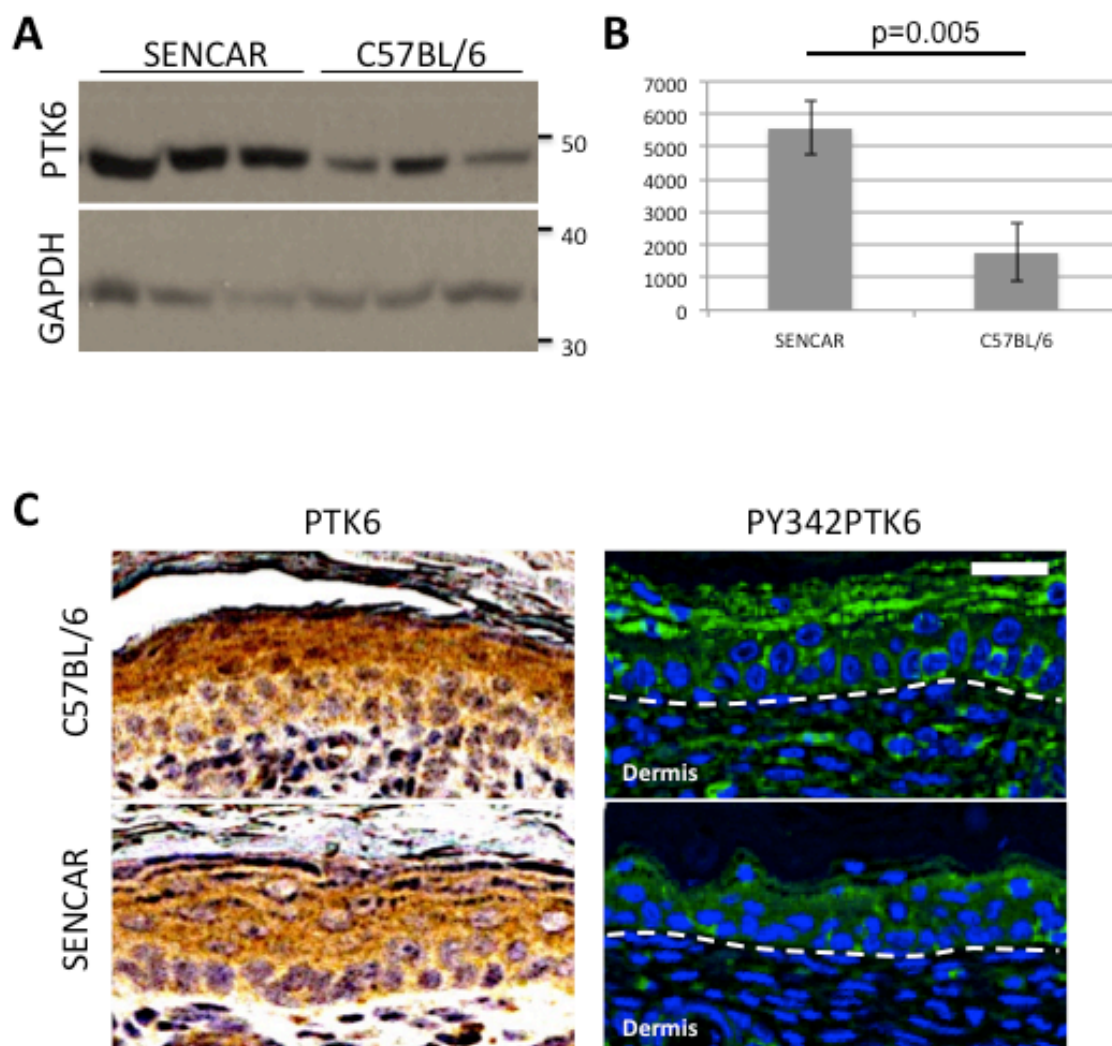the increased sensitivity of SENCAR mice carcinogenesis.

<center>33</center>

Figure 3: PTK6 Expression in SENCAR and C57BL/6 mice

A: Lysates of neonatal (4 days old) mouse skin were prepared and analyzed via immunoblot analysis. The membrane was incubated with antibodies against PTK6, which revealed stronger PTK6 expression in SENCAR pups than in C57BL/6 pups. GAPDH was used as a loading control.
B: Relative strength of luminescent signal was measured using a program called ImageJ. Intensity of PTK6 was normalized to intensity of GAPDH loading control and averaged across all samples. p-value = 0.005
C: Immunohistochemistry of total PTK6 expression in neonatal mice reveals differential staining pattern in SENCAR and C57BL/6 skin. Immunofluorescence shows that there is more phosphorylated PTK6 present in C57BL/6 neonatal skin than in SENCAR neonatal skin.
Size bar = 20 μm

A SENCAR C57BL/6

PTK6

GAPDH

50

40

30

B p=0.005

7000
6000
5000
4000
3000
2000
1000
0

SENCAR   C57BL/6

C PTK6   PY342PTK6

C57BL/6

SENCAR

Dermis

Dermis

B.   PTK6 expression and activation following exposure to UVB

While prior studies have shown PTK6 to be upregulated in response to different forms of DNA damage, such as gamma-irradiation (Haegebarth et al. 2009) or azoxymethane (AOM) treatment (Gierut et al. 2012), there were no studies on PTK6 expression following UVB irradiation. In order to observe the effect of UVB-induced DNA damage, I treated SENCAR *Ptk6+/+* mice with five doses of 220 mJ/cm^2 UVB over 10 days. During this period the mice experience erythema on the lower dorsal skin, but otherwise did not display any symptoms. After this short-term UVB treatment, PTK6 was found to be upregulated compared to untreated mice (Figure 4A). When quantified, the increase in PTK6 expression was found to be significant (p-value = 0.025) (Figure 4B). Immunofluorescence imaging revealed hyperplasia in UVB treated mouse skin, in which PTK6 was found throughout the skin, but was more concentrated in the suprabasal layer (Figure 4C). PTK6 also becomes phosphorylated at tyrosine residue 342 in UVB-treated skin, and Y342 phosphorylated PTK6 localizes primarily to the basal layer of the skin (Figure 4C). Phosphorylation of tyrosine 342 is required for full activation of PTK6and is used as a marker for active PTK6 (Lofgren et al. 2011, Peng et al. 2013). The antibody against Y342 phosphorylated PTK6 was tested against *Ptk6-/-* UVB-treated skin and no signal was detected indicating that the signal in *Ptk6+/+* skin is reliable (Figure 4C).

To further examine the contribution of PTK6 to tumorigenesis, I utilized an incrementally graded UVB tumorigenesis protocol. Wild-type mice were irradiated three times a week for 30 weeks with gradually increasing doses of irradiation. UVB is a relatively weak form of radiation and does not penetrate very far into tissues. The skins

Figure 4: PTK6 expression after UVB

A: Lysates of adult (8-weeks old) mouse skin after short-term UVB were prepared and analyzed via immunoblot analysis. The membrane was incubated with antibodies against PTK6, which revealed stronger PTK6 expression after UVB compared with the untreated group. GAPDH was used as a loading control.

B: Relative strength of luminescent signal was measured using a program called ImageJ. Intensity of PTK6 was normalized to intensity of GAPDH loading control and averaged across all samples. p-value = 0.025

C: Immunofluorescence of total PTK6 in untreated **(a)** and UVB-treated **(c)** skin, as well as Y342 phosphorylated PTK6 in untreated **(b)** and UVB-treated **(d)** skin. UVB-treated *Ptk6*-/- skin was incubated with the antibody against Y342 phosphorylated PTK6 **(e)** to verify specificity of the antibody against Y342 phosphorylated PTK6. Size bar = 20 μm

D: *Ptk6+/+* mouse tumors were incubated with total PTK6 **(a,d)** and phosphorylated PTK6 **(b,e)**. H&E stains were provided to examine morphology **(c,f)**. In hyperplastic skin **(a-c)**, PTK6 is expressed in all layers of the skin, and is Y342 phosphorylated at the membrane in all of these layers. In infiltrative dermis **(d-f)**, PTK6 is found in individual non-adhering cells and is Y342 phosphorylated in the cytoplasm.
Size bar = 20 μm
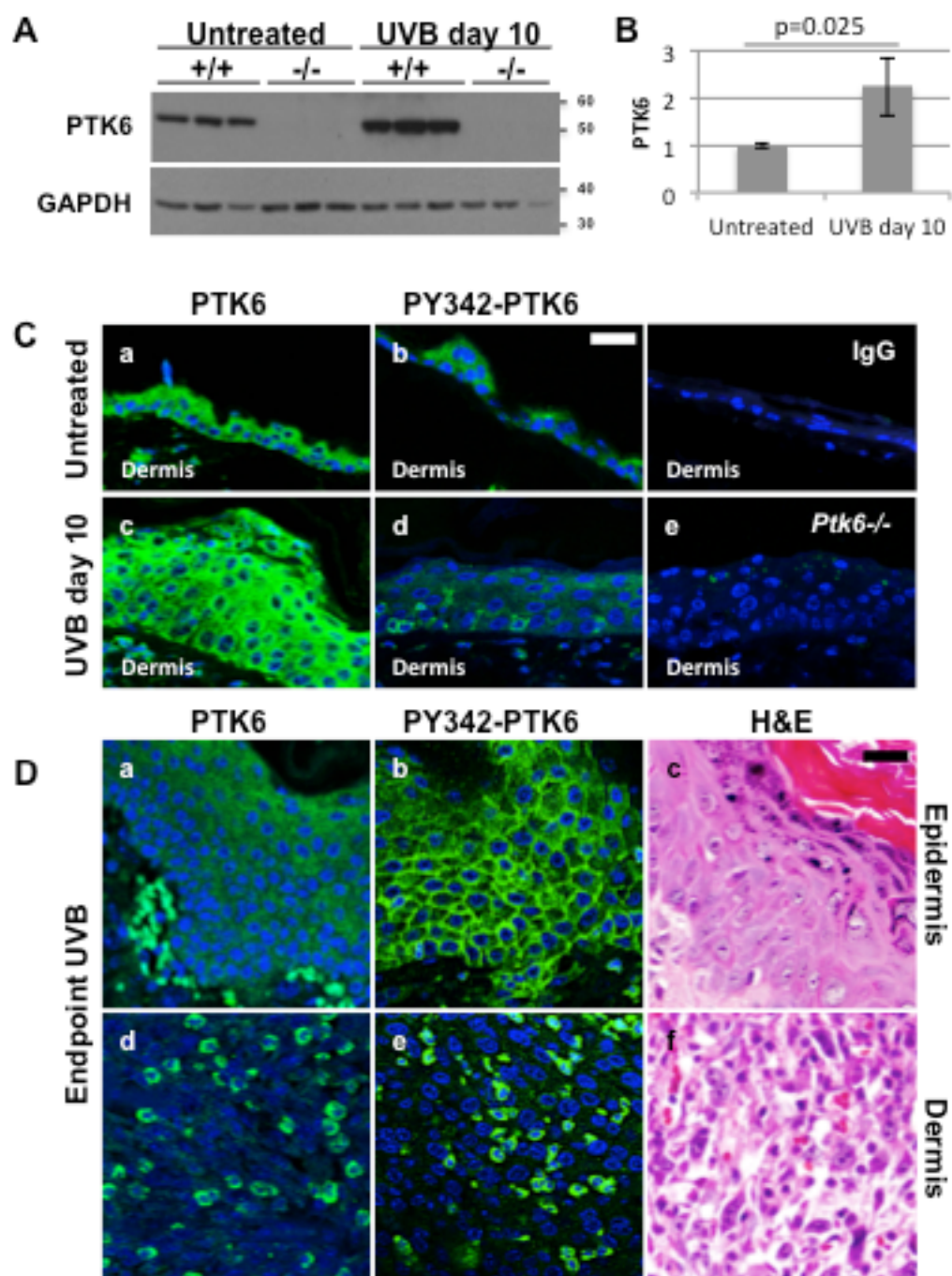
main barrier functions limits the impact of UVB. After irradiation, the skin becomes hyperplastic, increasing in thickness to prevent further damage. Increasing the dosage of UVB serves to overcome the skins adaptations against additional DNA damage. At the conclusion of UVB treatments, the mice were given a 13-week latency period for further tumor formation. We then examined skin tumors taken from these endpoint wild-type mice. In these skin tumors, we found considerable hyperplasia, as well as necroulcerative dermatitis and actinic keratosis. There were ulcerated infliltrative dermal-subcutaneous masses composed of spindle-shaped cells arranged in palisading interwoven bundles and sheets, which was highly cellular and a small amount of interspersed stromal collagen. These tumors were further observed to have a high rate of mitosis. These skin tumors were examined both in the hyperplastic epithelium and in infiltrative regions of the dermis for PTK6 expression and Y342 phosphorylation. PTK6 localizes to the cytoplasm of the epithelial cells in nucleated cell layers (Figure 4D) and Y342 phosphorylated PTK6 localizes to the membrane in all layers of the epidermis (Figure 4D). In the dermis, I examined an anaplasmic spindle cell squamous cell carcinoma. I observed multifocal cytoplasmic staining of both total PTK6 and phosphorylated PTK6 in individual, non-adhering cells (Figure 4D). There is no noticeable difference between the staining patters of total and phosphorylated PTK6. Phosphorylated PTK6 appears to be evenly distributed throughout the cells and is not concentrated at the membrane. In severe anaplasia, there is a notable lack of normal proteins/enzymes in the cell. The cells in the anaplastic spindle cell tumor lack the ability to adhere to each other, potentially due to the lack of desmosomes or tonofilaments.
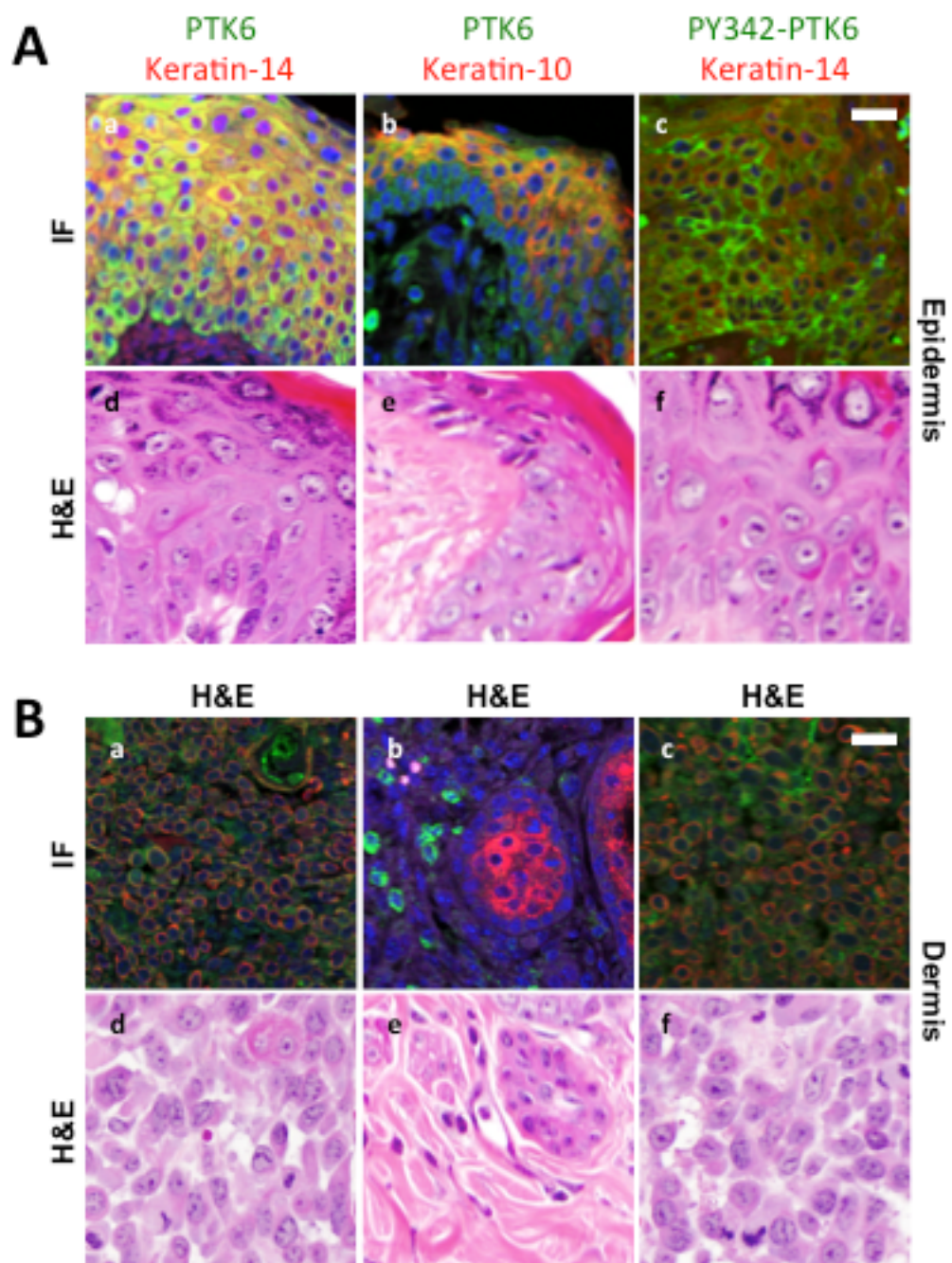
C.   Origin of PTK6 expressing cells

PTK6 expression is typically confined to epithelial cells and is not expressed in the dermis (Vasioukhin et al. 1995, Wang et al. 2005). It was therefore necessary to determine whether the infiltrative cells found in the dermis (Figure 4D) were epithelial-derived or whether this was an effect of UVB on the dermis. Epithelial skin cells typically express various types of keratin filaments, which distinguish it from the dermis (Fuchs et al. 2008). Keratin-14 specifically stains the mitotically active basal cell layer, while keratin-10 stains the differentiated suprabasal layer. We stained sections of the wild-type tumors to analyze the origins of PTK6-expressing Spindle Cell Tumors (SCT). We found that in hyperplastic skin, there is a diffuse pattern of PTK6 and keratin-14 expression in all layers of the skin (Figure 5A). While keratin-14 is normally limited to the basal layer of the epithelium, it expands into suprabasal layer in hyperplastic skin after UVB. There is a similar diffuse pattern of PTK6 and keratin-10 expression (Figure 5A), with expression of keratin-10 in cells of the suprabasal layer, but not in the basal layer. Phosphorylated PTK6 localizes to the membrane in all layers of the epithelium and co-localize with keratin-14 (Figure 5A). In anaplastic squamous cell carcinoma cells, there is multifocal expression of total PTK6 with keratin-14, confirming the epithelial origin of those cells (Figure 5B). In the dermis, PTK6 does not co-express with keratin-10, and instead we see that keratin-10 is expressed as part of a keratin pearl while PTK6 is expressed in the well-differentiated non-keratinized basal cells adjacent to it (Figure 5B). Phosphorylated PTK6 staining was similar to that of total PTK6, with multifocal expression of phosphorylated PTK6 with keratin-14 in anaplastic squamous cell carcinoma cells (Figure 5B). As noted earlier, in severe anaplasia there is a reduction in

Figure 5: PTK6-expressing cells are of epithelial origin

A: PTK6 (green) colocalizes with basal epithelial marker keratin-14 (red) throughout the hyperplastic epidermis **(a)**. PTK6 (green) colocalizes with differentiated epithelial marker keratin-10 (red) in the suprabasal layer of the hyperplastic epidermis **(b)**, but not the basal layer, suggesting a PTK6 expression correlates specifically with basal epithelial cells rather than squamous epithelial cells. Phosphorylated PTK6 (green) colocalizes with basal epithelial marker keratin-14 (red) in the hyperplastic epidermis **(c)**, showing that PTK6 is active in basal epithelial cells.
B: PTK6 (green) colocalizes with basal epithelial marker keratin-14 (red) in the infiltrative dermis **(a)**, suggesting an epithelial origin for PTK6-expressing infiltrative cells. PTK6 (green) does not colocalize with differentiated epithelial marker keratin-10 (red) in the infiltrative dermis **(b)**, indicating that invading non-adhering cells expressing PTK6 originate from the basal layer and not the squamous layer. Phosphorylated PTK6 (green) colocalizes with basal epithelial marker keratin-14 (red) in the infiltrative dermis **(c)**, suggesting that PTK6 activity plays a role in epithelial invasion into the dermis.
Size bar = 20 μm

A

PTK6 / Keratin-14   PTK6 / Keratin-10   PY342-PTK6 / Keratin-14

IF

H&E

Epidermis

B

H&E   H&E   H&E

IF

H&E

Dermis

protein/enzyme expression, resulting in a weaker signal in the keratin-14 expressing anaplastic squamous cell carcinoma cells compared with the keratin-10 expressing well-differentiated squamous cell carcinoma cells.

2.   PTK6 promotes UVB-induced tumorigenesis

A.   Background

The *Ptk6-/-* mouse model has been a powerful tool in understanding the role of PTK6 in maintaining homeostasis in epithelial tissues and regulating response to DNA damage. Disrupting the *Ptk6* frame eliminates endogenous PTK6, potentially altering the structural architecture in epithelial linings. In *Ptk6-/-* C57BL/6 mice, the intestine exhibits impaired differentiation and extended villus length (Haegebarth et al. 2006), and have impaired apoptosis following gamma-irradiation (Haegebarth et al. 2009). Additionally, disrupting *Ptk6* in the colon inhibits tumor formation after AOM treatment (Gierut et al. 2011). No studies have been done on the *Ptk6-/-* genotype in SENCAR mice to determine if there are similar morphological differences, or if disrupting *Ptk6* might protect against skin tumorigenesis. Since SENCAR mice have higher expression of PTK6 in the skin, which may contribute to the increased sensitivity of SENCAR mice to carcinogenesis, we hypothesized that PTK6 would have a similar effect of promoting tumorigenesis in DNA-damaged skin.

B.   *Ptk6-/-* mice are more resistant to UVB-induced injury

Both *Ptk6+/+* and *Ptk6-/-* mice were treated with the incrementally graded UVB tumorigenesis protocol, in which incrementally increasing doses of UVB were administered three times each week. *Ptk6+/+* mouse skin developed erythema on the lower dorsal skin, and this erythema developed into inflammatory lesions within the first two weeks of treatment (Figure 6). This inflammatory reaction fades as the skin becomes hyperplasic and adapts to the stress of UVB. This lesion began to heal by the third week and was completely healed after four weeks. In contrast, *Ptk6-/-* mice only developed a

Figure 6: *Ptk6*-/- mice are more resistant to UVB-induced skin injury than *Ptk6*+/+ mice

Ptk6+/+ and *Ptk6*-/- mice were treated with UVB three times a week. *Ptk6*+/+ mice (left panel) developed erythema and an inflammatory reaction on the lower dorsal skin within a week after beginning UVB treatments. *Ptk6*-/- mice developed a slight erythema but no inflammatory reaction. *Ptk6*+/+ mouse skin began to heal by week 3 and was almost completely healed by week 4. Size bar = 1 cm
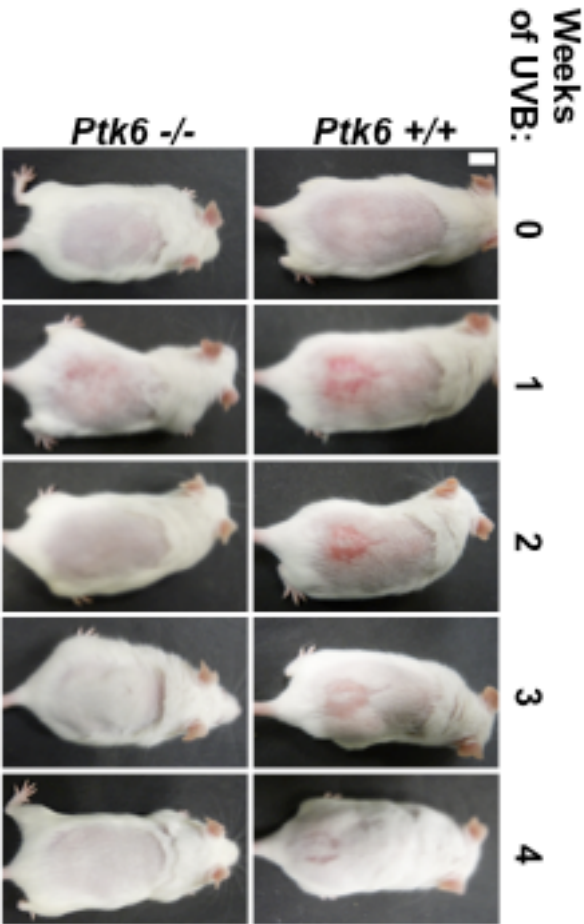
slight erythema, which healed by the end of the second week, and none of the mice developed lesions. No other symptoms developed during the early stages of the incrementally graded UVB protocol, and there were no other differences between the two genotypes after UVB.

C.   *Ptk6* **affects SENCAR mouse weight**

Disrupting the *Ptk6* gene impairs intestinal epithelial differentiation, which may be expected to negatively affect metabolism. In C57BL/6 mice, there were no detectable changes in weight in *Ptk6-/-* mice. By the conclusion of the incrementally graded UVB protocol, in which all mice were weighed each week, it became evident that SENCAR mouse metabolism was more strongly affected than C57BL/6 metabolism. In untreated SENCAR mice, *Ptk6+/+* mice became very obese, weighing up to 50 grams, while *Ptk6-/-* mice maintain a consistent body weight throughout their life, generally around 30 grams (Figure 7A). *Ptk6-/-* mice were also observed to be more active than *Ptk6+/+* mice. This weight differential could be a result of the higher activity, differences in intestinal absorption, or even changes in diet resulting from oral architectural changes, and further research will be needed to understand this phenotype. After UVB irradiation, *Ptk6+/+* mice do not become obese, and remain around the 30-gram range (Figure 7B). *Ptk6-/-* mouse weight did not appear to be affected. The additional stress caused by UVB irradiation may have had a variety of effects on the *Ptk6+/+* mice, including loss of appetite or increased physical exertion, although it is not clear at this time what the exact cause may have been.

Figure 7: Disruption of *Ptk6* reduces weight gain in SENCAR mice

A: Chart of average untreated *Ptk6*+/+ and *Ptk6*-/- mouse weight over the course of the experiment. *Ptk6*+/+ mice continue to gain weight after they reach adulthood and can reach up to 50 grams in weight. *Ptk6*-/- mice do not become obese and remain at an average of 30 grams per mouse throughout the experiment.
B: Chart of average UVB-treated *Ptk6*+/+ and *Ptk6*-/- mouse weight over the course of the experiment. There is no significant difference between the two genotypes, as they both maintain an average of 30 grams throughout the experiment.

A
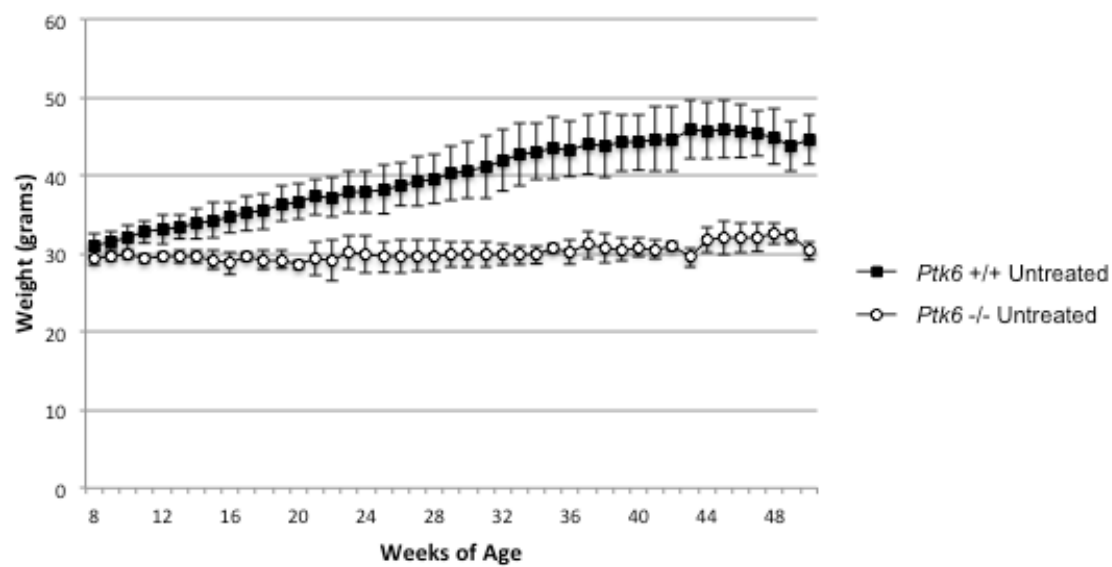
B
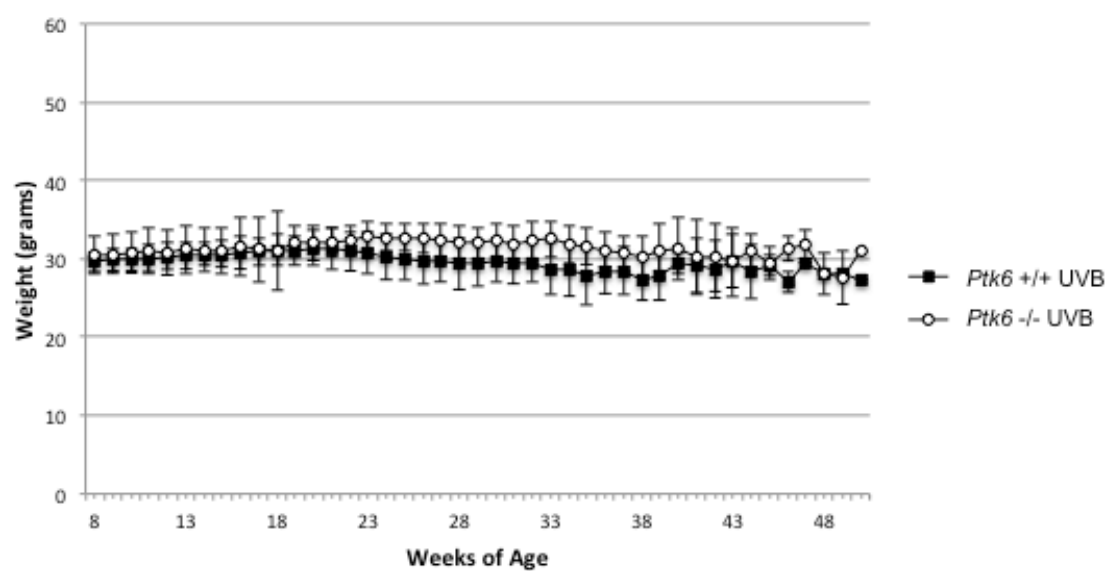
D.   *Ptk6-/-* mice exhibit delayed tumor formation and decreased mortality

While the endpoint of the experiment was expected to be 43 weeks (at 51 weeks of age), most of the experimental mice did not survive to the endpoint. Mice experience a sudden weight drop shortly before death, and were sacrificed when their weight dropped by more than 20%, which was generally about 6 grams, given an average weight of 30 grams. Most noticeably, the *Ptk6+/+* mice had a much higher mortality rate than the *Ptk6-/-* mice (Figure 8A), with only one *Ptk6+/+* mouse out of ten surviving to the end of the experiment, compared to half of the *Ptk6-/-* mice surviving at the end of the experiment. Earliest mortality for *Ptk6+/+* mice was at 35 weeks of age, and 28 weeks after initiation of UVB treatments (Figure 8A). In comparison, the earliest mortality for *Ptk6-/-* mice was at 41 weeks of age, and 33 weeks after initiation of UVB treatments. This higher level and earlier development of mortality remained consistent over the course of the experiment (Figure 8A).

Ptk6+/+ mice began developing tumors several weeks earlier than *Ptk6-/-* mice (Figure 8B), and more *Ptk6+/+* mice developed tumors. All of the *Ptk6+/+* mice developed tumors, while only half of the *Ptk6-/-* mice did. Additionally, the *Ptk6+/+* mice developed more tumors than did the *Ptk6-/-* mice (Figure 8C). *Ptk6+/+* mice developed a maximum tumor load of nearly four tumors per mouse, while *Ptk6-/-* mice only reached a maximum tumor load of 1.5 tumors per mouse. Quantitation of tumor load was made difficult by the fact that a papilloma can sometimes fall off, such that a smooth accumulation of tumors is not observed. Additionally, most of the mice did not survive until the end of the experiment. For quantitation purposes, I calculated the total number

Figure 8: *Ptk6*+/+ mice have higher mortality and a greater tumor load than *Ptk6*-/-mice

A: Kaplan-Meier survival chart of all experimental and control mice. All untreated control mice survived until the end of the experiment. *Ptk6*+/+ mice died earlier and in greater numbers than *Ptk6*-/- mice
B: Step chart showing percentage of tumor-free experimental mice over the course of the experiment. *Ptk6*+/+ mice developed tumors sooner than did *Ptk6*-/- mice. All *Ptk6*+/+ mice developed tumors, while only half of *Ptk6*-/- mice did.
C: Line graph showing average number of tumors formed per mouse in all experimental mice. Tumors that fell off or tumors on mice that died were still counted. *Ptk6*+/+ mice developed more tumors than did *Ptk6*-/- mice.
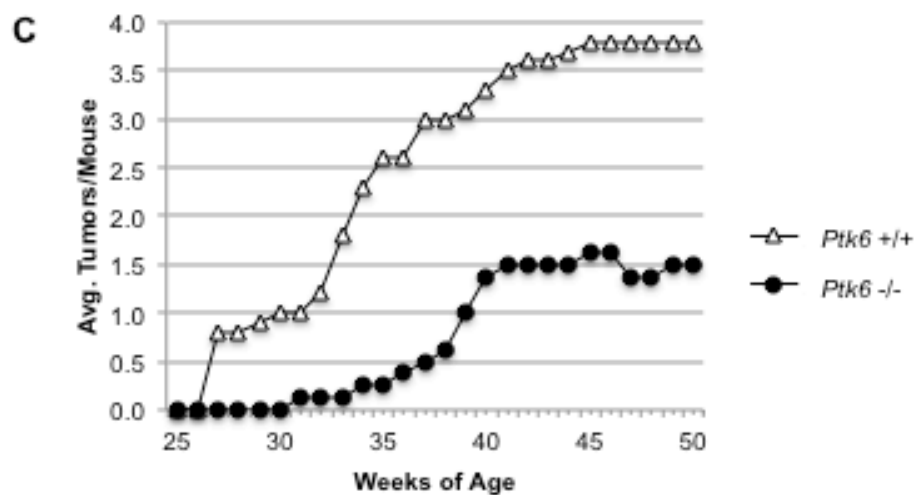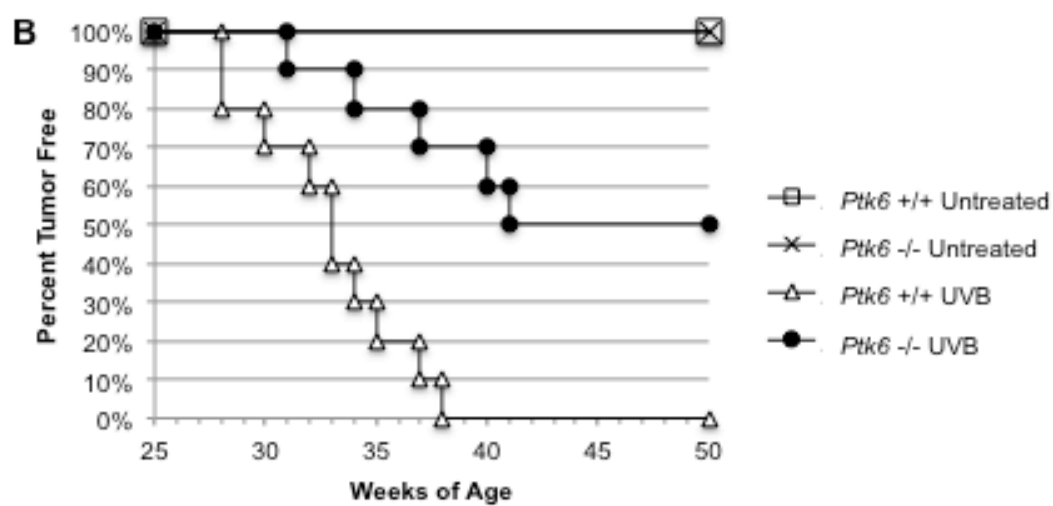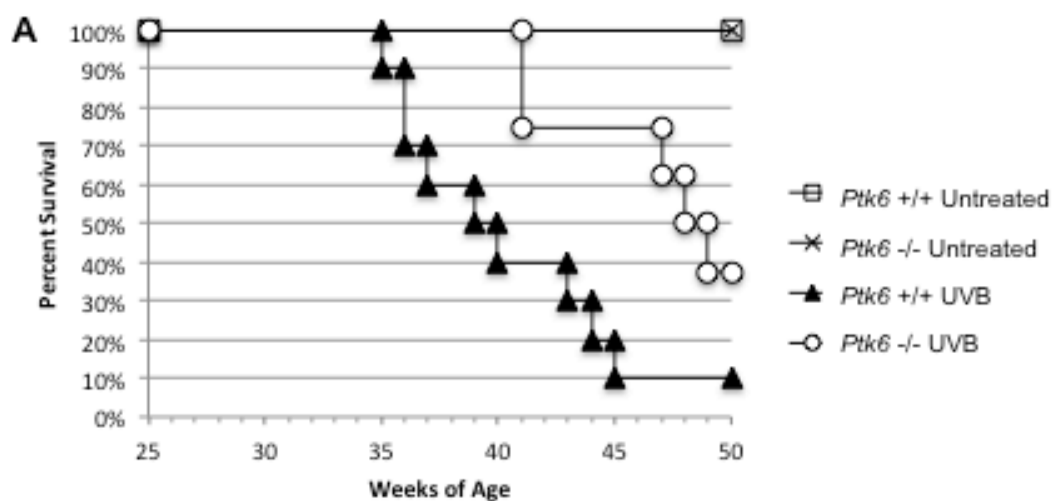
of tumors formed, even if they subsequently fell off or the mouse died. Tumor load also does not account for size of papilloma, some of which were very small.

Tumor load is not necessarily indicative of lethality, although particularly large tumors and ulcerations were usually indicators of oncoming death. *Ptk6+/+* mice were fairly consistent in tumor load and size before death (Figure 9A). *Ptk6-/-* mice developed fewer tumors, although these tumors typically were similar to the average size of *Ptk6+/+* tumors (Figure 9B). Tumor-bearing *Ptk6-/-* were more likely to die earlier, although not necessarily so, as one tumor-bearing mouse survived until the end of the experiment. None of the *Ptk6-/-* tumors became excessively large or ulcerated, unlike some of the *Ptk6+/+* tumors.

In both groups of mice we observed moderate hyperkeratosis and acanthosis of the epidermis with irregular formation of rete ridges. In wild-type mouse skin, we found severe ulceration of the epidermis as well as extensive necrosis. There was an ulcerated infiltrative dermal-subcutaneous mass composed of spindle-shaped cells arranged in palisading interwoven bundles and sheets. Wild-type skin typically had a much higher mitotic rate compared with PTK6-null skin and had greater progress in keratin pearl formation. PTK6-null skin exhibited a highly cellular dermal-subcutaneous mass composed of a large pleomorphic spindle in interwoven bundles.

Figure 9: Tumor Progression in *Ptk6+/+* and *Ptk6-/-* mice

A: *Ptk6+/+* mice before sacrifice. All *Ptk6+/+* mice developed tumors, and tumor size was not closely associated with mortality.
B: *Ptk6*-/- mice before sacrifice. Tumor development is not closely associated with mortality.
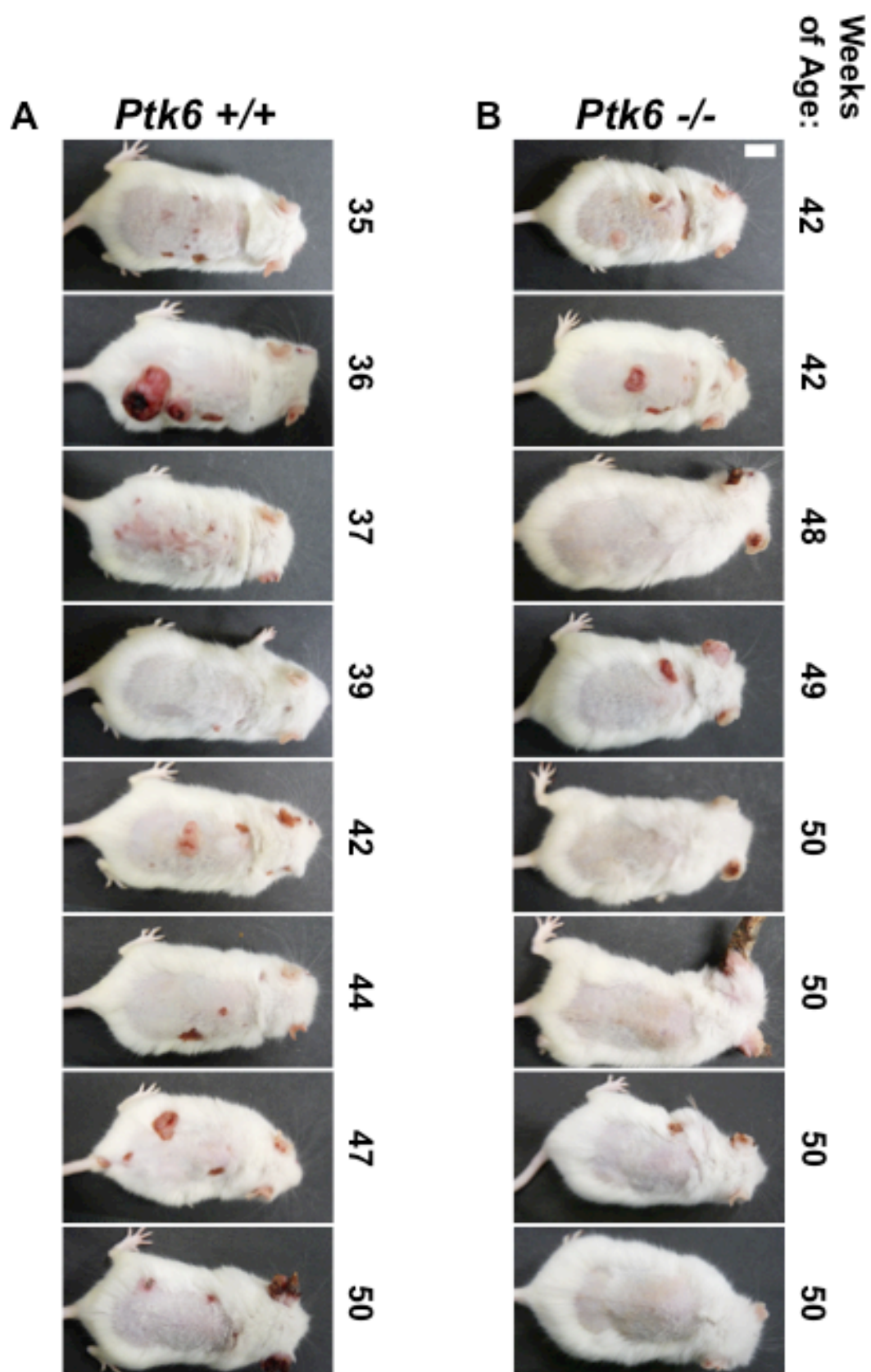
E.   Proliferation and differentiation

Ptk6+/+ mouse tumors have been shown to be more mitotically active than *Ptk6-/-* mouse tumors after long-term exposure to UVB. In order to better characterize how PTK6 affects proliferation in mouse skin, mice were injected with BrdU 2 hours prior to sacrifice and immunohistochemistry was used to examine BrdU incorporation, which identifies cells in S-phase. Despite having a higher mitotic rate, *Ptk6+/+* mouse skin did not have a higher level of BrdU incorporation than *Ptk6-/-* mouse skin (Figure 10A) in either the epithelial surface (a, d) or in the infiltrated dermis (b, e). BrdU stains for cell in S-phase of the cell cycle, so differences between quantitation of BrdU and quantitation of mitosis are not necessarily contradictory, as cell may become stuck in S-phase and only undergo mitosis in *Ptk6+/+* skin. Immunofluorescence revealed that phosphorylated PTK6 does not colocalize with BrdU, suggesting that PTK6 does not directly drive proliferation to UVB-induced carcinogenesis (Figure 10A - c, f). When quantified, *Ptk6-/-* mouse skin was found to have slightly higher levels of BrdU incorporation, but this difference was not significant (Figure 10B).

To further examine how PTK6 may affect proliferation in mouse skin, I stained 4-day old *Ptk6+/+* and *Ptk6-/-* SENCAR mouse skin with antibodies against ki67, a protein involved in ribosomal transcription which is commonly used by pathologists to characterize proliferation in tissues. There was very little ki67 in *Ptk6+/+* neonatal mouse skin. In comparison, there were high levels of ki67 in the basal layer of *Ptk6-/-* neonatal mouse skin (Figure 11A). I UVB irradiated the mice with a moderate dose (250 mJ/cm^2) and sacrificed them three hours later to identify short-term alterations in cell signaling. *Ptk6+/+* neonatal skin was mildly more proliferative after UVB, while *Ptk6-/-* neonatal

Figure 10: Proliferation in *Ptk6*+/+ and *Ptk6*-/- skin tumors

A: BrdU stained cells are present in both the *Ptk6*+/+ epithelial layers **(a)** and in the infiltrative dermis **(d)**. BrdU stained cells are present in both the *Ptk6*-/- epithelial layers **(b)** and in the infiltrative dermis **(e)**. In *Ptk6*+/+ skin tumors, phosphorylated PTK6 (green) does not co-localize with BrdU (red) in either the epithelial layers of the skin **(c)** or in the infiltrative dermis **(f)**.
B: Quantitation of BrdU-stained cells in *Ptk6*+/+ and *Ptk6*-/- skin tumors.
p-value = 0.158
Size bar = 20 μm
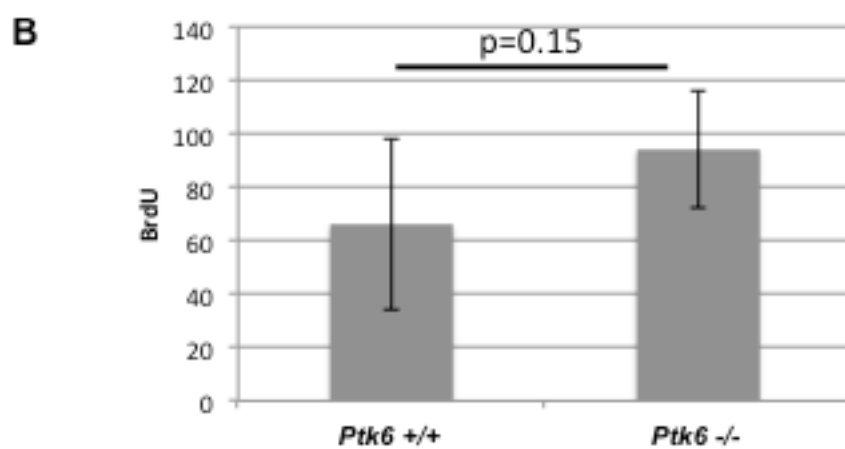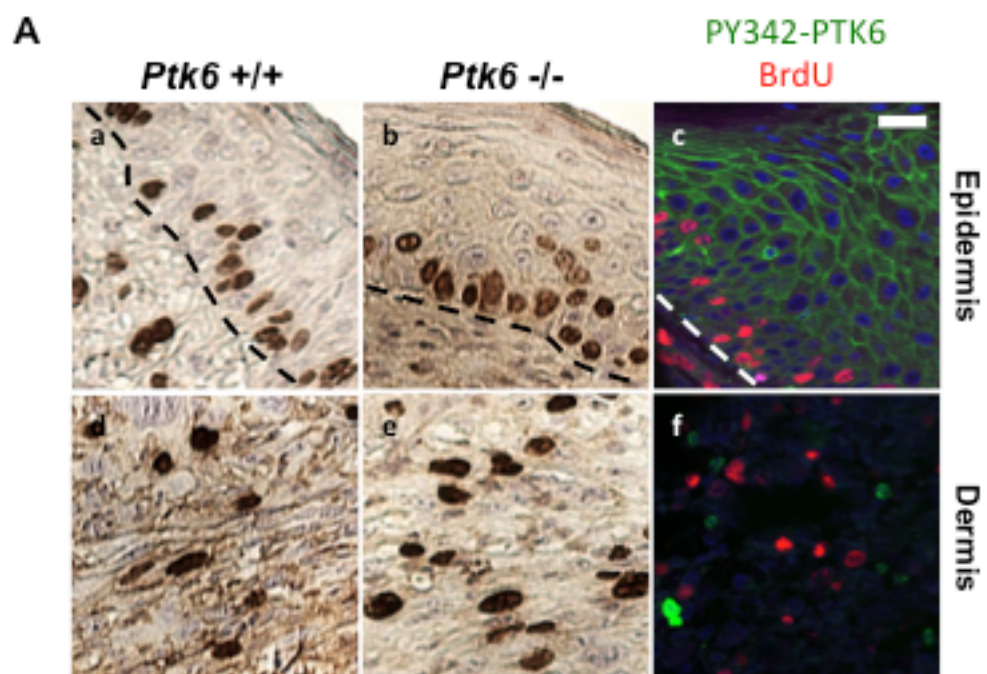
Figure 11: Proliferation and architecture of neonatal mouse skin

A: Immunohistochemistry of *Ptk6*+/+ and *Ptk6*-/- neonatal (4-days old) mouse skin incubated with antibodies against ki67. *Ptk6*+/+ has relatively little ki67-stained cells in the basal layer, while most basal layer cells in *Ptk6*-/- neonatal mouse skin are positively stained for ki67. This difference is maintained 3 hours after UVB treatment.
B: Quantitation of ki67-stained cells in *Ptk6*+/+ and *Ptk6*-/- neonatal mouse skin.
C: Immunofluorescence for keratin-14 (green) and ki67 (red). There is more ki67 present in the basal layer of *Ptk6*-/- neonatal mouse skin. Keratin-14 remains confined to the basal layer, as is ki67.
D: Immunofluorescence for keratin-14 (green) and keratin-10 (red). There does not appear to be a significant difference in keratin expression between *Ptk6*+/+ and *Ptk6*-/- neonatal mouse skin, suggesting that there is little difference in skin architecture.
Size bar = 20 μm

A

Ptk6 +/+   *Ptk6 -/-*

Untreated

UVB 3 hr

B

p=0.000002   p=0.00975

% ki67-positive basal layer cells

90%
80%
70%
60%
50%
40%
30%
20%
10%
0%

+/+   -/-   +/+   -/-

Control   UVB 3 hours

C

Ptk6 +/+   *Ptk6 -/-*

Keratin-14
ki67

Dermis   Dermis

D

Ptk6 +/+   *Ptk6 -/-*

Keratin-14
Keratin-10

Dermis   Dermis
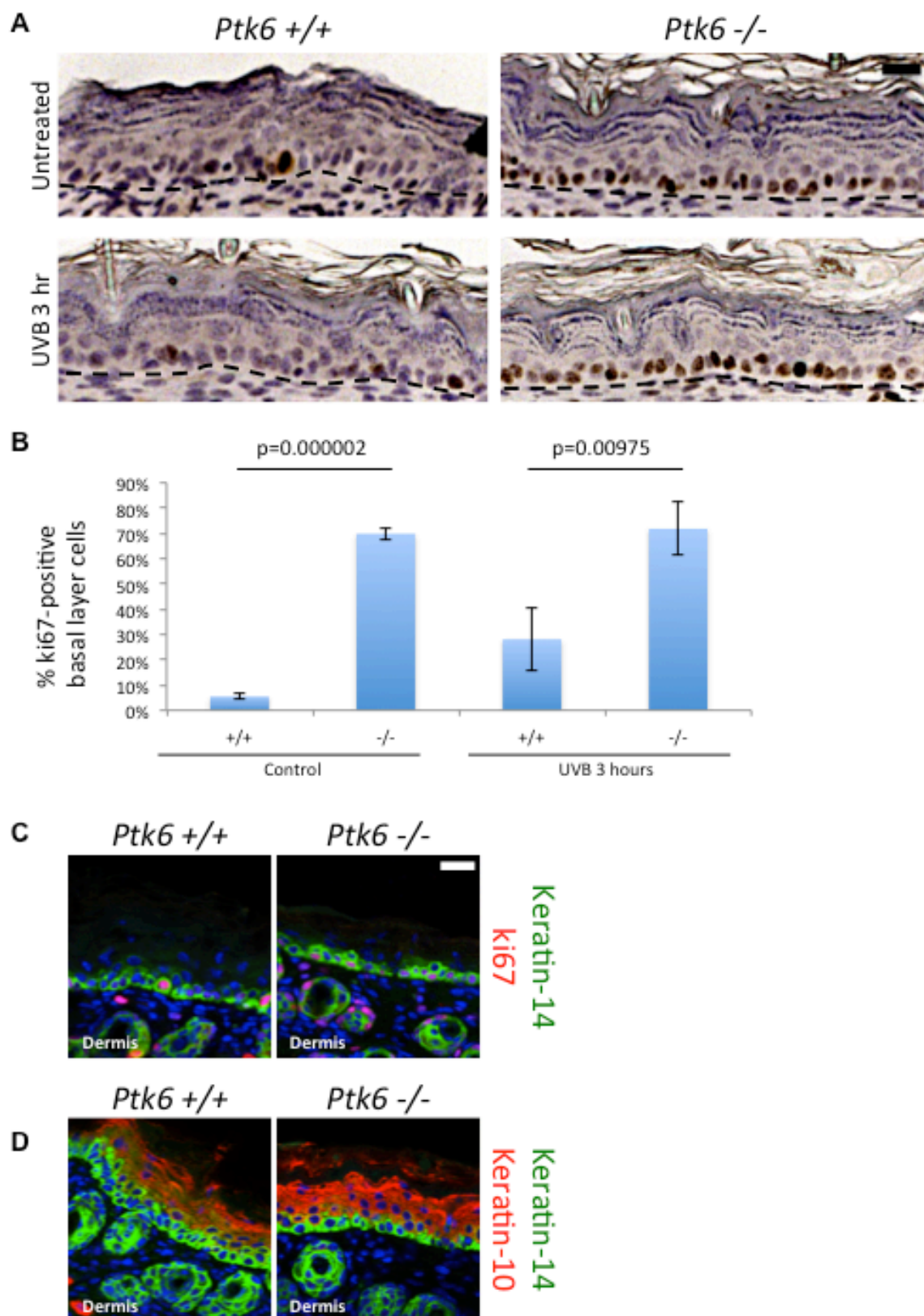
skin remained unchanged (Figure 11A). When quantified, it was determined that the higher expression of ki67 in *Ptk6*-/- neonatal mouse skin was significant both before and after UVB (Figure 11B). In order to better understand how PTK6 affects the architecture of the skin, I performed immunofluorescence in sections of neonatal mouse skin with antibodies specific for ki67 and keratin-14. Keratin-14 expression remained confined to the basal layer in both *Ptk6*+/+ and *Ptk6*-/- neonatal skin (Figure 11C). Additionally, I performed immunofluorescence in sections of neonatal mouse skin with antibodies specific for both keratin-14 and keratin-10, and determined that there is no clear difference in keratin expression between the two genotypes (Figure 11D).

While *Ptk6*-/- neonatal mouse skin had higher ki67 content than *Ptk6*+/+ neonatal mouse skin, there does not seem to be a corresponding difference in adult mouse skin. In adult (8 week old) mice that were treated with the short-term UVB protocol (5 times for 10 days), there was not difference in ki67 staining between genotypes, either before or after UVB treatment (Figure 12A), despite a difference in neonatal mouse skin. Similarly there is no apparent difference in BrdU staining between genotypes either before or after UVB treatment (Figure 12B). BrdU cells were confined to the basal layer in both genotypes. Keratin-14 expression extends into the suprabasal layers after UVB, and is not confined to the basal layer. Keratin-14 is expressed in all layers of the skin, while keratin-10 is confined to the suprabasal layers of the skin (Figure 12C). This expression pattern is conserved in both *Ptk6*+/+ and *Ptk6*-/- mouse skin.

Additionally, there does not seem to be a significant difference in UVB-induced apoptosis, as measured by TUNEL assay. While *Ptk6*+/+ mouse skin is more sensitive to UVB, there does not seem to be an architectural difference.

Figure 12: Architecture of UVB-treated skin

A: Immunofluorescence for ki67 in untreated and UVB-treated *Ptk6+/+* and *Ptk6-/-* adult mouse skin. There is no apparent difference in ki67 expression between genotypes.
B: Immunofluorescence for keratin-14 (green) and BrdU (red) in untreated and UVB-treated adult mouse skin. There are equivalent levels of BrdU in adult *Ptk6+/+* and *Ptk6-/-* mouse skin both before and after UVB treatment. BrdU-stained cells localize to the keratin-14-stained basal layer in both genotypes.
C: Immunofluorescence for keratin-14 (green) and keratin-10 (red). There does not appear to be a significant difference in keratin expression between *Ptk6+/+* and *Ptk6-/-* mouse skin either before or after UVB treatment. PTK6 does not seem to affect skin architecture in adult skin.
D: TUNEL assay to measure apoptosis. There is very little apoptosis before or after UVB after 10 days, and there is no detectable difference between *Ptk6+/+* and *Ptk6-/-* skin.
Size bar = 20 μm
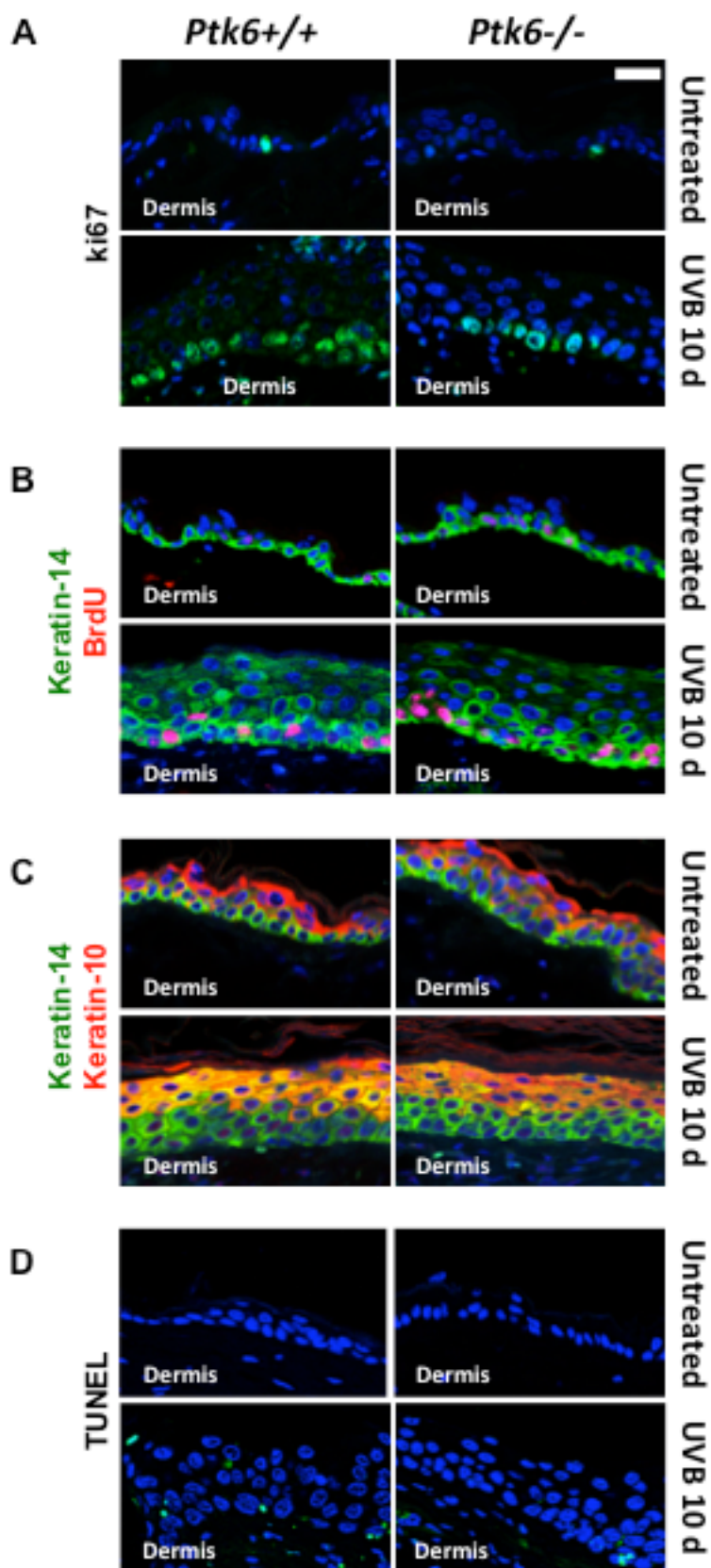
3.   **Disruption of *Ptk6* results alters cell signaling after UVB**

A.   **PTK6 promotes STAT3 activation**

STAT3 promotes proliferation in many cell types, and has previously been shown to promote UVB-induced carcinogenesis in skin (Kim 2007). PTK6 directly phosphorylates at tyrosine residue 705, which activates STAT3, causing it to dimerize and translocate to the nucleus and transcribe target genes (Liu 2006), so upregulation of PTK6 activity following UVB treatment may promote STAT3 activation. Similar experiments have been done in C57BL/6 mouse colon, in which the *Ptk6-/-* mouse colon had less Y705 phosphorylation of STAT3 after AOM treatment than the *Ptk6+/+* mouse colon (Gierut et al. 2011), and it is possible PTK6 may similarly target STAT3 in SENCAR skin after UVB.

Protein lysates prepared from full thickness short-term irradiated skin were subjected to immunoblotting to assess STAT3 expression and activation after UVB-induced skin damage. There is slightly more Y705 phosphorylation of STAT3 in untreated *Ptk6-/-* mouse skin than in *Ptk6+/+* mouse skin, but this increase is not statistically significant (Figure 13A). After UVB, STAT3 is significantly phosphorylated in *Ptk6+/+* skin but not in *Ptk6-/-* skin. This activation was quantified, and it was determined that this difference is statistically significant (Figure 13B). When analyzed using immunofluorescence, we found significantly more nuclear-targeted phosphorylated STAT3 in *Ptk6+/+* skin than in *Ptk6-/-* skin (Figure 13C). Similarly, there was more nuclear-targeted phosphorylated STAT3 in the epithelial layers of *Ptk6+/+* endpoint mouse skin tumors compared with *Ptk6-/-* skin endpoint mouse skin tumors (Figure 13D). Ultimately, UVB-induced STAT3 activation is significantly enhanced by PTK6.

**Figure 13: PTK6 promotes STAT3 Y705 phosphorylation after UVB**

A: Immunoblot of phosphorylated STAT3 before and after short-term UVB in *Ptk6*+/+ and *Ptk6*-/- mouse skin. There are higher levels of P-Y705 STAT3 in *Ptk6*+/+ UVB-treated mouse skin than in *Ptk6*-/- UVB-treated mouse skin.
B: Relative strength of luminescent signal was measured using a program called ImageJ. Intensity of P-Y705 STAT3 was normalized to intensity of total STAT3 and to the GAPDH loading control, and averaged across all samples. There is no significant difference between *Ptk6*+/+ and *Ptk6*-/- untreated skin (p-value = 0.19). There is a significant difference between *Ptk6*+/+ and *Ptk6*-/- UVB-treated skin (p-value = 0.009).
C: Immunohistochemistry of total and phosphorylated STAT3 expression in adult short-term UVB-treated mice reveals differential staining pattern between *Ptk6*+/+ and *Ptk6*-/- mouse skin. Immunofluorescence shows that in UVB-treated mice there is more phosphorylated STAT3 present in *Ptk6*+/+ mouse skin than in *Ptk6*-/- mouse skin.
D: Immunohistochemistry of total and phosphorylated STAT3 expression in adult endpoint UVB-treated mouse tumors reveals differential staining pattern between *Ptk6*+/+ and *Ptk6*-/- skin tumors. There is more phosphorylated STAT3 present in *Ptk6*+/+ skin tumors than in *Ptk6*-/- skin tumors.
Size bar = 20 μm
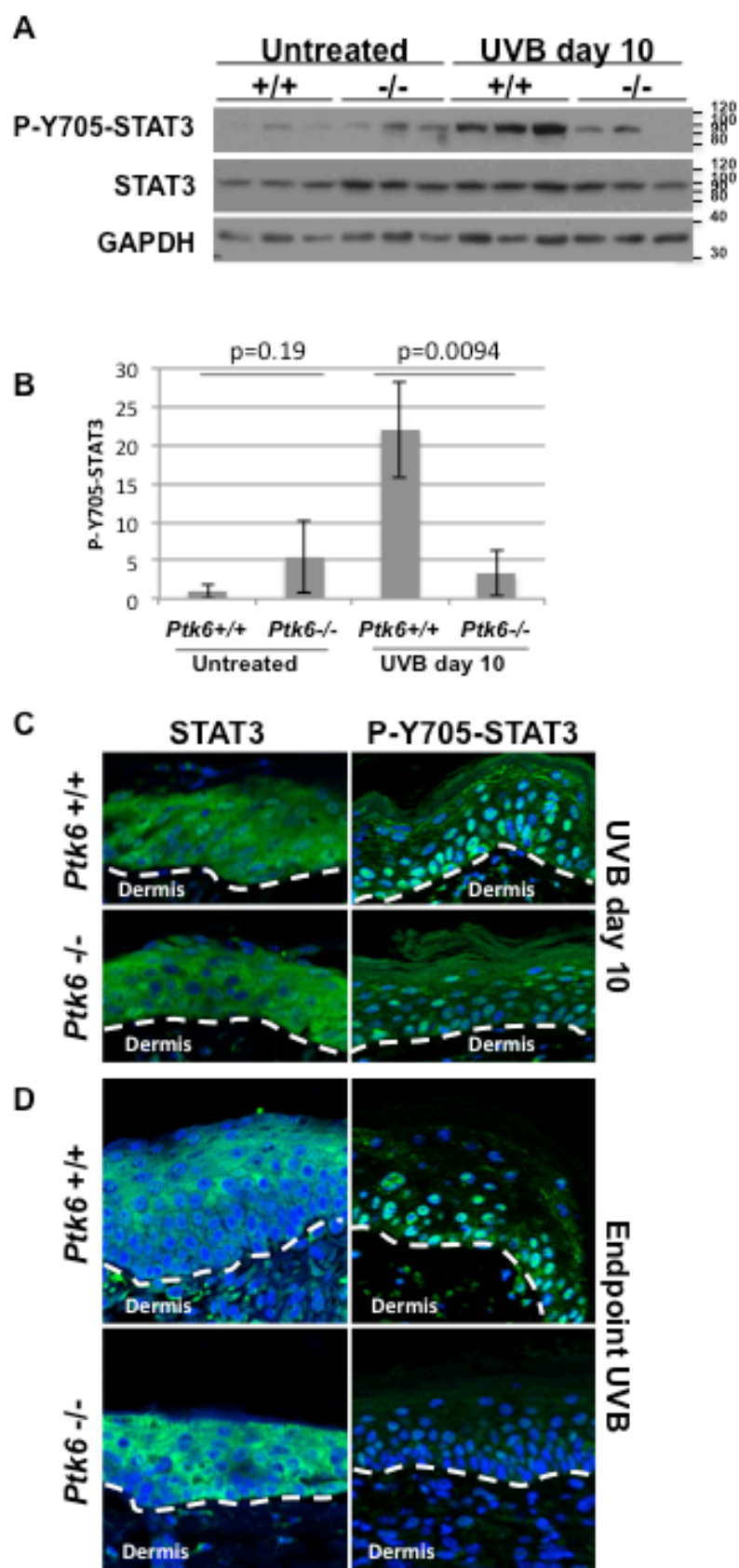
B.   PTK6 promotes FAK activation

Suppression of anoikis and promotion of anchorage-independent survival further promotes oncogenesis, and Focal Adhesion Kinase (FAK) plays an important role in this pathway. Phosphorylation of FAK at multiple tyrosine residues causes its activation and promotes downstream signaling. FAK is a direct target of PTK6 and is involved in regulating cell signaling at focal adhesion complexes (Zheng et al. 2012). FAK is phosphorylated at multiple sites, including Y576/Y577, which is important for maximum activation, and Y925, which is a high affinity Grb2 binding site (Schlaepfer et al. 2004). Phosphorylation of FAK results in greater motility, which can promote invasion and metastasis.

We used immunofluorescence with antibodies against two phosphorylation sites of FAK, Y925 and Y576/Y577 to examine sections of skin. In untreated skin, FAK is not phosphorylated at either Y576/577 or Y925, and disruption of *Ptk6* has no effect (Figure 14A). After short-term UVB, where the mice are treated 5 times in 10 days and then sacrificed, FAK is phosphorylated at both sites and localizes to the membrane in *Ptk6+/+* skin, but is not phosphorylated at either site in *Ptk6-/-* skin (Figure 14B). In endpoint mouse skin tumors, FAK continues to be highly phosphorylated on both tyrosine residues at the membrane in *Ptk6+/+* hyperplastic skin (Figure 14C). FAK is phosphorylated on both tyrosine residues at the membrane in *Ptk6-/-* skin, but not at strongly as in *Ptk6+/+* skin.

Figure 14: PTK6 promotes FAK phosphorylation

A: FAK is expressed throughout the epidermis in adult mouse skin, but is not phosphorylated in either *Ptk6*+/+ or *Ptk6*-/- adult mouse skin.
B: After 10 days of regular UVB treatment, FAK becomes phosphorylated at the membrane in *Ptk6*+/+ adult mouse skin at both phosphorylation sites. There is no phosphorylation of FAK at either site in *Ptk6*-/- mouse skin.
C: FAK is phosphorylated at both Y576/Y577 and at Y925 at the membrane in both *Ptk6*+/+ and *Ptk6*-/- mouse skin tumors, but is much more pervasive in *Ptk6*+/+ mouse skin tumors.
Size bar = 20 μm

C.   PTK6 promotes phosphorylation of BCAR1

To further understand how PTK6 may activate oncogenic signaling, we decided to examine Y165 phosphorylation of BCAR1. BCAR1 is important in regulating peripheral adhesion complexes, is phosphorylated at multiple residues by Src, FAK, and other kinases, and is Y165 phosphorylated by PTK6 (Zheng et al. 2012). Tyrosine 165 is located in the substrate domain, where phosphorylation results amplification of BCAR1 activity and in binding with SH2 domains, PTB domains or C-Crk (Bouton et al. 2001). We found that BCAR1 is already phosphorylated on Y165 and targeted to the membrane in untreated *Ptk6+/+* skin, but not in *Ptk6-/-* skin (Figure 15A). Following short-term UVB treatments, where the mice are treated 5 times in 10 days and then sacrificed, there is an increase in phosphorylation of BCAR1 on Y165 at the membrane in both genotypes, but there is still more Y165 phosphorylation of BCAR1 at the membrane in *Ptk6+/+* skin than in *Ptk6-/-* skin (Figure 15B). Finally, we examined the endpoint mouse skin tumors, and found that BCAR1 is highly phosphorylated in endpoint *Ptk6+/+* skin, but is much less so in *Ptk6-/-* skin (Figure 15C).

D.   Cell signaling pathways in *Ptk6+/+* and *Ptk6-/-* mice after UVB

In addition to STAT3, FAK, and BCAR1, PTK6 targets a variety of cell signaling pathways, most notably ERK1/2, ERK5, and AKT (Brauer et al. 2010). Lysates were made of short-term UVB-treated *Ptk6+/+* and *Ptk6-/-* mouse skin and immunoblotting was performed with antibodies specific for phosphorylation of these pathways. Phosphorylation of the ERK1/2 pathway does not seem to be significantly affected by UVB irradiation or by the disruption of *Ptk6* (Figure 16). However, AKT appears to be more strongly Thr308 phosphorylated in adult UVB-treated *Ptk6-/-* mouse skin than in
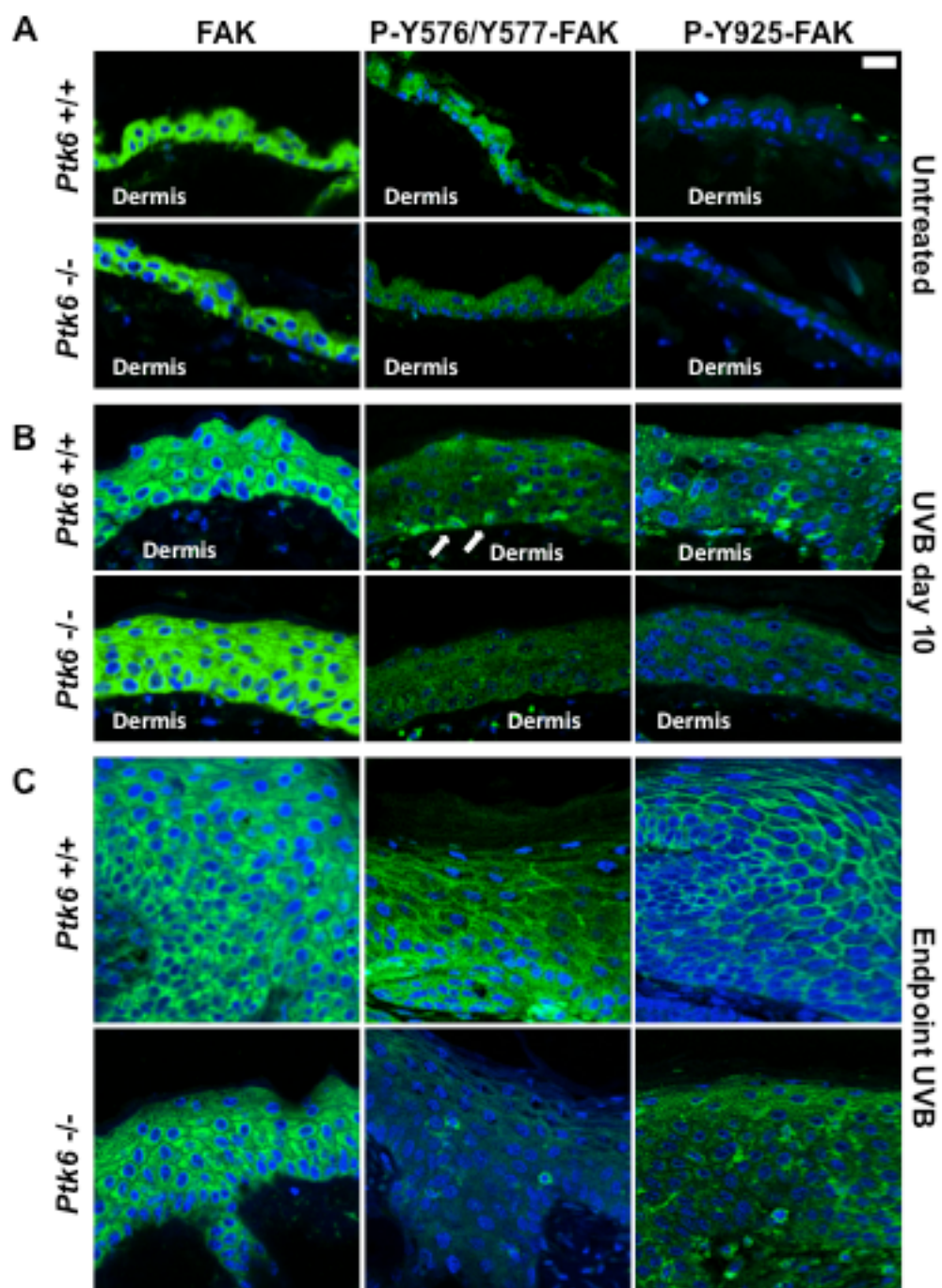
Figure 15: PTK6 promotes BCAR1 phosphorylation

A: BCAR1 is expressed throughout the epidermis in adult mouse skin. BCAR1 is phosphorylated in the basal layer of *Ptk6+/+* mouse skin. There is no phosphorylation of BCAR1 in *Ptk6-/-* mouse skin.
B: Within 10 days of regular UVB treatment, BCAR1 phosphorylation increases in both genotypes. Phosphorylation of BCAR1 remains higher in *Ptk6+/+* mouse skin than in *Ptk6-/-* mouse skin.
C: BCAR1 is phosphorylated in both *Ptk6+/+* and *Ptk6-/-* mouse skin tumors, but is much more pervasive in *Ptk6+/+* mouse skin tumors.
Size bar = 20 μm

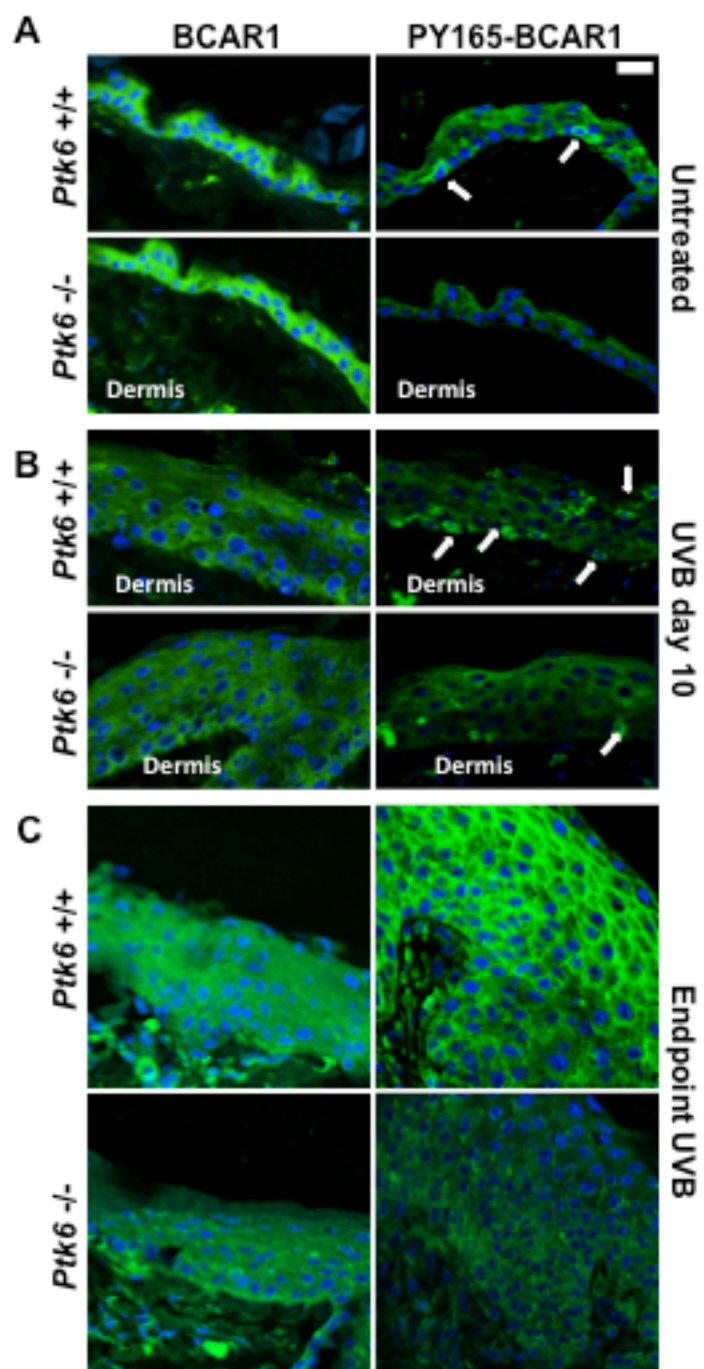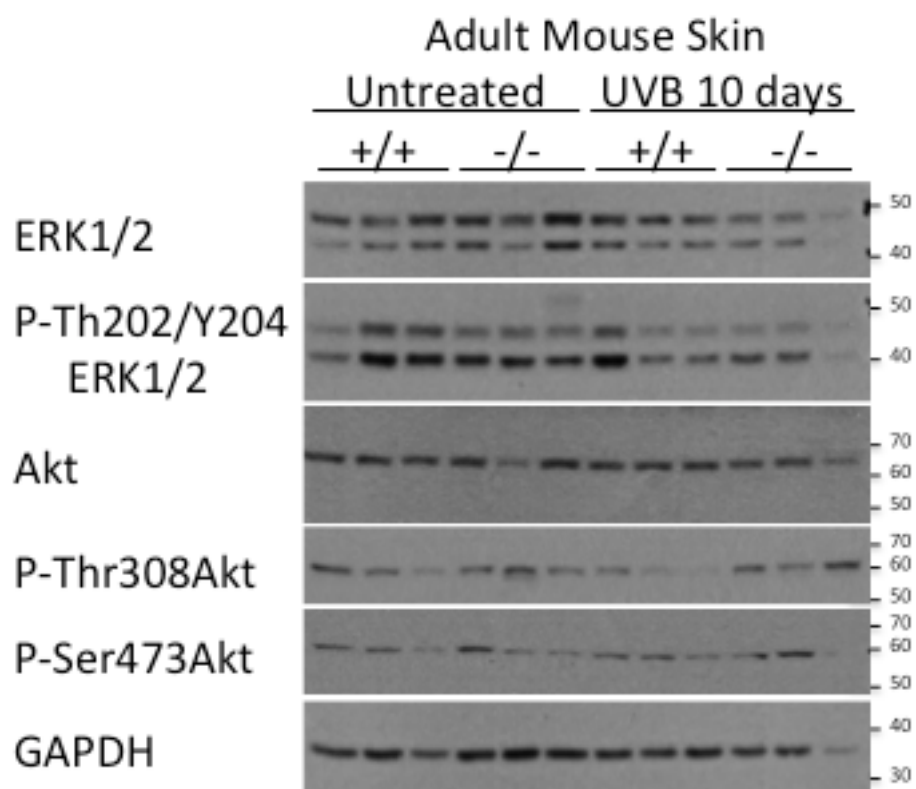**Figure 16: Cell signaling pathways in *Ptk6+/+* and *Ptk6-/-* mouse skin**

Lysates of short-term UVB treated mouse skin were run on an SDS-PAGE and subjected to immunoblot analysis for downstream signaling targets of PTK6, particularly AKT and ERK1/2. There is little consistent difference between UVB-treated adult *Ptk6+/+* and *Ptk6-/-* mouse skin in these signaling pathways.

Adult Mouse Skin

adult UVB-treated *Ptk6+/+* mouse skin. There was some individual variation between animals, but when the signal was compared across groups and individual variations accounted for, there was no consistent difference between any of these mice. Immunofluorescence was used to further examine the localization of phosphorylated ERK1/2, ERK5, and AKT (Figure 17). There is a small increase in phosphorylated ERK5 in UVB-treated *Ptk6+/+* mouse skin, but none of these pathways were significantly different in *Ptk6+/+ and* Ptk6-/- mouse skin after UVB irradiation.

I also examined these signaling pathways in neonatal mice to determine if the increased thickness and more rapid turnover might involve higher activation of those pathways (Figure 18). STAT3 phosphorylation, which is impaired in adult UVB-treated *Ptk6*-/- mouse skin, is not impaired in neonatal *Ptk6*-/- mouse skin. The ERK5 and AKT pathways were not affected by UVB treatment or by disrupting *Ptk6*. Interestingly, ERK1/2 becomes heavily phosphorylated three hours after UVB treatment in neonatal *Ptk6*-/- skin. It is possible that neonatal skin, which is still developing and is more proliferative than adult skin, is more sensitive to ERK1/2 pathway activation than adult skin, and does not rely as heavily on the STAT3 pathway. In endpoint *Ptk6+/+* mouse skin tumors, ERK1/2 was strongly phosphorylated, but there was little ERK1/2 phosphorylation in *Ptk6*-/- mouse skin tumors (Figure 19). There did not appear to be any significant difference in S473 phosphorylation of AKT or localization of active β-catenin.

Figure 17: Cell signaling localization in *Ptk6*+/+ and *Ptk6*-/- mouse skin

Immunofluorescence using antibodies against several signaling pathways, particularly AKT, ERK1/2, ERK5, and β-catenin in short-term UVB treated adult mouse skin (10 days after 5 treatments). There was little consistent significant difference between UVB-treated adult *Ptk6*+/+ and *Ptk6*-/- mouse skin in these signaling pathways.
Size bar = 20 μm
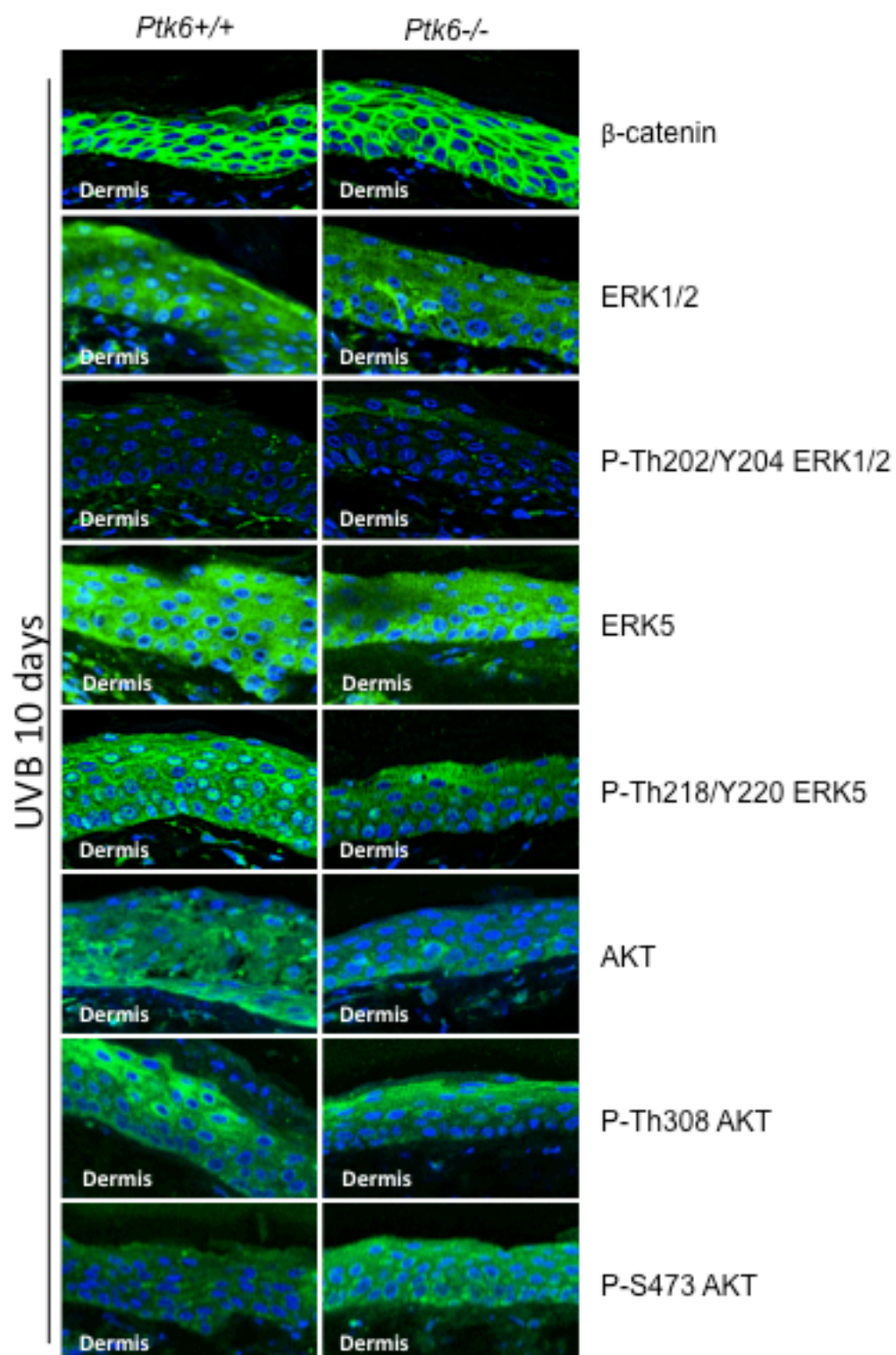
Figure 18: Cell signaling in *Ptk6+/+* and *Ptk6-/-* neonatal mouse skin

A: STAT3 becomes phosphorylated 3 hours after UVB treatment, but there is no significant difference between *Ptk6+/+* and *Ptk6-/-* neonatal mouse skin
B: ERK1/2 becomes highly phosphorylated in *Ptk6-/-* neonatal mouse skin 3 hours after UVB treatment, but not in *Ptk6+/+* neonatal mouse skin.
C: ERK5 phosphorylation is increased after UVB treatment, but there is no significant difference between between *Ptk6+/+* and *Ptk6-/-* neonatal mouse skin
D: AKT Th308 phosphorylation is not affected after UVB treatment in either *Ptk6+/+* and *Ptk6-/-* neonatal mouse skin
E: There is no significant difference in caspase 3 cleavage between *Ptk6+/+* and *Ptk6-/-* neonatal mouse skin
Size bar = 20 μm
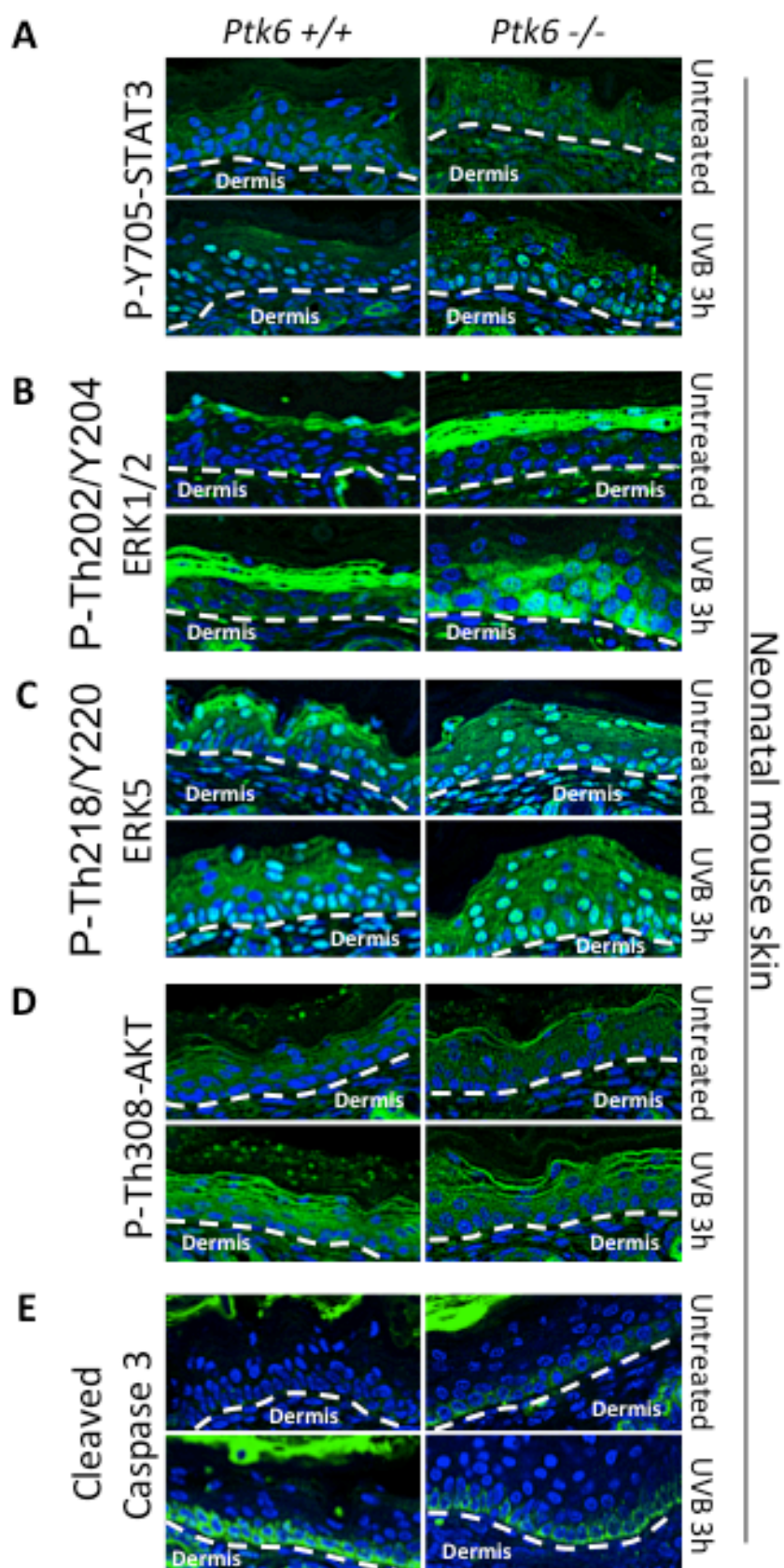
Figure 19: Cell signaling in mouse skin tumors

Immunofluorescence on *Ptk6*+/+ and *Ptk6*-/- mouse skin tumors using antibodies specific for active β-catenin, PS473-AKT, PTh202/Y204-ERK1/2. Only ERK1/2 showed any difference in phosphorylation, and was more strongly phosphorylated in *Ptk6*+/+ mouse skin tumors.
Size bar = 20 μm

4.   PTK6 is activated in human squamous cell carcinomas

A.   PTK6 phosphorylation localizes to the basal layer in human skin

We detected phosphorylation of PTK6 at Tyrosine residue 342 in UVB-damaged mouse skin, and we wanted to determine this phosphorylation also occurred in human tissue samples. We acquired patient biopsy samples from Dr. Yu-Ying He at the University of Chicago. These samples included normal skin, actinic keratosis, and squamous cell carcinomas. These s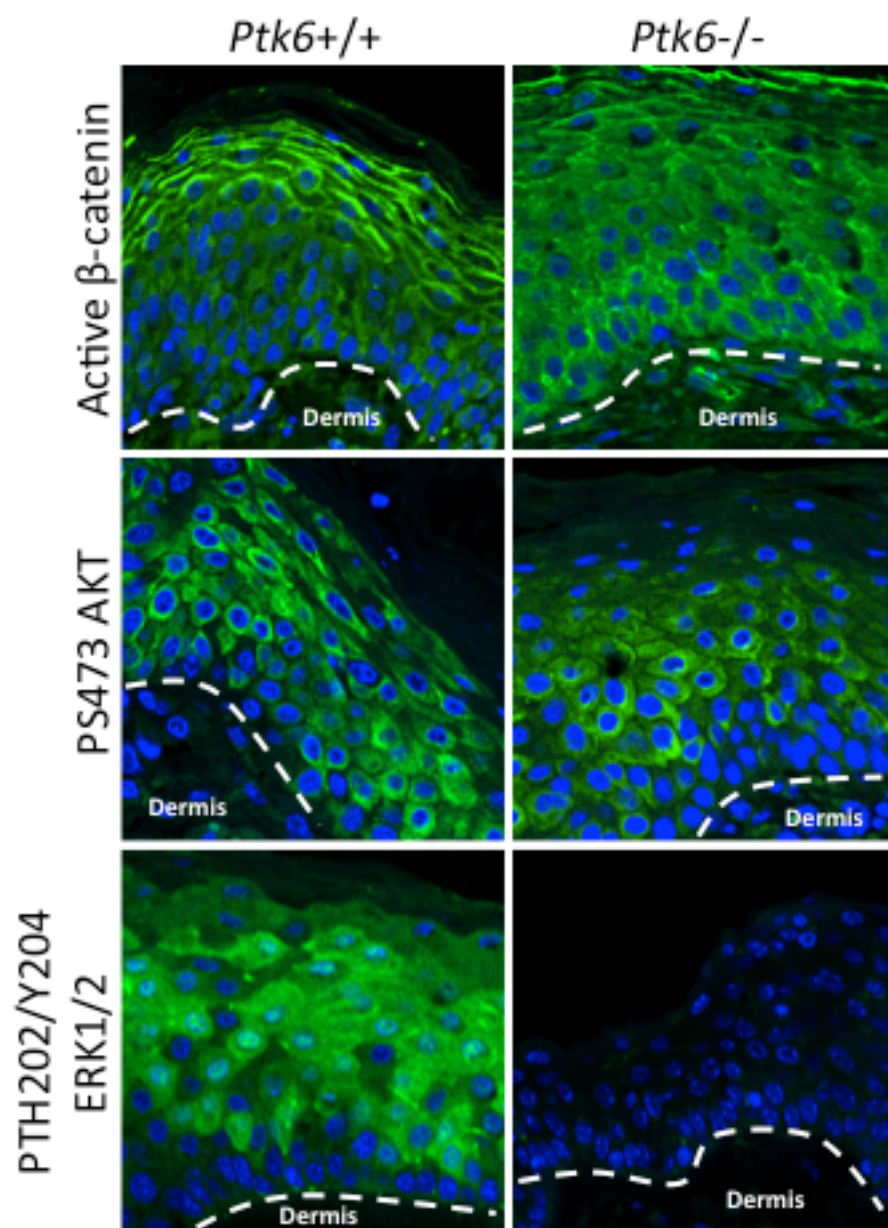amples were stained with the anti-PY342-PTK6 antibody, and some were also stained with anti-human PTK6. In normal human skin, PTK6 is expressed in the suprabasal layer of the epidermis, with minimal expression in the basal layer (Figure 20A). PTK6 is not strongly Y342 phosphorylated, but when it was phosphorylated, it localized to the membrane in the basal layer. In SCC, PTK6 becomes much more strongly Y342 phosphorylated at the basal layer, although most PTK6 expression remains confined to the suprabasal layer (Figure 20B). Total levels of PTK6 do not seem to be strongly affected in SCC. We did not observe a decrease in PTK6 expression in these samples, as has been reported in other publications. There is little overlap between total and phosphorylated PTK6 signals, suggesting different roles for PTK6 before and after phosphorylation.

B.   PTK6 expression decreases in Squamous Cell Carcinoma

We obtained a dataset on gene expression profiles in human HNSCC (Lambert et al. 2014). In the Lambert Dataset, patient samples were classified according to skin type as actinic keratosis, well-differentiated SCC, moderately-differentiated SCC, and poorly-differentiated SCC. After examining PTK6 expression in all samples, I found that PTK6 expression decreases in less differentiated SCC (Figure 20). PTK6 expression is

Figure 20: PTK6 expression and activation in human SCC

A: Expression of PTK6 is localized to the suprabasal layer of normal human skin. There are low levels of PTK6 phosphorylation in the basal layer of normal human skin.
B: PTK6 is phosphorylated at the membrane of the basal layer in human squamous cell carcinoma samples. Total PTK6 was expressed mostly in the suprabasal layer.

Size bar = 20 μm
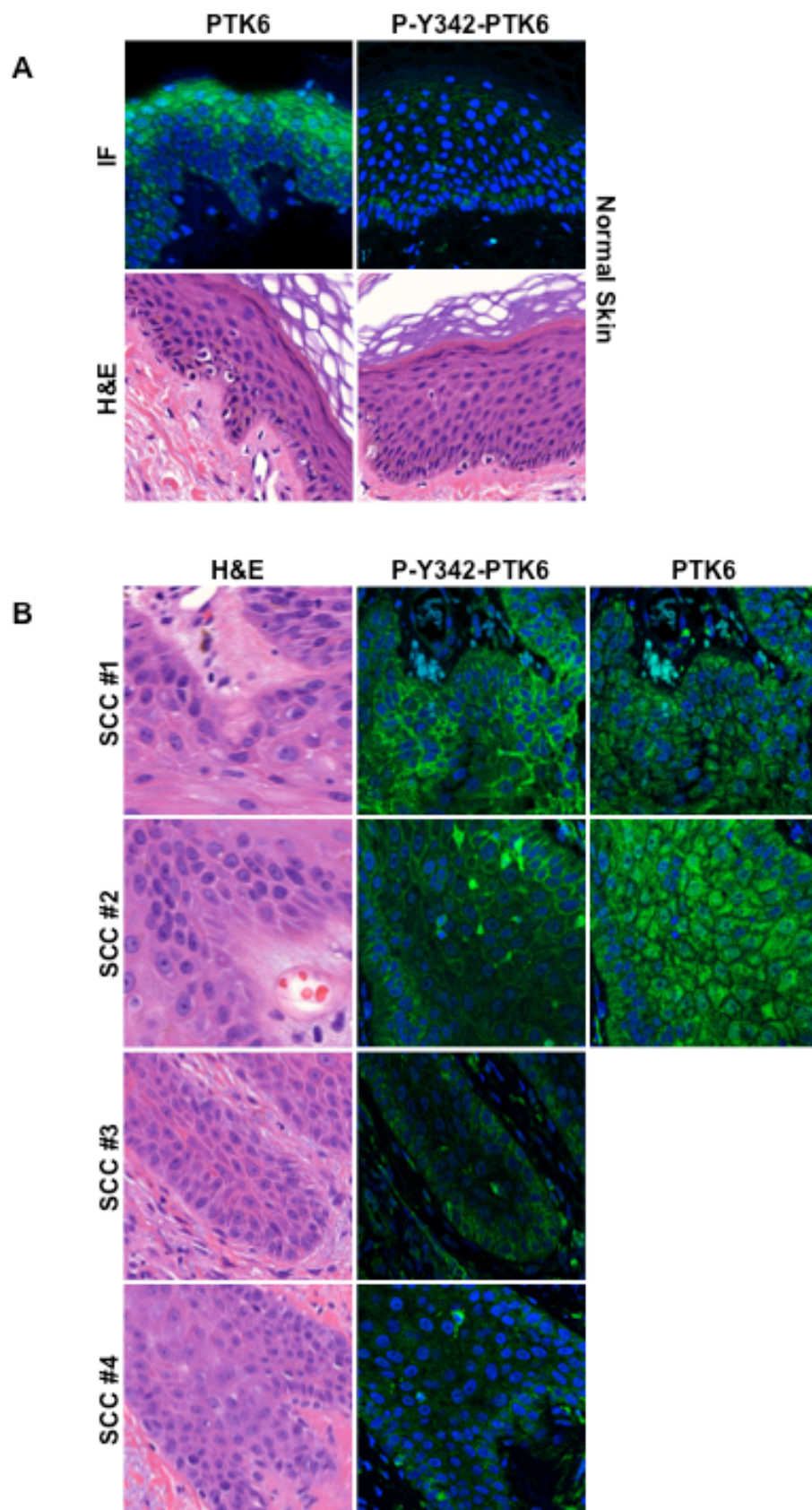
Figure 21: PTK6 expression decreases in poorly-differentiated SCC

Bar chart of PTK6 expression from the Lambert dataset of SCC (Lambert et al. 2014). Data is sorted according to skin type and development of differentiation. PTK6 transcription significantly decreases in less differentiated SCC. There are significant differences between actinic keratosis and SCC, as well as between well-differentiated SCC and poorly-differentiated SCC.
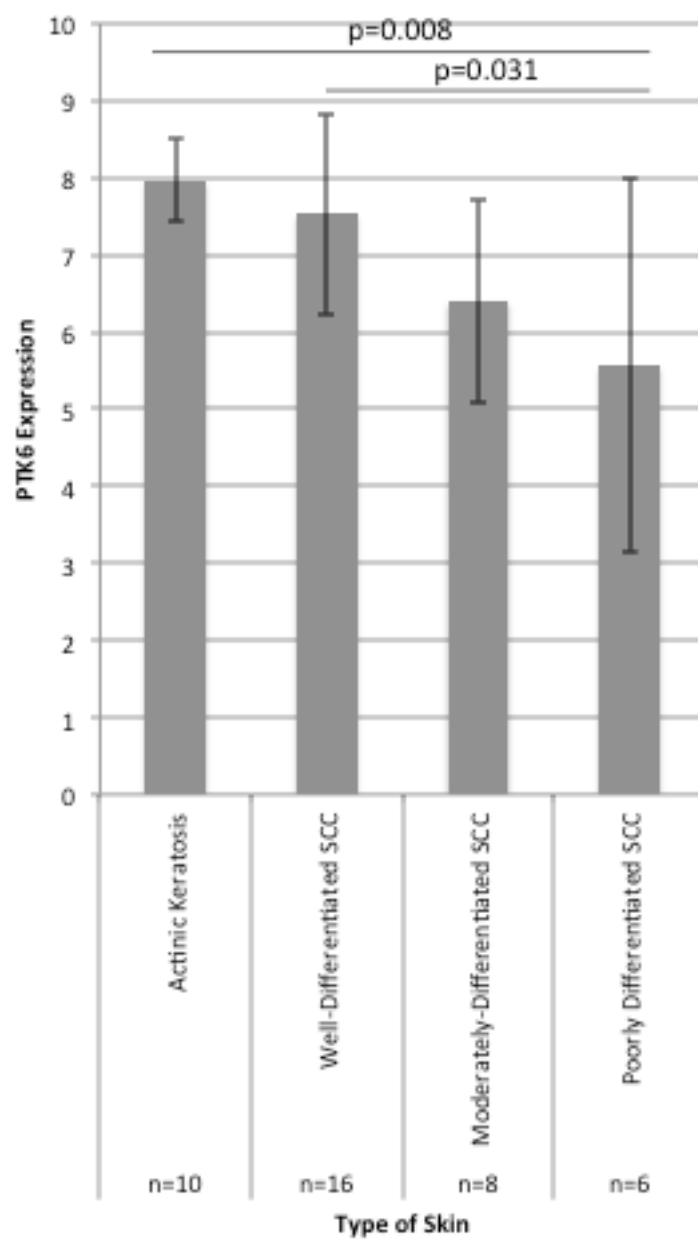
significantly decreased in SCC compared with actinic keratosis. Additionally, among the SCC samples, there was a significant difference between well-differentiated SCC and poorly-differentiated SCC.

I examined additional published datasets containing PTK6 expression in different types of SCC in different epithelial tissues, such as the cervix, esophagus, and oral mucosa. In these tissues, PTK6 expression consistently decreases in squamous cell carcinomas relative to normal tissue (Figure 22). Oral Squamous Cell Carcinomas were obtained from patients at the University of Medicine and Dentistry of New Jersey (Toruner et al. 2004). There was a significant decrease in PTK6 mRNA expression in OSCC cells compared with normal oral tissue (Figure 22A). A study for Head and Neck Squamous Cell Carcinoma included cancer tissues harvested from 22 patients and compared those tissues to similar tissues at distant locations from the tumor in the same patient (Kuriakose et al. 2004). There was significantly less PTK6 mRNA detected in the cancerous tissue compared with the normal tissue (Figure 22B). Cervical cancer tissues were obtained from patients in Spain and Columbia and frozen for use in research at Johns Hopkins Hospital and the University of Michigan Medical School (Zhai et al. 2007). In the epithelial linings of the cervix, PTK6 expression decreases in *in situ* lesions, and remains low after these lesions develop into squamous cell carcinomas (Figure 22C). A study of esophageal SCC in China (Hu et al. 2010) found a significant decrease in PTK6 mRNA expression in esophageal SCC compared with normal esophageal tissue (Figure 22D). These data support previous finding in which PTK6 expression decreases in SCC compared with normal human skin (Wang et al. 2005).

Figure 22: PTK6 mRNA expression decreases in human SCC

A: Expression of PTK6 mRNA in oral SCC obtained from the Toruner dataset (Toruner et al. 2004). Clinical samples were obtained and frozen for use in genetic screens.
B: Expression of PTK6 mRNA in HNSCC obtained from the Kuriakose dataset (Kuriakose et al. 2004). Clinical samples were obtained and frozen for use in genetic screens.
C: Expression of PTK6 mRNA in cervical SCC obtained from the Zhai dataset (Zhai et al. 2007). Clinical samples were obtained and frozen for use in genetic screens.
D: Expression of PTK6 mRNA in esophageal SCC obtained from the Hu dataset (Hu et al. 2010). Clinical samples were obtained and frozen for use in genetic screens.

A Toruner 2004
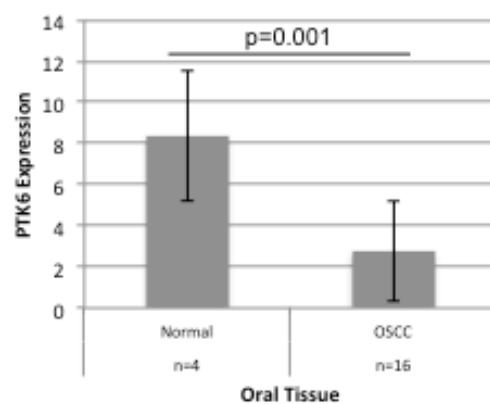
B Kuriakose 2004
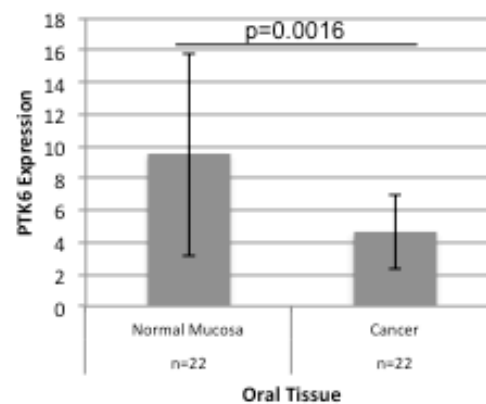
C Zhai 2007
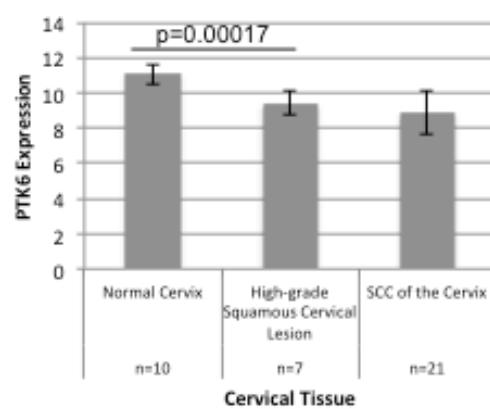
D Hu 2010
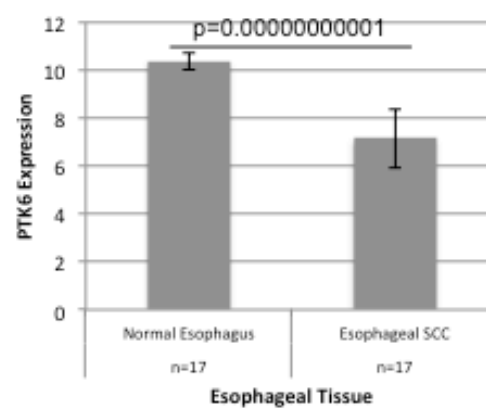
C.   PTK6 expression decreases in early carcinogenesis and then recovers

We used Oncomine to examine reported changes in PTK6 expression in Head and Neck Cancer (HNSCC). In the Ginos dataset (Ginos et al. 2004), mRNA was analyzed and relative levels of PTK6 were measured and sorted according multiple classifications, including tumor grade. Using the N-stage classification, which measures tumor development in the lymph nodes, we found that PTK6 mRNA decreases significantly in early stage of lymph node tumorigenesis (Figure 23). In lymph nodes with even higher number of tumors, PTK6 expression returns to normal levels. Statistical analysis determined that the decrease in PTK6 in N1 cancers is significant from both N0 and N2. In comparison, N0 and N2 cancers had the same level of PTK6 expression. It is possible that PTK6 expression decreases in the beginning stages of carcinogenesis, but then increases later as PTK6 assumes the role of an oncogene.

D.   Knockdown of PTK6 in Keratinocytes

One major tool for studying keratinocyte cells *in vitro* are HaCaT cells. HaCaT cells, a spontaneously immortalized human keratinocyte cell line frequently used for *in vitro* skin experiments (Deyrieux et al. 2007). HaCaT cells were cultured from an elderly Caucasian male, and were cultured under conditions of low calcium and high temperature, from which the name HaCaT (Human adult-Calcium-Temperature) derived. HaCaT cells contain mutant *p53*, which is typical of UV-damaged keratinocytes, and have increased telomerase activity. These cells can be used to study cellular effects of differentiation and ultraviolet irradiation on human cells (Deyrieux et al. 2007, Faurschou 2010). HaCaT cells can be efficiently transfected using Lipofectamine 2000 (Deyrieux et al. 2007) for transient transfections, as well as lentivirus for permanent transfections.

Figure 23: PTK6 expression in human HNSCC

Boxplot of PTK6 transcription from the Ginos dataset of HNSCC. Data is sorted according to N-stages, reflecting tumor development in lymph nodes. PTK6 transcription decreases in N1 cancers, but returns to normal in N2 and N3.
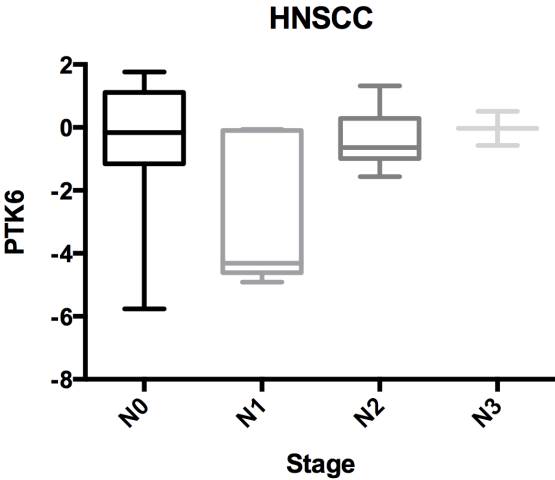
To identify whether PTK6 might have an effect on cell proliferation and differentiation, we generated PTK6 knockdown HaCaT cells using stable introduction of shRNA. We transfected these cells with two different shRNAs, #49 and #52, to knock down PTK6. We confirmed the knockdown of PTK6 by probing with two different antibodies against human PTK6 (Figure 24A). Both antibodies detected PTK6 expression in the scramble cell lines, although the Millipore monoclonal antibody detected PTK6 expression early in differentiation (day 2), while the G6 polyclonal antibody only detected PTK6 expression later in differentiation (day 9). Both antibodies detected a decrease in PTK6 expression in both shRNA knockdown cell lines. We also have preliminary data suggesting that keratin-14 expression, which is a marker for the mitotically active basal cell layer, decreases in the scramble cells after becoming confluent, but not in the shRNA knockdown cells after becoming confluent (not shown). We then analyzed relative growth of control and PTK6 knockdown HaCaT cells. Cells were plated at $1x10^3$ cells/60mm plate. The cells were then grown for two weeks, changing media every few days. The cells were resuspended and quantified using the Countess automated cell counter (Invitrogen) and then graphed (Figure 24B). There does not seem to be a significant difference in cell growth, either before of after achieving confluence, suggesting that PTK6 does not have a major effect on keratinocyte growth.

When the cells reached the desired density, they were irradiated with 25 mJ/cm^2 of UVB and harvested 10 minutes, 30 minutes, and 60 minutes after UVB treatment. Immunoblotting against these cell lysates showed a reduction of PTK6 in the shRNA knockdown cells. We used immunoblotting with antibodies specific for several cell signaling pathways affected by PTK6, primarily AKT, ERK1/2, ERK5, STAT3, FAK,

Figure 24: PTK6 is knocked down in HaCaT cells

A: Immunoblot analysis shows that PTK6 is successfully knocked down by both shRNA #49 and shRNA #52 constructs. Cells were harvested while they were preconfluent (60% confluent), 2 days after becoming confluent, and 9 days after becoming confluent. The Millipore monoclonal antibody detected PTK6 expression two days after differentiation, but the G6 polyclonal antibody did not. Both antibodies detected PTK6 9 days after confluence.

B: Growth curve of PTK6 knockdown HaCaT cells. Knocking down PTK6 does not have a significant impact of keratinocyte growth.

A

B
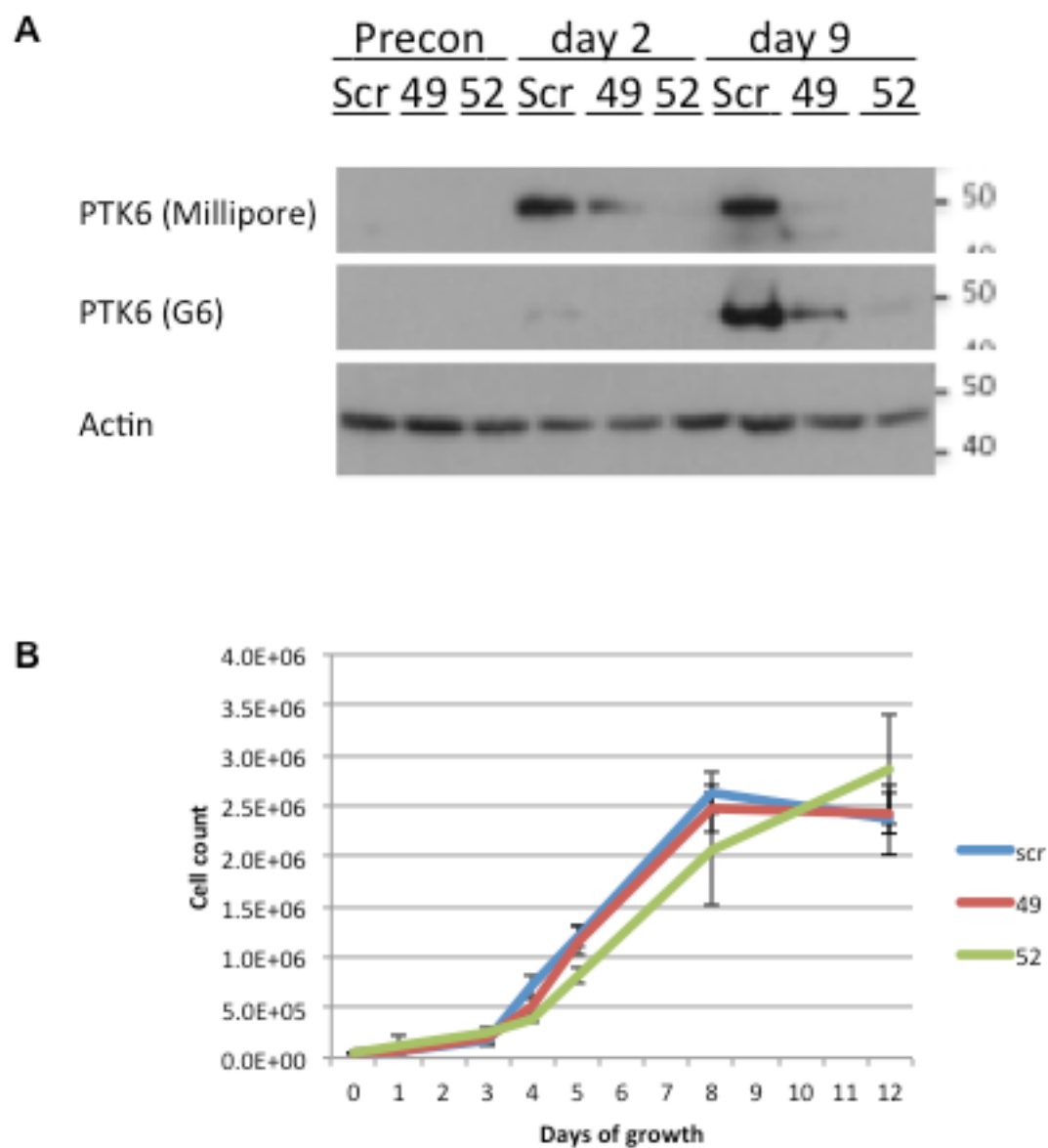
ErbB2 and EGFR. Few of these pathways were significantly affected by knocking down

PTK6 at the time points studied (Figure 25). There appears to be a slight difference in

AKT phosphorylation, and further studies will need to confirm this finding.

Figure 25: Cell signaling in PTK6 knockdown in HaCaT cells

HaCaT cells were exposed to UVB irradiation, and the lysates run on an SDS-PAGE and analyzed by immunoblotting. Antibodies against STAT3, ERK5, ERK1/2, EGFR, ErbB2, FAK, and AKT were used to identify differences in cell signaling. PTK6 is knocked down in shRNA cell lines. None of these cell-signaling pathways were significantly affected by knocking down PTK6.

UVB 25mJ/cm²: Untreated   10 min   30 min   60 hr

Scr 49 52 Scr 49 52 Scr 49 52 Scr 49 52

PTK6 — 50

P-Y705 STAT3 — 100 90 80

STAT3 — 100 90 80

P-FAK — 160 120

FAK — 160 120

EGFR — 220 160

ErbB2 — 160 120

B-Catenin — 100 90 80

P-Th308-AKT — 60

P-S473-AKT — 60

AKT — 60

P-Th218/Y220 ERK5 — 120 100 90 80

ERK5 — 160 120 100

P-Th202/Y204 ERK1/2 — 40

ERK1/2 — 40

Actin — 50 40
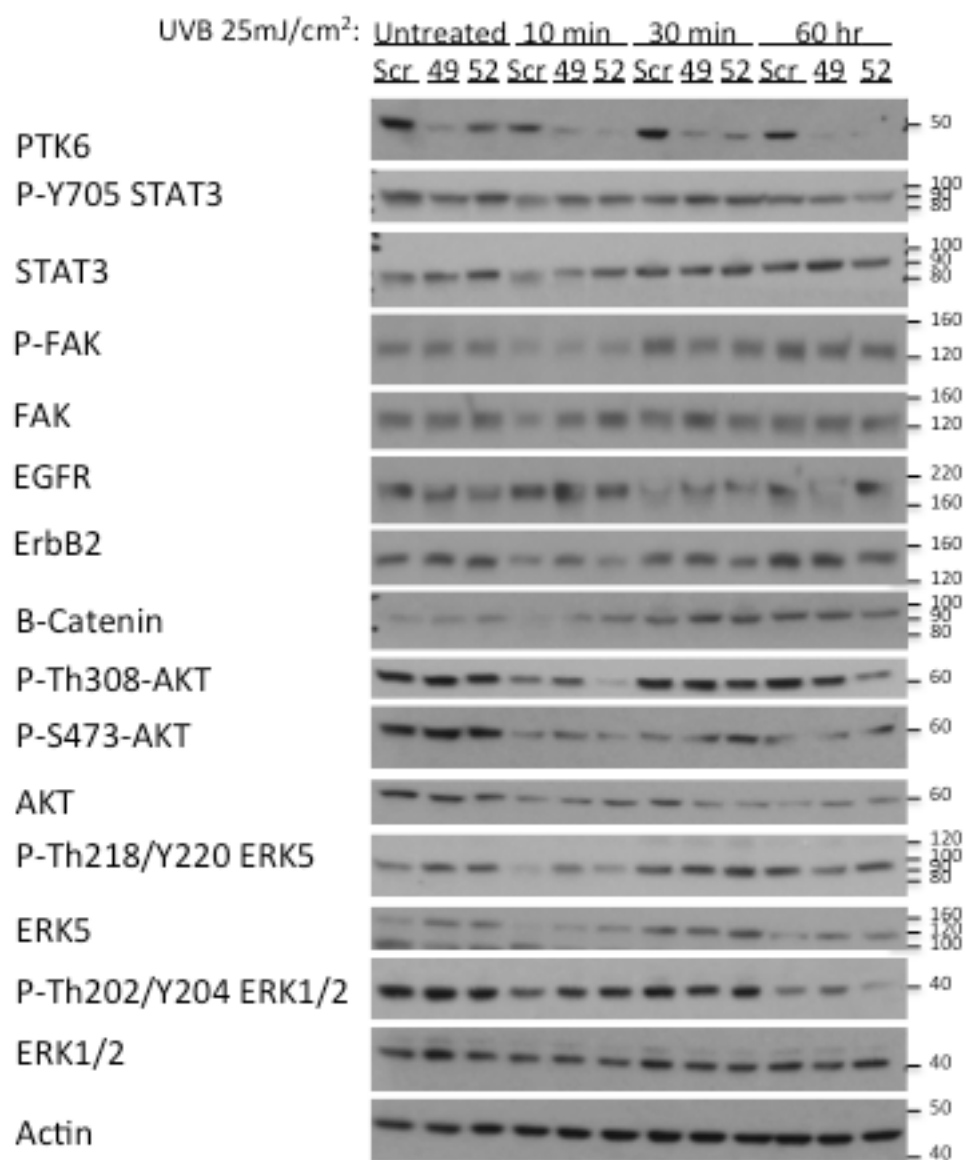
IV. DISCUSSION

1. Significance

PTK6 was first identified and characterized as promoting differentiation in skin. However, most recent research into PTK6 function in normal epithelial tissue has focused on the gastrointestinal tract, and PTK6 function has not been examined in skin *in vivo*. I hypothesized that as in other tissues, PTK6 could play two different roles in skin. I hypothesized that PTK6 would promote terminal differentiation and inhibit growth in normal skin, but would promote carcinogenesis under conditions of DNA damage. In order to resolve my hypothesis, I used the SENCAR mouse strain, which is particularly sensitive to carcinogenesis. SENCAR mice were selectively bred for sensitivity to developing skin tumors, and are 10-20 times more sensitive to DMBA/TPA induced skin cancer than CD-1 mice (DiGiovanni et al. 1980). SENCAR mice exhibit persistent hyperplasia as a result of sustained basal cell proliferation (Strickland 1986). After injury, basal skin cells in SENCAR mice do not return to their normal state of proliferation, and this elevated basal cell proliferation may promote sensitivity to carcinogenesis. We have shown that PTK6 expression, localization, and Y342 phosphorylation in SENCAR mice is abnormal compared with C57BL/6 mice (Figure 3), and may contribute to the increased sensitivity of SENCAR mice to tumorigenesis. *Ptk6*-/- SENCAR mice were resistant to inflammation (Figure 6) and tumor formation (Figures 8, 9), supporting our hypothesis that PTK6 promotes carcinogenesis after DNA damage.

Ptk6-/- mouse skin also exhibited impaired phosphorylation of STAT3, FAK, and BCAR1 (Figures 13, 14, 15). STAT3, FAK, and BCAR1 are all activated by Src and are important for promoting cell survival, proliferation, and migration. PTK6 promotes

STAT3 Y705 phosphorylation, dimerization, and translocation to the nucleus, where STAT3 promotes transcription of genes that inhibit apoptosis and promote proliferation, as well as genes that promote EMT. This data supports data previously generated in our lab showing that PTK6 promotes STAT3 activation in the colon after DNA damage (Gierut et al. 2011). FAK promotes activation of the AKT and MAPK pathways, and promotes migration, and PTK6 activation of FAK reinforces previous data in our lab (Zheng et al. 2012). BCAR1 similarly promotes cytoskeletal remodeling, migration, and invasion, and our data provides further support to previous data showing BCAR1 activation by PTK6 (Zheng et al. 2012). *Ptk6+/+* mouse skin tumors are also more mitotically active than *Ptk6-/-* mouse skin tumors, although PTK6 does not directly promote proliferation (Figure 10).

In contrast, *Ptk6-/-* neonatal mouse skin is more proliferative than *Ptk6+/+* neonatal mouse skin, which supports our hypothesis that PTK6 normally inhibits cell growth (Figure 11). There was no significant difference in epidermal architecture (Figures 11, 12). It appears that in normal mouse skin, abnormal PTK6 expression and activation does not have a significant impact. After DNA damage, SENCAR mouse skin becomes more proliferative in the basal layer and remains proliferative after the damage has been repaired (Strickland 1986). PTK6 has been shown to be Y342 phosphoyrlated primarily in areas of low PTK6 expression (Figures 3, 20). Normal SENCAR mouse skin has high expression, and low activation, of PTK6 in the basal layer, but PTK6 becomes active in the basal layer after DNA damage, which may then promote tumorigenesis.

2.   **PTK6 expression in normal skin**

The skin is one of the first tissues in which PTK6 was studied. PTK6 was originally cloned from melanocytes (Mitchell et al. 1994), and was localized to the granular layers of the skin during embryonic development (Vasioukhin et al. 1995). While PTK6 localization to differentiated cell layers has been previously reported in mouse skin (V. Vasioukhin 1997), we found that suprabasal localization was lost in SENCAR mouse skin (Figure 3C). We also determined that SENCAR mice, which are prone to forming skin tumors, have elevated expression of PTK6 compared with tumor-resistant C57BL/6 mice (Figures 3A, 3B). While phosphorylation of PTK6 at tyrosine 342 has never been studied in mouse skin, we found that PTK6 is Y342 phosphorylated in the basal layer in C57BL/6 mice, despite low expression (Figure 3C). Furthermore, this Y342 phosphorylation was lost in SENCAR mice. PTK6 localization to the suprabasal layer has also been reported in human skin (Wang et al. 2005). Our findings confirm that PTK6 localizes to the suprabasal layer in human skin (Figure 20A) and also explore Y342 phosphorylation. We found that PTK6 is minimally phosphorylated at Y342 in normal human skin, and that Y342 phosphorylated PTK6 localizes to the basal layer, as it does in neonatal mouse skin (Figure 20A). Throughout our studies, we have frequently found that Y342 phosphorylated PTK6 localizes to where there is low expression of PTK6.

A *Ptk6*-null mouse model was established in the C57BL/6 genetic background to study the role of PTK6 *in vivo*. Most studies so far have focused on the gastrointestinal tract, and *Ptk6-/-* mouse skin has not been well characterized. In the *Ptk6-/-* mouse intestine, there is increased proliferation in intestinal crypt cells compared to in *Ptk6+/+* intestinal crypts, along with greater cell turnover and proliferation throughout the

intestinal epithelia (Haegebarth et al. 2006). We found that in neonatal mouse skin, disruption of *Ptk6* causes the basal layer to become more proliferative, with a high percentage of basal cells expressing proliferation marker ki67 (Figures 11A, 11B). In adult SENCAR mouse skin, however, there was no significant difference in proliferation, as measured by both ki67 expression and BrdU incorporation (Figures 12A, 12B).

Ptk6-null mice also exhibit reduced differentiation of intestinal epithelial linings (Haegebarth et al. 2006), and villus length is significantly longer than in the wild type intestine, along with an expanded proliferation zone and delayed enterocyte differentiation. In contrast, we did not detect a significant difference in skin architecture. Keratin expression remained consistent between genotypes in both neonatal mouse skin and adult mouse skin, with keratin-14 confined to the basal layer and keratin-10 confined to the suprabasal layer, and minimal overlap between the epithelial markers (Figures 11C, 11D, 12C). We did not detect a significant difference in epidermal thickness in either adult or neonatal mouse skin. We also did not detect a significant difference in cell turnover in adult mouse skin, as measured using a TUNEL assay (Figure 12D). There may be an increase in apoptosis in neonatal mouse skin, as measured by cleaved caspase-3, and further examination is required (Figure 18).

In the gastrointestinal tract of *Ptk6*-/- mice, the cell signaling pathways can be affected. For example, *Ptk6*-/- intestinal epithelia display greater activation of AKT, as well as increased levels of nuclear β-catenin, which plays a role in regulating the Wnt pathway and regulates epithelial turnover in the skin and gastrointestinal tract (Haegebarth et al. 2006). PTK6 inhibits β-catenin by directly phosphorylating it and targeting it for degradation (Palka-Hamblin et al. 2010). However, we did not observe a

difference in cell signaling between *Ptk6+/+* and *Ptk6-/-* adult or neonatal mice. Phosphorylation of ERK1/2, ERK5, AKT, FAK and β-catenin was unaffected by disruption of *Ptk6*. However, we did see a decrease in Y165 phosphorylation of BCAR1 in adult *Ptk6-/-* mouse skin. Otherwise, disruption of *Ptk6* does not seem to have a significant impact on keratinocyte homeostasis and development.

Expression of PTK6 in normal epithelial tissues has also been extensively studied in cell culture. The role of PTK6 in differentiation was confirmed using embryonic mouse keratinocyte (EMK) cells, in which overexpression of PTK6 promotes expression of the skin differentiation marker filaggrin, and calcium induced differentiation of embryonic mouse keratinocytes promotes PTK6 activity (V. Vasioukhin 1997). Additionally, in HaCaT cells, confluence induces expression and co-localization of both PTK6 and the skin differentiation marker keratin-10 (Wang et al. 2005). We have generated stable PTK6 knockdown cell lines in the HaCaT keratinocyte cell line to further study the effect of knocking down PTK6 on keratinocytes. We have confirmed effective disruption in PTK6 expression (Figure 24A), but have not seen a significant effect on cell growth (Figure 24B). We expect to use this model in the future to better understand how PTK6 affects keratinocyte proliferation, differentiation, and cell signaling.

3.   PTK6 is upregulated and activated by UVB-induced DNA damage

The effect of DNA damage on PTK6 expression and activation has been best characterized in the gastrointestinal tract. In the intestine, PTK6 is expressed in the differentiated villus cells, but not in the proliferating crypt cells (Haegebarth et al. 2006), similar to PTK6 expression in the suprabasal layers of the skin but not in the basal layer.

PTK6 is induced in the intestinal crypt cell 6 hours after gamma-irradiation (Haegebarth et al. 2009). In SENCAR mouse skin, localization to the suprabasal layer is lost, so induction of PTK6 expression in the basal layer was not examined. In squamous cell carcinomas, PTK6 expression is reduced (Petro et al. 2004). However, in primary human keratinocytes, reduction in PTK6 expression results in a decrease in epidermal growth factor receptor (EGFR) along with an increase in keratin-10 (Tupper et al. 2011), suggesting that under certain conditions, PTK6 may depart from its typical role in differentiation and act as an oncogene.

After UVB irradiating SENCAR mice 5 times in 10 days, PTK6 expression increases significantly in SENCAR mouse skin (Figures 4A, 4B). Additionally, PTK6 is Y342 phosphorylated and localizes to the membrane in the basal layer (Figure 4C). In endpoint mouse skin tumors, PTK6 expression is ubiquitous in the epithelium, and PTK6-expressing cells have infiltrated the dermis (Figure 4D). PTK6 is Y342 phosphorylated at the membrane in both the epithelium and in the dermis. These cells have been confirmed to be of epithelial origin, and express keratin-14, indicating that they originated from the basal cell layer (Figures 5a, 5c, 5d, 5f).

In normal oral tissue and in well-differentiated oral squamous cell carcinomas (OSCCs), PTK6 localizes to the cytoplasm and the nucleus (Petro et al. 2004). In poorly differentiated OSCCs, PTK6 was excluded from the nucleus and exhibit perinuclear localization. In our study, Cells in the dermis that express keratin-10 compose well-differentiated squamous cell carcinomas and do not express PTK6 (Figures 5b, 5e), suggesting that PTK6 is specifically associated with anaplastic and poorly differentiated

squamous cell carcinomas. We did not observe clear differences in localization of total PTK6, and PTK6 was generally excluded from the nucleus in all PTK6-expressing cells.

In human squamous cell carcinomas (SCCs), we found that PTK6 was primarily expressed in differentiated squamous cell tissue and was Y342 phosphorylated in the undifferentiated basal cell layer (Figure 20B). This remains consistent with previous data in normal skin, in which PTK6 is Y342 phosphorylated primarily when it is lowly expressed. After examining a dataset of Head and Neck Squamous Cell Carcinomas (HNSCCs), we found that PTK6 mRNA transcription significantly dropped in the early (N1) stage of tumorigenesis in the lymph nodes, but returned to normal as the cancer progressed to higher (N2, N3) stages of tumorigenesis (Figure 23). It may be that PTK6 expression is down-regulated, while remaining PTK6 is Y342 phosphorylated and promotes carcinogenesis.

4. PTK6 promotes tumorigenesis in SENCAR mice

As in intestinal and epidermal epithelial cells, PTK6 is upregulated in colon cancer, despite normally being expressed in only differentiated colon epithelial cells (Llor et al. 1999). When treated with azoxymethane (AOM), *Ptk6*-/- mice exhibit increased resistance to colonic tumor formation compared with wild type mice (Gierut et al. 2011). We found that *Ptk6*-/- mice are similarly resistant to UVB-induced inflammation (Figure 6), tumor formation (Figures 8B, 8C), and mortality (Figure 8A). Mortality was not closely linked with tumor size or load (Figure 9), and there was no evidence of metastasis of tumors outside of the epidermis. As a result, we were unable to ascertain a clear cause of death, despite a significant difference in mortality between the two genotypes. Interestingly, UVB irradiation also eliminated the weight difference between *Ptk6*+/+ and

Ptk6-/- mice, with *Ptk6*+/+ remaining at an average weight of about 30 grams (Figure 7B). It is possible that this change may be due to the added stress caused by the UVB treatments.

Proliferation increases in the basal layer in both genotypes, and there is no significant difference between them as detected by either ki67 expression (Figure 12A) or BrdU incorporation (Figure 12B). H&E stained sections of mouse skin tumors showed a higher mitotic rate in *Ptk6*+/+ skin tumors compared with *Ptk6*-/- skin tumors. We examined these tumors for BrdU incorporation to measure proliferation, and determined that there was no significant difference in BrdU incorporation between *Ptk6*+/+ and *Ptk6*-/- mouse skin tumors (Figures 10A, 10B). BrdU incorporation reports cells in S-phase, so it may be that *Ptk6*-/- cells are stuck in S-phase but are unable to complete mitosis. Additionally, cell in which PTK6 is Y342 phosphorylated at the membrane do not incorporate BrdU (Figure 10A), suggesting that while *Ptk6*+/+ skin tumors have a higher mitotic rate, PTK6 is not directly promoting proliferation.

Despite increased resistance to UVB-induced inflammation, *Ptk6*-/- did not exhibit any significant alterations to the architecture of the skin, as measured by keratin localization (Figure 12C). Keratin-14 expression expands into the suprabasal layer, while keratin-10 remains confined to the suprabasal layer. Disruption of *Ptk6* did not enlarge or diminish the proliferative zones before or after UVB treatment.

In other PTK6-expressing tissues, PTK6 has a major impact on cell survival. In the colonic crypt cells after AOM treatment, and there is more apoptosis in *Ptk6*+/+ crypts than in *Ptk6*-/- crypts (Gierut et al. 2010). In an immortalized nontransformed Rat1A cell line, expression of PTK6 sensitizes the cell to apoptotic stimuli, such as serum

deprivation and UV irradiation (Haegebarth et al. 2005). Additional studies show that after gamma irradiation, PTK6-induction in the intestinal crypt cells promote DNA-damaged induced apoptosis. Disrupting *Ptk6* results in an increase in the MAPK pro-survival signaling pathway and impedes apoptosis in irradiated mice, and *Ptk6+/+* intestinal crypt cells are more proliferative after gamma irradiation (Haegebarth et al. 2009). However, *Ptk6+/+* and *Ptk6-/-* UVB-treated mouse skin did not exhibit a significant difference in cell death, as measured by TUNEL assay (Figure 12D). When neonatal mouse skin was exposed to UVB, there was no significant difference in cleaved caspace-3 in either genotype (Figure 18E). These data suggest that PTK6 does not directly promote cell turnover in UVB-irradiated skin.

5.   PTK6 promotes cell signaling pathways after UVB irradiation

Previous work from our lab showed that disruption of PTK6 inhibits STAT3 Y705 phosphorylation activation after AOM treatment (Gierut et al. 2011). STAT3 is an important transcription factor that promotes proliferation and survival in the gastrointestinal tract and in skin. UVB irradiation causes G1 cell cycle arrest in keratinocytes, which is usually followed by proapoptotic signals. STAT3 can target these pathways to prevent apoptosis and promote proliferation (Sano et al. 2008). Disruption of *Stat3* significantly increases keratinocyte stem cell apoptosis following treatment with DMBA/TPA carcinogens (Kim et al. 2009), showing how STAT3 promotes survival of DNA-damaged cells. STAT3 has also been shown to interact with Twist, a transcription factor known to promote the epithelial-mesenchymal transition (EMT) (Macias et al. 2013). We found that STAT3 Y705 phosphorylation (Figures 13A, 13B) and localization to the nucleus (Figures 13C) is impaired in *Ptk6-/-* short-term UVB-treated mouse skin.

STAT3 remains more active in *Ptk6*+/+ mouse epithelial skin cells at the endpoint UVB-treated mouse skin tumors (Figure 13D). These data suggest that PTK6 plays an important role in Y705 phosphorylation of STAT3 following UVB irradiation, which would help promote skin carcinogenesis and EMT. However, we did not observe a similar effect in UVB-treated neonatal mouse skin (Figure 18A). It is possible that we need a longer time-point in the neonatal mice to observe efficient STAT3 Y705 phosphorylation. It is also possible that neonatal mouse skin, which is still developing, responds differently to UVB irradiation than adult mouse skin.

BCAR1 is a docking protein that can be activated by Src and promote activation of ERK and AKT pathways. BCAR1 interacts with a wide variety of cell signaling pathways, and BCAR1 phosphorylation is a key event for cytoskeletal reorganization (Barrett et al. 2013). Activation of BCAR can promote lamellipodia formation, which promotes cell mobility and migration (Mitra et al. 2005). PTK6 directly phosphorylates BCAR1 on tyrosine 165 (Zheng et al. 2012), and we have already shown impaired Y165 phosphorylation in *Ptk6*-/- mouse skin (Figure 15A), which may indicate impaired migration of basal cells into the suprabasal layer. We found that Y165 phosphorylation of BCAR1 remains impaired after UVB irradiation. Short-term UVB-treated *Ptk6*-/- displayed minimal BCAR1 Y165 phosphorylation at the membrane, compared with robust Y165 phosphorylation at the membrane in *Ptk6*+/+ mouse skin (Figure 15B). This difference was maintained in endpoint mouse skin tumors, in which there was significantly less Y165 phosphorylation of BCAR1 in *Ptk6*-/- mouse skin tumors than *Ptk6*+/+ mouse skin tumors (Figure 15C). Reduced BCAR1 activation, especially coupled with reduced STAT3 activation, after UVB irradiation could potentially impair

epidermal hyperplasia following DNA damage. Hyperplasia serves to thicken the skin to protect against further DNA damage, but this function can be potentially oncogenic. PTK6 activation may strengthen the oncogenic potential of hyperplasia and promote carcinogenesis.

Like BCAR1, FAK is involved in integrin signaling and promotes survival and migration, and is also a substrate of PTK6 (Zheng et al. 2012). FAK is a tyrosine kinase that promotes activation of numerous signaling cascades, such as AKT and the MAPK pathway. Defective FAK expression in skin epithelial cells results in an impaired hair cycle (Essayem et al. 2006), and FAK expression progressively increases in skin papillomas, squamous cell carcinomas (SCC), and spindle cell carcinomas (SCT) (McLean et al. 2005). Integrin clustering as a result of cell-cell interactions causes phosphorylation of FAK. FAK is phosphorylated at Y925, which leads to further activation of the MAPK pathway (McLean et al. 2005, Mitra et al. 2005, Essayem et al. 2006), as well as Y576/Y577 in the kinase domain, which is required for full activation (McLean et al. 2005, Mitra et al. 2005). PTK6 phosphorylates FAK at both of these sites, and may play similar role to Src. Neither site is phosphorylated in normal mouse skin in either genotype (Figure 14A). After short-term UVB irradiation, FAK is phosphorylated at both sites in *Ptk6+/+* mouse skin, but not in *Ptk6-/-* mouse skin (Figure 14B). In the endpoint mouse skin tumors, this difference is maintained, and there is significantly less phosphorylation of FAK at both sites in *Ptk6-/-* mouse skin tumors than in *Ptk6+/+* mouse skin tumors (Figure 14C). PTK6 phosphorylation of Y576/Y577 in UVB-treated mouse suggests that PTK6 plays an important role in activation of FAK downstream targets, such as AKT, in keratinocytes after UVB-induced DNA damage.

Phosphorylation of Y925 suggests that PTK6 may also be important for the activation of the Ras/MAPK pathway in UVB-treated skin. By activating FAK, PTK6 has the potential to initiate cytoskeletal remodeling and to promote migration and invasion.

There are many other pathway which are affected by PTK6 in response to DNA damage, including AKT, ERK1/2, ERK5, and β-catenin (Brauer et al. 2010). We examined these pathways for phosphorylation after UVB irradiation and found that PTK6 had little effect on them. ERK1/2 and AKT phosphorylation was unaffected by disruption of *Ptk6* in neonatal mouse skin, either before or after UVB irradiation (Figure 16). In adult short-term UVB-treated skin, there was no significant difference in phosphorylation or localization of AKT, ERK1/2, ERK5, or β-catenin (Figure 17). Similarly, there was no significant difference in phosphorylation or localization of AKT or ERK5, in UVB-treated neonatal mouse skin (Figures 18C, 18D). In endpoint mouse skin tumors, there was no difference in active β-catenin localization or AKT phosphorylation (Figure 19). We did observe a significant difference in ERK1/2 phosphorylation after UVB. In neonatal mouse skin, there was extensive ERK1/2 phosphorylation after UVB in *Ptk6*-/- skin, and minimal ERK1/2 phosphorylation in *Ptk6*+/+ skin (Figure 18B). However, there was significantly more phosphorylation of ERK1/2 in *Ptk6*+/+ mouse skin tumors than in *Ptk6*-/- mouse skin tumors (Figure 19). It is possible that the difference in in neonatal UVB-treated skin and in adult mouse skin tumors may reflect the role of ERK1/2 phosphorylation in adult mouse skin and neonatal mouse skin.

Stable shRNA knockdown of PTK6 also impaired basal STAT3 activation in HCT116 human colon cancer cells, and PTK6 also promotes STAT3 activation in YAMC cells (Gierut et al. 2012). We generated HaCaT cells with a stable stable

knockdown of PTK6 to determine if a similar effect occurred in keratinocytes. Control and knockdown HaCaT cells were exposed to a low dose of UVB irradiation and analyzed via immunoblotting. None of the signaling pathways examined showed a consistent significant difference in phosphorylation in PTK6 knockdown HaCaT cells (Figure 25). Some cell signaling pathways merit further study, such as ERK5 and ERK1/2, as they may have a slight increase in phosphorylation immediately after UVB irradiation. Further experiments performed under different levels of UVB and different time-points may yield different results, and additional studies are needed.

Additionally, we found that disruption of *Ptk6* has a significant impact on weight gain in SENCAR mice (Figure 7A). *Ptk6+/+* mice became highly obese, weighing up to 50 grams, while *Ptk6-/-* mice remained slim, with an average weight of about 30 grams. *Ptk6-/-* were also much more active than *Ptk6+/+* mice, which remained fairly sedate. There are a variety of possible explanations for this weight difference. Disruption of *Ptk6* has been shown to affect differentiation of C57BL/6 intestinal epithelium, and *Ptk6-/-* mice may have impaired intestinal absorption. *Ptk6-/-* may also have impaired oral epithelial linings, which may impact tooth development or appetite. Finally, there may be additional behavioral anomalies that have not yet been explored.

6.   Conclusion

Although PTK6 was first identified in melanocytes, and its role in differentiation characterized in keratinocytes, relatively little work has been done to study the role of PTK6 in skin. Most of the research on PTK6 either focuses on its role in the gastrointestinal tract or in tissues where it is normally minimally expressed but overexpressed in cancer. My work in this field has characterized the role of PTK6 in skin

development and carcinogenesis. Additional work is needed to further understand how PTK6 can promote both differentiation in normal skin and carcinogenesis in DNA-damaged skin.

My work is also the first to address Y342 phosphorylation in human and mouse skin. I found that PTK6 Y342 phosphorylation is frequently inversely proportional to its expression. In normal and cancerous human skin, Y342 PTK6 phosphorylation occurs in the basal layer, in which minimal PTK6 is expressed. PTK6 is also Y342 phosphorylated in the basal layer in C57BL/6 mice, which contains minimal PTK6 protein. This suggests that PTK6 may perform two different functions, one that is independent of Y342 phosphorylation, and another when it is phosphorylated.

In the course of my research, I found that PTK6 localization in skin is not consistent in all mouse strains, and that cancer sensitive mice have abnormal PTK6 expression and localization. I also found that in this cancer sensitive mouse strain, PTK6 is responsible for differences in weight and behavior. These mice also have impaired Y342 phosphorylation of PTK6 in the basal cell layer of normal skin.

PTK6 promotes tumorigenesis in cancer-sensitive mice, which corresponds to previous work done in the colon (Gierut et al. 2011). Similarly, PTK6 phosphorylation of STAT3, FAK, and BCAR1 is impaired in all UVB-treated tissues, which matches work done in the colon (Gierut et al. 2011) and in the prostate (Zheng et al. 2012, Zheng et al. 2012). While the role of PTK6 in skin may not be identical to its role in the gastrointestinal tract or in prostate, there is a commonality to its function in these tissues. PTK6 is activated following UVB irradiation and translocates to the membrane (Figure 26). PTK6 activates STAT3, which translocates to the nucleus to promote survival and

Figure 26: Model for PTK6 function in UVB-treated skin

After UVB irradiation, PTK6 is Y342 phosphorylated and translocates to the membrane. PTK6 Y705 phosphorylates STAT3, which translocates to the nucleus to promote survival and proliferation. PTK6 phosphorylates FAK on Y576/Y577 and on Y925, and BCAR1 on Y165. FAK and BCAR1 then promote migration and invasion.
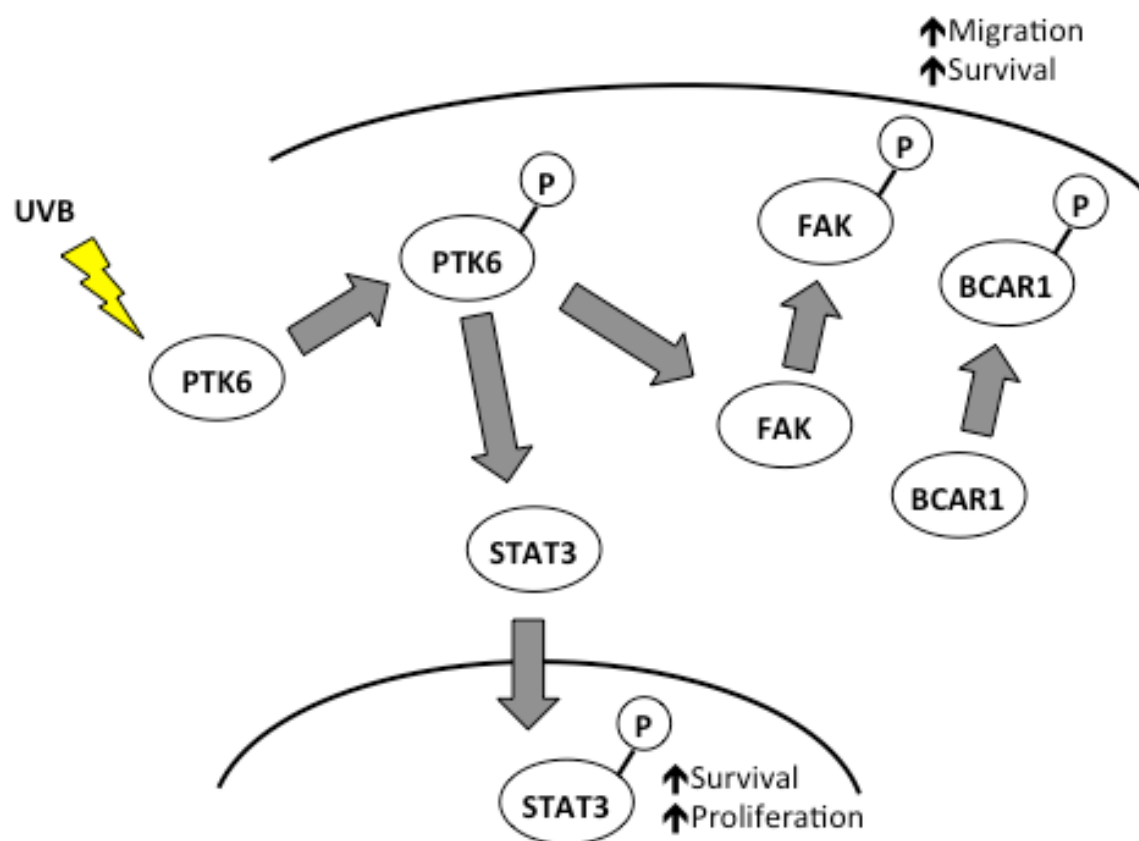
proliferation. PTK6 also activates BCAR1 and FAK, which promote survival and migration.

Ultimately, my research into PTK6 function in UVB-treated skin has helped us to further our model what role PTK6 plays in epithelial tissues. My data seems to support the idea that PTK6 protein expression promotes differentiation in inhibition of cells growth in normal epithelial tissues. After DNA damage, PTK6 becomes Y342 phosphorylated and promotes proliferation. This theory is supported by the fact that PTK6 is typically down-regulated in skin squamous cell carcinomas and in head and neck squamous cell carcinomas. PTK6 activity has never been studied in human skin before, and hopefully my research will enable further exploration into PTK6 function in skin carcinogenesis.

V. Cited Literature

Ai, M., K. Liang, Y. Lu, S. Qiu and Z. Fan (2013). "Brk/PTK6 cooperates with HER2 and Src in regulating breast cancer cell survival and epithelial-to-mesenchymal transition." Cancer biology & therapy **14**(3): 237-245. .

Aubele, M., A. K. Walch, N. Ludyga, H. Braselmann, M. J. Atkinson, B. Luber, G. Auer, S. Tapio, T. Cooke and J. M. Bartlett (2008). "Prognostic value of protein tyrosine kinase 6 (PTK6) for long-term survival of breast cancer patients." Br J Cancer **99**(7): 1089-1095.

Balsas, P., N. Lopez-Royuela, P. Galan-Malo, A. Anel, I. Marzo and J. Naval (2009). "Cooperation between Apo2L/TRAIL and bortezomib in multiple myeloma apoptosis." Biochem Pharmacol **77**(5): 804-812.

Barker, K. T., L. E. Jackson and M. R. Crompton (1997). "BRK tyrosine kinase expression in a high proportion of human breast carcinomas." Oncogene **15**(7): 799-805.

Barrett, A., C. Pellet-Many, I. C. Zachary, I. M. Evans and P. Frankel (2013). "p130Cas: a key signalling node in health and disease." Cell Signal **25**(4): 766-777.

Born, M., L. Quintanilla-Fend, H. Braselmann, U. Reich, M. Richter, P. Hutzler and M. Aubele (2005). "Simultaneous over-expression of the Her2/neu and PTK6 tyrosine kinases in archival invasive ductal breast carcinomas." J Pathol **205**(5): 592-596.

Bose, P., N. T. Brockton and J. C. Dort (2013). "Head and neck cancer: from anatomy to biology." Int J Cancer **133**(9): 2013-2023.

Bouton, A. H., R. B. Riggins and P. J. Bruce-Staskal (2001). "Functions of the adapter protein Cas: signal convergence and the determination of cellular responses." Oncogene **20**(44): 6448-6458.

Brauer, P. M. and A. L. Tyner (2009). "RAKing in AKT: a tumor suppressor function for the intracellular tyrosine kinase FRK." Cell Cycle **8**(17): 2728-2732.

Brauer, P. M. and A. L. Tyner (2010). "Building a better understanding of the intracellular tyrosine kinase PTK6 - BRK by BRK." Biochimica et biophysica acta **1806**(1): 66-73.

Brauer, P. M., Y. Zheng, M. D. Evans, C. Dominguez-Brauer, D. M. Peehl and A. L. Tyner (2011). "The Alternative Splice Variant of Protein Tyrosine Kinase 6 Negatively Regulates Growth and Enhances PTK6-Mediated Inhibition of beta-Catenin." PLoS One **6**(3): e14789.

Brauer, P. M., Y. Zheng, L. Wang and A. L. Tyner (2010). "Cytoplasmic retention of protein tyrosine kinase 6 promotes growth of prostate tumor cells." Cell cycle **9**(20): 4190-4199.

Brinkman, A., S. van der Flier, E. M. Kok and L. C. Dorssers (2000). "BCAR1, a human homologue of the adapter protein p130Cas, and antiestrogen resistance in breast cancer cells." J Natl Cancer Inst **92**(2): 112-120.

Cabodi, S., A. Tinnirello, B. Bisaro, G. Tornillo, M. del Pilar Camacho-Leal, G. Forni, R. Cojoca, M. Iezzi, A. Amici, M. Montani, A. Eva, P. Di Stefano, S. K. Muthuswamy, G. Tarone, E. Turco and P. Defilippi (2010). "p130Cas is an essential transducer element in ErbB2 transformation." FASEB journal : official publication of the Federation of American Societies for Experimental Biology **24**(10): 3796-3808.

Cabodi, S., A. Tinnirello, P. Di Stefano, B. Bisaro, E. Ambrosino, I. Castellano, A. Sapino, R. Arisio, F. Cavallo, G. Forni, M. Glukhova, L. Silengo, F. Altruda, E. Turco, G. Tarone and P. Defilippi (2006). "p130Cas as a new regulator of mammary epithelial cell proliferation, survival, and HER2-neu oncogene-dependent breast tumorigenesis." Cancer Res **66**(9): 4672-4680.

Chakraborty, G., S. Jain and G. C. Kundu (2008). "Osteopontin promotes vascular endothelial growth factor-dependent breast tumor growth and angiogenesis via autocrine and paracrine mechanisms." Cancer Res **68**(1): 152-161.

Chan, K. S., S. Sano, K. Kiguchi, J. Anders, N. Komazawa, J. Takeda and J. DiGiovanni (2004). "Disruption of Stat3 reveals a critical role in both the initiation and the promotion stages of epithelial carcinogenesis." J Clin Invest **114**(5): 720-728.

Chen, H. Y., C. H. Shen, Y. T. Tsai, F. C. Lin, Y. P. Huang and R. H. Chen (2004). "Brk activates rac1 and promotes cell migration and invasion by phosphorylating paxillin." Mol Cell Biol **24**(24): 10558-10572.

Cohen, R. B. (2014). "Current challenges and clinical investigations of epidermal growth factor receptor (EGFR)- and ErbB family-targeted agents in the treatment of head and neck squamous cell carcinoma (HNSCC)." Cancer Treat Rev **40**(4): 567-577.

Cowley, G. P., J. A. Smith and B. A. Gusterson (1986). "Increased EGF receptors on human squamous carcinoma cell lines." Br J Cancer **53**(2): 223-229.

Derry, J. J., G. S. Prins, V. Ray and A. L. Tyner (2003). "Altered localization and activity of the intracellular tyrosine kinase BRK/Sik in prostate tumor cells." Oncogene **22**(27): 4212-4220.

Derry, J. J., S. Richard, H. Valderrama Carvajal, X. Ye, V. Vasioukhin, A. W. Cochrane, T. Chen and A. L. Tyner (2000). "Sik (BRK) phosphorylates Sam68 in the nucleus and negatively regulates its RNA binding ability." Mol Cell Biol **20**(16): 6114-6126.

Deyrieux, A. F. and V. G. Wilson (2007). "In vitro culture conditions to study keratinocyte differentiation using the HaCaT cell line." Cytotechnology **54**(2): 77-83.

DiGiovanni, J., T. J. Slaga and R. K. Boutwell (1980). "Comparison of the tumor-initiating activity of 7,12-dimethylbenz[a]anthracene and benzo[a]pyrene in female SENCAR and CS-1 mice." Carcinogenesis **1**(5): 381-389.

Dorssers, L. C., N. Grebenchtchikov, A. Brinkman, M. P. Look, S. P. van Broekhoven, D. de Jong, H. A. Peters, H. Portengen, M. E. Meijer-van Gelder, J. G. Klijn, D. T. van Tienoven, A. Geurts-Moespot, P. N. Span, J. A. Foekens and F. C. Sweep (2004). "The prognostic value of BCAR1 in patients with primary breast cancer." Clin Cancer Res **10**(18 Pt 1): 6194-6202.

Easty, D. J., P. J. Mitchell, K. Patel, V. A. Florenes, R. A. Spritz and D. C. Bennett (1997). "Loss of expression of receptor tyrosine kinase family genes PTK7 and SEK in metastatic melanoma." Int J Cancer **71**(6): 1061-1065.

Essayem, S., B. Kovacic-Milivojevic, C. Baumbusch, S. McDonagh, G. Dolganov, K. Howerton, N. Larocque, T. Mauro, A. Ramirez, D. M. Ramos, S. J. Fisher, J. L. Jorcano, H. E. Beggs, L. F. Reichardt and D. Ilic (2006). "Hair cycle and wound healing in mice with a keratinocyte-restricted deletion of FAK." Oncogene **25**(7): 1081-1089.

Fan, G., G. Lin, R. Lucito and N. K. Tonks (2013). "Protein-tyrosine phosphatase 1B antagonized signaling by insulin-like growth factor-1 receptor and kinase BRK/PTK6 in ovarian cancer cells." The Journal of biological chemistry **288**(34): 24923-24934.

Faurschou, A. (2010). "Role of tumor necrosis factor-alpha in the regulation of keratinocyte cell cycle and DNA repair after ultraviolet-B radiation." Dan Med Bull **57**(10): B4179.

Fromont, G., G. Vallancien, P. Validire, P. Levillain and O. Cussenot (2007). "BCAR1 expression in prostate cancer: association with 16q23 LOH status, tumor progression and EGFR/KAI1 staining." Prostate **67**(3): 268-273.

Fuchs, E. and J. A. Nowak (2008). "Building Epithelial Tissues from Skin Stem Cells." Cold Spring Harb Symp Quant Biol.

Gaffney, D. C., H. P. Soyer and F. Simpson (2014). "The epidermal growth factor receptor in squamous cell carcinoma: An emerging drug target." Australas J Dermatol **55**(1): 24-34.

Gao, Y., V. Cimica and N. C. Reich (2012). "Suppressor of cytokine signaling 3 inhibits breast tumor kinase activation of STAT3." The Journal of biological chemistry **287**(25): 20904-20912.

Gierut, J., Y. Zheng, W. Bie, R. E. Carroll, S. Ball-Kell, A. Haegebarth and A. L. Tyner (2011). "Disruption of the Mouse Protein Tyrosine Kinase 6 Gene Prevents STAT3 Activation and Confers Resistance to Azoxymethane." Gastroenterology **141**(4): 1371-1380 e1372.

Gierut, J. J., P. S. Mathur, W. Bie, J. Han and A. L. Tyner (2012). "Targeting Protein Tyrosine Kinase 6 Enhances Apoptosis of Colon Cancer Cells Following DNA Damage." Molecular cancer therapeutics **11**(11): 2311-2320.

Gierut, J. J., A. O. Perekatt, J. Han and A. L. Tyner (2010). "Protein Tyrosine Kinase 6 promotes apoptosis of p53-/- human colon cancer cells after DNA-damage.   ." Gastroenterology W1748.

Ginos, M. A., G. P. Page, B. S. Michalowicz, K. J. Patel, S. E. Volker, S. E. Pambuccian, F. G. Ondrey, G. L. Adams and P. M. Gaffney (2004). "Identification of a gene expression signature associated with recurrent disease in squamous cell carcinoma of the head and neck." Cancer Res **64**(1): 55-63.

Goel, R. K., S. Miah, K. Black, N. Kalra, C. Dai and K. E. Lukong (2013). "The unique N-terminal region of SRMS regulates enzymatic activity and phosphorylation of its novel substrate docking protein 1." FEBS J **280**(18): 4539-4559.

Grivennikov, S. I. and M. Karin (2010). "Dangerous liaisons: STAT3 and NF-kappaB collaboration and crosstalk in cancer." Cytokine Growth Factor Rev **21**(1): 11-19.

Haegebarth, A., W. Bie, R. Yang, S. E. Crawford, V. Vasioukhin, E. Fuchs and A. L. Tyner (2006). "Protein tyrosine kinase 6 negatively regulates growth and promotes enterocyte differentiation in the small intestine." Molecular and Cellular Biology **26**(13): 4949-4957.

Haegebarth, A., D. Heap, W. Bie, J. J. Derry, S. Richard and A. L. Tyner (2004). "The nuclear tyrosine kinase BRK/Sik phosphorylates and inhibits the RNA-binding activities of the Sam68-like mammalian proteins SLM-1 and SLM-2." J Biol Chem **279**(52): 54398-54404.

Haegebarth, A., R. Nunez and A. L. Tyner (2005). "The Intracellular Tyrosine Kinase Brk Sensitizes Non-Transformed Cells to Inducers of Apoptosis." Cell Cycle **4**(9): 1239-1246.

Haegebarth, A., A. O. Perekatt, W. Bie, J. J. Gierut and A. L. Tyner (2009). "Induction of protein tyrosine kinase 6 in mouse intestinal crypt epithelial cells promotes DNA damage-induced apoptosis." Gastroenterology **137**(3): 945-954.

Han, C. Y., S. C. Lim, H. S. Choi and K. W. Kang (2008). "Induction of ErbB2 by ultraviolet A irradiation: potential role in malignant transformation of keratinocytes." Cancer Sci **99**(3): 502-509.

Harvey, A. J. and M. R. Crompton (2003). "Use of RNA interference to validate Brk as a novel therapeutic target in breast cancer: Brk promotes breast carcinoma cell proliferation." Oncogene **22**(32): 5006-5010.

Harvey, A. J., C. J. Pennington, S. Porter, R. S. Burmi, D. R. Edwards, W. Court, S. A. Eccles and M. R. Crompton (2009). "Brk protects breast cancer cells from autophagic cell death induced by loss of anchorage." <u>Am J Pathol</u> **175**(3): 1226-1234.

Honda, H., H. Oda, T. Nakamoto, Z. Honda, R. Sakai, T. Suzuki, T. Saito, K. Nakamura, K. Nakao, T. Ishikawa, M. Katsuki, Y. Yazaki and H. Hirai (1998). "Cardiovascular anomaly, impaired actin bundling and resistance to Src-induced transformation in mice lacking p130Cas." <u>Nat Genet</u> **19**(4): 361-365.

Hu, N., R. J. Clifford, H. H. Yang, C. Wang, A. M. Goldstein, T. Ding, P. R. Taylor and M. P. Lee (2010). "Genome wide analysis of DNA copy number neutral loss of heterozygosity (CNNLOH) and its relation to gene expression in esophageal squamous cell carcinoma." <u>BMC Genomics</u> **11**: 576.

Ikeda, O., Y. Sekine, A. Mizushima, M. Nakasuji, Y. Miyasaka, C. Yamamoto, R. Muromoto, A. Nanbo, K. Oritani, A. Yoshimura and T. Matsuda (2010). "Interactions of STAP-2 with Brk and STAT3 participate in cell growth of human breast cancer cells." <u>J Biol Chem</u> **285**(49): 38093-38103.

Imamoto, A., X. J. Wang, H. Fujiki, S. E. Walker, L. M. Beltran and J. DiGiovanni (1993). "Comparison of 12-O-tetradecanoylphorbol-13-acetate and teleocidin for induction of epidermal hyperplasia, activation of epidermal PKC isozymes and skin tumor promotion in SENCAR and C57BL/6 mice." <u>Carcinogenesis</u> **14**(4): 719-724.

Irie, H. Y., Y. Shrestha, L. M. Selfors, F. Frye, N. Iida, Z. Wang, L. Zou, J. Yao, Y. Lu, C. B. Epstein, S. Natesan, A. L. Richardson, K. Polyak, G. B. Mills, W. C. Hahn and J. S. Brugge (2010). "PTK6 regulates IGF-1-induced anchorage-independent survival." <u>PLoS One</u> **5**(7): e11729.

Kamalati, T., H. E. Jolin, M. J. Fry and M. R. Crompton (2000). "Expression of the BRK tyrosine kinase in mammary epithelial cells enhances the coupling of EGF signalling to PI 3-kinase and Akt, via erbB3 phosphorylation." <u>Oncogene</u> **19**(48): 5471-5476.

Kamalati, T., H. E. Jolin, P. J. Mitchell, K. T. Barker, L. E. Jackson, C. J. Dean, M. J. Page, B. A. Gusterson and M. R. Crompton (1996). "Brk, a breast tumor-derived non-receptor protein-tyrosine kinase, sensitizes mammary epithelial cells to epidermal growth factor." <u>J Biol Chem</u> **271**(48): 30956-30963.

Kang, S. A., E. S. Lee, H. Y. Yoon, P. A. Randazzo and S. T. Lee (2010). "PTK6 inhibits down-regulation of EGF receptor through phosphorylation of ARAP1." <u>The Journal of biological chemistry</u> **285**(34): 26013-26021.

Kanner, S. B., A. B. Reynolds and J. T. Parsons (1991). "Tyrosine phosphorylation of a 120-kilodalton pp60src substrate upon epidermal growth factor and platelet-derived growth factor receptor stimulation and in polyomavirus middle-T-antigen-transformed cells." <u>Mol Cell Biol</u> **11**(2): 713-720.

Kasprzycka, M., M. Majewski, Z. J. Wang, A. Ptasznik, M. Wysocka, Q. Zhang, M. Marzec, P. Gimotty, M. R. Crompton and M. A. Wasik (2006). "Expression and Oncogenic Role of Brk (PTK6/Sik) Protein Tyrosine Kinase in Lymphocytes." Am J Pathol **168**(5): 1631-1641.

Kawachi, Y., H. Nakauchi and F. Otsuka (1994). "Identification of a novel cDNA clone encoding protein tyrosine kinase in murine skin." J Dermatol **21**(8): 533-538.

Kim, D. J., K. S. Chan, S. Sano and J. Digiovanni (2007). "Signal transducer and activator of transcription 3 (Stat3) in epithelial carcinogenesis." Mol Carcinog **46**(8): 725-731.

Kim, D. J., K. Kataoka, D. Rao, K. Kiguchi, G. Cotsarelis and J. Digiovanni (2009). "Targeted disruption of stat3 reveals a major role for follicular stem cells in skin tumor initiation." Cancer Res **69**(19): 7587-7594.

Kohmura, N., T. Yagi, Y. Tomooka, M. Oyanagi, R. Kominami, N. Takeda, J. Chiba, Y. Ikawa and S. Aizawa (1994). "A novel nonreceptor tyrosine kinase, Srm: cloning and targeted disruption." Mol Cell Biol **14**(10): 6915-6925.

Kuriakose, M. A., W. T. Chen, Z. M. He, A. G. Sikora, P. Zhang, Z. Y. Zhang, W. L. Qiu, D. F. Hsu, C. McMunn-Coffran, S. M. Brown, E. M. Elango, M. D. Delacure and F. A. Chen (2004). "Selection and validation of differentially expressed genes in head and neck cancer." Cell Mol Life Sci **61**(11): 1372-1383.

Lambert, S. R., N. Mladkova, A. Gulati, R. Hamoudi, K. Purdie, R. Cerio, I. Leigh, C. Proby and C. A. Harwood (2014). "Key differences identified between actinic keratosis and cutaneous squamous cell carcinoma by transcriptome profiling." Br J Cancer **110**(2): 520-529.

Lee, S. T., K. M. Strunk and R. A. Spritz (1993). "A survey of protein tyrosine kinase mRNAs expressed in normal human melanocytes." Oncogene **8**(12): 3403-3410.

Leemans, C. R., B. J. Braakhuis and R. H. Brakenhoff (2011). "The molecular biology of head and neck cancer." Nat Rev Cancer **11**(1): 9-22.

Lewis, D. A., S. A. Hurwitz and D. F. Spandau (2003). "UVB-induced apoptosis in normal human keratinocytes: role of the erbB receptor family." Exp Cell Res **284**(2): 316-327.

Li, X., Y. Lu, K. Liang, J. M. Hsu, C. Albarracin, G. B. Mills, M. C. Hung and Z. Fan (2012). "Brk/PTK6 sustains activated EGFR signaling through inhibiting EGFR degradation and transactivating EGFR." Oncogene **31**(40): 4372-4383.

Li, X., Y. Lu, K. Liang, J. M. Hsu, C. Albarracin, G. B. Mills, M. C. Hung and Z. Fan (2012). "Brk/PTK6 sustains activated EGFR signaling through inhibiting EGFR degradation and transactivating EGFR." Oncogene.

Lim, S. T., X. L. Chen, Y. Lim, D. A. Hanson, T. T. Vo, K. Howerton, N. Larocque, S. J. Fisher, D. D. Schlaepfer and D. Ilic (2008). "Nuclear FAK promotes cell proliferation and survival through FERM-enhanced p53 degradation." Mol Cell **29**(1): 9-22.

Lippens, S., E. Hoste, P. Vandenabeele, P. Agostinis and W. Declercq (2009). "Cell death in the skin." Apoptosis **14**(4): 549-569.

Liu, F. and S. E. Millar (2010). "Wnt/beta-catenin signaling in oral tissue development and disease." J Dent Res **89**(4): 318-330.

Liu, L., Y. Gao, H. Qiu, W. T. Miller, V. Poli and N. C. Reich (2006). "Identification of STAT3 as a specific substrate of breast tumor kinase." Oncogene **25**(35): 4904-4912.

Llor, X., M. S. Serfas, W. Bie, V. Vasioukhin, M. Polonskaia, J. Derry, C. M. Abbott and A. L. Tyner (1999). "BRK/Sik expression in the gastrointestinal tract and in colon tumors." Clin Cancer Res **5**(7): 1767-1777.

Locatelli, A., K. A. Lofgren, A. R. Daniel, N. E. Castro and C. A. Lange (2012). "Mechanisms of HGF/Met signaling to Brk and Sam68 in breast cancer progression." Hormones & cancer **3**(1-2): 14-25.

Lofgren, K. A., J. H. Ostrander, D. Housa, G. K. Hubbard, A. Locatelli, R. L. Bliss, K. L. Schwertfeger and C. A. Lange (2011). "Mammary gland specific expression of Brk/PTK6 promotes delayed involution and tumor formation associated with activation of p38 MAPK." Breast cancer research : BCR **13**(5): R89.

Ludyga, N., N. Anastasov, I. Gonzalez-Vasconcellos, M. Ram, H. Hofler and M. Aubele (2011). "Impact of protein tyrosine kinase 6 (PTK6) on human epidermal growth factor receptor (HER) signalling in breast cancer." Molecular bioSystems **7**(5): 1603-1612.

Ludyga, N., N. Anastasov, M. Rosemann, J. Seiler, N. Lohmann, H. Braselmann, K. Mengele, M. Schmitt, H. Hofler and M. Aubele (2013). "Effects of simultaneous knockdown of HER2 and PTK6 on malignancy and tumor progression in human breast cancer cells." Molecular cancer research : MCR **11**(4): 381-392.

Lukong, K. E., M. E. Huot and S. Richard (2009). "BRK phosphorylates PSF promoting its cytoplasmic localization and cell cycle arrest." Cell Signal **21**(9): 1415-1422.

Lukong, K. E., D. Larocque, A. L. Tyner and S. Richard (2005). "Tyrosine phosphorylation of sam68 by breast tumor kinase regulates intranuclear localization and cell cycle progression." J Biol Chem **280**(46): 38639-38647.

Lukong, K. E. and S. Richard (2008). "Breast tumor kinase BRK requires kinesin-2 subunit KAP3A in modulation of cell migration." Cell Signal **20**(2): 432-442.

Lynch, D., J. Svoboda, S. Putta, H. E. Hofland, W. H. Chern and L. A. Hansen (2007). "Mouse skin models for carcinogenic hazard identification: utilities and challenges." Toxicol Pathol **35**(7): 853-864.

Ma, S., J. Y. Bao, P. S. Kwan, Y. P. Chan, C. M. Tong, L. Fu, N. Zhang, A. H. Tong, Y. R. Qin, S. W. Tsao, K. W. Chan, S. Lok and X. Y. Guan (2012). "Identification of PTK6, via RNA Sequencing Analysis, as a Suppressor of Esophageal Squamous Cell Carcinoma." Gastroenterology.

Macias, E., D. Rao and J. Digiovanni (2013). "Role of stat3 in skin carcinogenesis: insights gained from relevant mouse models." J Skin Cancer **2013**: 684050.

McLean, G. W., N. O. Carragher, E. Avizienyte, J. Evans, V. G. Brunton and M. C. Frame (2005). "The role of focal-adhesion kinase in cancer - a new therapeutic opportunity." Nat Rev Cancer **5**(7): 505-515.

Mitchell, P. J., K. T. Barker, J. E. Martindale, T. Kamalati, P. N. Lowe, M. J. Page, B. A. Gusterson and M. R. Crompton (1994). "Cloning and characterisation of cDNAs encoding a novel non-receptor tyrosine kinase, brk, expressed in human breast tumours." Oncogene **9**: 2383-2390.

Mitchell, P. J., E. A. Sara and M. R. Crompton (2000). "A novel adaptor-like protein which is a substrate for the non-receptor tyrosine kinase, BRK." Oncogene **19**(37): 4273-4282.

Mitra, S. K., D. A. Hanson and D. D. Schlaepfer (2005). "Focal adhesion kinase: in command and control of cell motility." Nat Rev Mol Cell Biol **6**(1): 56-68.

Nesnow, S., H. Bergman and T. J. Slaga (1986). "Comparison of the tumorigenic response of SENCAR and C57BL/6 mice to benzo(a)pyrene and the inter-experimental variability over a three-year period." Environ Health Perspect **68**: 19-25.

Ostrander, J. H., A. R. Daniel, K. Lofgren, C. G. Kleer and C. A. Lange (2007). "Breast tumor kinase (protein tyrosine kinase 6) regulates heregulin-induced activation of ERK5 and p38 MAP kinases in breast cancer cells." Cancer Research **67**(9): 4199-4209.

Palka-Hamblin, H. L., J. J. Gierut, W. Bie, P. M. Brauer, Y. Zheng, J. M. Asara and A. L. Tyner (2010). "Identification of beta-catenin as a target of the intracellular tyrosine kinase PTK6." J Cell Sci **123**(Pt 2): 236-245.

Park, S. H., K. H. Lee, H. Kim and S. T. Lee (1997). "Assignment of the human PTK6 gene encoding a non-receptor protein tyrosine kinase to 20q13.3 by fluorescence in situ hybridization." Cytogenet Cell Genet **77**(3-4): 271-272.

Parsons, J. T. (2003). "Focal adhesion kinase: the first ten years." J Cell Sci **116**(Pt 8): 1409-1416.

Peng, M., S. M. Ball-Kell, R. R. Franks, H. Xie and A. L. Tyner (2013). "Protein tyrosine kinase 6 regulates mammary gland tumorigenesis in mouse models." Oncogenesis **2**: e81.

Peng, M., R. Emmadi, Z. Wang, E. L. Wiley, P. H. Gann, S. Khan, N. Banerji, W. McDonald, S. Asztalos, T. N. D. Pham, D. A. Tonetti and A. L. Tyner (2014).

"PTK6/BRK is Expressed in the Normal Mammary Gland and Activated at the Plasma Membrane in Breast Tumors." Oncotarget **In Press**.

Petch, L. A., S. M. Bockholt, A. Bouton, J. T. Parsons and K. Burridge (1995). "Adhesion-induced tyrosine phosphorylation of the p130 src substrate." J Cell Sci **108 (Pt 4)**: 1371-1379.

Petro, B. J., R. C. Tan, A. L. Tyner, M. W. Lingen and K. Watanabe (2004). "Differential expression of the non-receptor tyrosine kinase BRK in oral squamous cell carcinoma and normal oral epithelium." Oral Oncol **40**(10): 1040-1047.

Provenzano, P. P., D. R. Inman, K. W. Eliceiri, H. E. Beggs and P. J. Keely (2008). "Mammary epithelial-specific disruption of focal adhesion kinase retards tumor formation and metastasis in a transgenic mouse model of human breast cancer." Am J Pathol **173**(5): 1551-1565.

Qiu, H. and W. T. Miller (2002). "Regulation of the nonreceptor tyrosine kinase Brk by autophosphorylation and by autoinhibition." J Biol Chem **277**(37): 34634-34641.

Qiu, H. and W. T. Miller (2004). "Role of the Brk SH3 domain in substrate recognition." Oncogene **23**(12): 2216-2223.

Qiu, H., F. Zappacosta, W. Su, R. S. Annan and W. T. Miller (2005). "Interaction between Brk kinase and insulin receptor substrate-4." Oncogene.

Rastogi, R. P., Richa, A. Kumar, M. B. Tyagi and R. P. Sinha (2010). "Molecular mechanisms of ultraviolet radiation-induced DNA damage and repair." J Nucleic Acids **2010**: 592980.

Regan Anderson, T. M., D. L. Peacock, A. R. Daniel, G. K. Hubbard, K. A. Lofgren, B. J. Girard, A. Schorg, D. Hoogewijs, R. H. Wenger, T. N. Seagroves and C. A. Lange (2013). "Breast Tumor Kinase (Brk/PTK6) Is a Mediator of Hypoxia-Associated Breast Cancer Progression." Cancer research **73**(18): 5810-5820.

Reynolds, A. B., S. B. Kanner, H. C. Wang and J. T. Parsons (1989). "Stable association of activated pp60src with two tyrosine-phosphorylated cellular proteins." Mol Cell Biol **9**(9): 3951-3958.

Rho, O., D. J. Kim, K. Kiguchi and J. Digiovanni (2011). "Growth factor signaling pathways as targets for prevention of epithelial carcinogenesis." Mol Carcinog **50**(4): 264-279.

Sakai, R., A. Iwamatsu, N. Hirano, S. Ogawa, T. Tanaka, H. Mano, Y. Yazaki and H. Hirai (1994). "A novel signaling molecule, p130, forms stable complexes in vivo with v-Crk and v-Src in a tyrosine phosphorylation-dependent manner." Embo J **13**(16): 3748-3756.

Sano, S., K. S. Chan, S. Carbajal, J. Clifford, M. Peavey, K. Kiguchi, S. Itami, B. J. Nickoloff and J. DiGiovanni (2005). "Stat3 links activated keratinocytes and immunocytes required for development of psoriasis in a novel transgenic mouse model." Nat Med **11**(1): 43-49.

Sano, S., K. S. Chan and J. DiGiovanni (2008). "Impact of Stat3 activation upon skin biology: a dichotomy of its role between homeostasis and diseases." J Dermatol Sci **50**(1): 1-14.

Sano, S., S. Itami, K. Takeda, M. Tarutani, Y. Yamaguchi, H. Miura, K. Yoshikawa, S. Akira and J. Takeda (1999). "Keratinocyte-specific ablation of Stat3 exhibits impaired skin remodeling, but does not affect skin morphogenesis." Embo J **18**(17): 4657-4668.

Sano, S., M. Kira, S. Takagi, K. Yoshikawa, J. Takeda and S. Itami (2000). "Two distinct signaling pathways in hair cycle induction: Stat3-dependent and -independent pathways." Proc Natl Acad Sci U S A **97**(25): 13824-13829.

Schaefer, F., Y. Chen, T. Tsao, P. Nouri and R. Rabkin (2001). "Impaired JAK-STAT signal transduction contributes to growth hormone resistance in chronic uremia." J Clin Invest **108**(3): 467-475.

Schaller, M. D. (2001). "Paxillin: a focal adhesion-associated adaptor protein." Oncogene **20**(44): 6459-6472.

Schlaepfer, D. D. and S. K. Mitra (2004). "Multiple connections link FAK to cell motility and invasion." Curr Opin Genet Dev **14**(1): 92-101.

Schmandt, R. E., M. Bennett, S. Clifford, A. Thornton, F. Jiang, R. R. Broaddus, C. C. Sun, K. H. Lu, A. K. Sood and D. M. Gershenson (2006). "The BRK Tyrosine Kinase is Expressed in High-Grade Serous Carcinoma of the Ovary." Cancer Biol Ther **5**(9): 1136-1141.

Sellier, C., F. Rau, Y. Liu, F. Tassone, R. K. Hukema, R. Gattoni, A. Schneider, S. Richard, R. Willemsen, D. J. Elliott, P. J. Hagerman and N. Charlet-Berguerand (2010). "Sam68 sequestration and partial loss of function are associated with splicing alterations in FXTAS patients." EMBO **29**(7): 1248-1261.

Serfas, M. S. and A. L. Tyner (2003). "Brk, Srm, Frk, and Src42A form a distinct family of intracellular Src-like tyrosine kinases." Oncol Res **13**(6-10): 409-419.

Shen, C. H., H. Y. Chen, M. S. Lin, F. Y. Li, C. C. Chang, M. L. Kuo, J. Settleman and R. H. Chen (2008). "Breast tumor kinase phosphorylates p190RhoGAP to regulate rho and ras and promote breast carcinoma growth, migration, and invasion." Cancer Res **68**(19): 7779-7787.

Siyanova, E. Y., M. S. Serfas, I. A. Mazo and A. L. Tyner (1994). "Tyrosine kinase gene expression in the mouse small intestine." Oncogene **9**(7): 2053-2057.

Slaga, T. J. (1986). "SENCAR mouse skin tumorigenesis model versus other strains and stocks of mice." Environ Health Perspect **68**: 27-32.

Slaga, T. J., J. O'Connell, J. Rotstein, G. Patskan, R. Morris, C. M. Aldaz and C. J. Conti (1986). "Critical genetic determinants and molecular events in multistage skin carcinogenesis." Symp Fundam Cancer Res **39**: 31-44.

Smith, H. W., P. Marra and C. J. Marshall (2008). "uPAR promotes formation of the p130Cas-Crk complex to activate Rac through DOCK180." J Cell Biol **182**(4): 777-790.

Strickland, P. T. (1982). "Tumor induction in Sencar mice in response to ultraviolet radiation." Carcinogenesis **3**(12): 1487-1489.

Strickland, P. T. (1986). "Abnormal wound healing in UV-irradiated skin of Sencar mice." J Invest Dermatol **86**(1): 37-41.

Strickland, P. T. (1986). "Photocarcinogenesis and persistent hyperplasia in UV-irradiated SENCAR mouse skin." Environ Health Perspect **68**: 131-134.

Strickland, P. T. (1986). "Photocarcinogenesis by near-ultraviolet (UVA) radiation in Sencar mice." J Invest Dermatol **87**(2): 272-275.

Tachibana, K., T. Urano, H. Fujita, Y. Ohashi, K. Kamiguchi, S. Iwata, H. Hirai and C. Morimoto (1997). "Tyrosine phosphorylation of Crk-associated substrates by focal adhesion kinase. A putative mechanism for the integrin-mediated tyrosine phosphorylation of Crk-associated substrates." J Biol Chem **272**(46): 29083-29090.

Theocharis, S. E., J. T. Klijanienko, E. Padoy, S. Athanassiou and X. X. Sastre-Garau (2009). "Focal adhesion kinase (FAK) immunocytochemical expression in breast ductal invasive carcinoma (DIC): correlation with clinicopathological parameters and tumor proliferative capacity." Med Sci Monit **15**(8): BR221-226.

Toruner, G. A., C. Ulger, M. Alkan, A. T. Galante, J. Rinaggio, R. Wilk, B. Tian, P. Soteropoulos, M. R. Hameed, M. N. Schwalb and J. J. Dermody (2004). "Association between gene expression profile and tumor invasion in oral squamous cell carcinoma." Cancer Genet Cytogenet **154**(1): 27-35.

Tupper, J., M. R. Crompton and A. J. Harvey (2011). "Breast tumor kinase (Brk/PTK6) plays a role in the differentiation of primary keratinocytes." Archives of dermatological research **303**(4): 293-297.

Turkson, J. (2004). "STAT proteins as novel targets for cancer drug discovery." Expert Opin Ther Targets **8**(5): 409-422.

V. Vasioukhin, A. L. T. (1997). "A role for the epithelial-cell specific tyrosine kinase Sik during keratinocyte differentiation." Proc. Natl. Acad. Sci **94**: 14477-14482.

Van Laethem, A., M. Garmyn and P. Agostinis (2009). "Starting and propagating apoptotic signals in UVB irradiated keratinocytes." Photochem Photobiol Sci **8**(3): 299-308.

Vasioukhin, V., M. S. Serfas, E. Y. Siyanova, M. Polonskaia, V. J. Costigan, B. Liu, A. Thomason and A. L. Tyner (1995). "A novel intracellular epithelial cell tyrosine kinase is expressed in the skin and gastrointestinal tract." Oncogene **10**(2): 349-357.

Wang, T. C., S. H. Jee, T. F. Tsai, Y. L. Huang, W. L. Tsai and R. H. Chen (2005). "Role of breast tumour kinase in the in vitro differentiation of HaCaT cells." Br J Dermatol **153**(2): 282-289.

Weaver, A. M. and C. M. Silva (2007). "Signal transducer and activator of transcription 5b: a new target of breast tumor kinase/protein tyrosine kinase 6." Breast Cancer Res **9**(6): R79.

Xia, H., R. S. Nho, J. Kahm, J. Kleidon and C. A. Henke (2004). "Focal adhesion kinase is upstream of phosphatidylinositol 3-kinase/Akt in regulating fibroblast survival in response to contraction of type I collagen matrices via a beta 1 integrin viability signaling pathway." J Biol Chem **279**(31): 33024-33034.

Xiang, B., K. Chatti, H. Qiu, B. Lakshmi, A. Krasnitz, J. Hicks, M. Yu, W. T. Miller and S. K. Muthuswamy (2008). "Brk is coamplified with ErbB2 to promote proliferation in breast cancer." Proc Natl Acad Sci U S A **105**(34): 12463-12468.

Yim, E. K., G. Peng, H. Dai, R. Hu, K. Li, Y. Lu, G. B. Mills, F. Meric-Bernstam, B. T. Hennessy, R. J. Craven and S. Y. Lin (2009). "Rak functions as a tumor suppressor by regulating PTEN protein stability and function." Cancer Cell **15**(4): 304-314.

Yim, E. K., S. Siwko and S. Y. Lin (2009). "Exploring Rak tyrosine kinase function in breast cancer." Cell Cycle **8**(15): 2360-2364.

Yu, L. F., Y. B. Zhu, M. M. Qiao, J. Zhong, S. P. Tu and Y. L. Wu (2004). "[Constitutive activation and clinical significance of Stat3 in human gastric cancer tissues and cell lines]." Zhonghua Yi Xue Za Zhi **84**(24): 2064-2069.

Zhai, Y., R. Kuick, B. Nan, I. Ota, S. J. Weiss, C. L. Trimble, E. R. Fearon and K. R. Cho (2007). "Gene expression analysis of preinvasive and invasive cervical squamous cell carcinomas identifies HOXC10 as a key mediator of invasion." Cancer Res **67**(21): 10163-10172.

Zhang, P., J. H. Ostrander, E. J. Faivre, A. Olsen, D. Fitzsimmons and C. A. Lange (2005). "Regulated association of protein kinase B/Akt with breast tumor kinase." J Biol Chem **280**(3): 1982-1991.

Zheng, Y., J. M. Asara and A. L. Tyner (2012). "Protein-tyrosine Kinase 6 Promotes Peripheral Adhesion Complex Formation and Cell Migration by Phosphorylating p130 CRK-associated Substrate." The Journal of biological chemistry **287**(1): 148-158.

Zheng, Y., J. M. Asara and A. L. Tyner (2012). "Protein-tyrosine kinase 6 promotes peripheral adhesion complex formation and cell migration by phosphorylating p130 CRK-associated substrate." J Biol Chem **287**(1): 148-158.

Zheng, Y., J. Gierut, Z. Wang, J. Miao, J. M. Asara and A. L. Tyner (2012). "Protein tyrosine kinase 6 protects cells from anoikis by directly phosphorylating focal adhesion kinase and activating AKT." Oncogene.

Zheng, Y., M. Peng, Z. Wang, J. M. Asara and A. L. Tyner (2010). "Protein tyrosine kinase 6 directly phosphorylates AKT and promotes AKT activation in response to epidermal growth factor." Molecular and Cellular Biology **30**(17): 4280-4292.

Zouq, N. K., J. A. Keeble, J. Lindsay, A. J. Valentijn, L. Zhang, D. Mills, C. E. Turner, C. H. Streuli and A. P. Gilmore (2009). "FAK engages multiple pathways to maintain survival of fibroblasts and epithelia: differential roles for paxillin and p130Cas." J Cell Sci **122**(Pt 3): 357-367.

VI. VITA

NAME: Michael Chastkofsky

EDUCATION: Bachelor of Science, Biochemistry and Molecular Biology,
                 University of Georgia, Athens, GA, 2003

                 Master of Science, Biomolecular Chemistry,
                 University of Wisconsin – Madison, Madison, WI, 2006

                 PhD., Oral Science,
                 University of Illinois – Chicago, Chicago, IL, 2014

HONORS: HOPE Scholarship, 2001
                 Alpha Delta Lambda Honor Society, 2001
                 CURO Scholarship, 2002
                 Delta Epsilon Iota Honor Society, 2002
                 Golden Key Honor Society, 2002
                 Magna Cum Laude, 2003
                 Karavolas Scholarship, 2003
                 1st Place, Clinic and Research Day Forum, 2013

PUBLICATIONS: Baker DL, Youssef OA, **Chastkofsky MI**, Dy DA, Terns RM,
                 Terns MP. RNA-guided RNA modification: functional
                 organization of the archaeal H/ACA RNP. Genes and
                 Development. 2005 May 15;19(10):1238-48.